2021

PERIOCULAR MESENCHYME HETEROGENEITY DURING MORPHOGENESIS OF THE VERTEBRATE OCULAR ANTERIOR SEGMENT

Kristyn L. Van Der Meulen
University of Kentucky, vandermeulenk2015@gmail.com
Digital Object Identifier: https://doi.org/10.13023/etd.2021.047

STUDENT AGREEMENT:

I represent that my thesis or dissertation and abstract are my original work. Proper attribution has been given to all outside sources. I understand that I am solely responsible for obtaining any needed copyright permissions. I have obtained needed written permission statement(s) from the owner(s) of each third-party copyrighted matter to be included in my work, allowing electronic distribution (if such use is not permitted by the fair use doctrine) which will be submitted to UKnowledge as Additional File.

I hereby grant to The University of Kentucky and its agents the irrevocable, non-exclusive, and royalty-free license to archive and make accessible my work in whole or in part in all forms of media, now or hereafter known. I agree that the document mentioned above may be made available immediately for worldwide access unless an embargo applies.

I retain all other ownership rights to the copyright of my work. I also retain the right to use in future works (such as articles or books) all or part of my work. I understand that I am free to register the copyright to my work.

REVIEW, APPROVAL AND ACCEPTANCE

The document mentioned above has been reviewed and accepted by the student's advisor, on behalf of the advisory committee, and by the Director of Graduate Studies (DGS), on behalf of the program; we verify that this is the final, approved version of the student's thesis including all changes required by the advisory committee. The undersigned agree to abide by the statements above.

Kristyn L. Van Der Meulen, Student

Dr. Jakub Famulski, Major Professor

Dr. David Weisrock, Director of Graduate Studies

PERIOCULAR MESENCHYME HETEROGENEITY DURING MORPHOGENESIS OF THE VERTEBRATE OCULAR ANTERIOR SEGMENT

DISSERTATION

A dissertation submitted in partial fulfillment of the requirements for the degree of Doctor of Philosophy in the College of Arts and Sciences at the University of Kentucky

By
Kristyn L. Van Der Meulen
Lexington, Kentucky

Director: Dr. Jakub K. Famulski, Assistant Professor of Biology
Lexington, Kentucky

2021

ABSTRACT OF DISSERTATION

PERIOCULAR MESENCHYME HETEROGENEITY DURING MORPHOGENESIS OF THE VERTEBRATE OCULAR ANTERIOR SEGMENT

The vertebrate eye is a complex organ, responsible for the primary sense with which we interact with our environment: vision. Development of the eye is a tightly regulated process, controlled by a vast network of genes. This process begins with eye morphogenesis, when the eye structure is formed through a series of morphogenetic movements and culminates in the creation of the optic cup, lens, and presumptive optic stalk. Next, retinal differentiation creates the critical cell layers of the retina needed to process light waves that enter the eye, including rod and cone photoreceptors, interneurons, and support cells. Failure in either one of these steps can result in developmental congenital defects or disorders which can range from relatively minor visual impairment to blindness. While extensive research has already been done to understand congenital blinding disorders, we have only begun to scratch the surface of understanding key parts of eye development and the intrinsic and extrinsic factors that go into regulating the process. While many researchers focus their work on eye morphogenesis or retinal differentiation in relation to these disorders, little attention is given to a process that overlaps with both stages: formation of the anterior segment (AS). The AS is a collection of individual structures located in the front third of the eye and has different developmental origins from the rest of the eye. AS structures are formed from a specialized group of neural crest-derived cells called Periocular Mesenchyme (POM) cells, which migrate around the forming optic cup to colonize the space between the anterior most regions of the optic cup and the surface ectoderm. Once positioned in this space, POM cells will specify into their cell types and form structures that include the corneal stroma and endothelium, the iris and ciliary body, and drainage network of the iridocorneal angle. Failure in the migration or specification of these cells can result in Anterior Segment Dysgenesis and a spectrum of visual impairment. Presently, little is understood about this transient cell population, its origins within the neural crest, its migration to the AS, or its genetic makeup during colonization and differentiation of the AS. In this dissertation, I examine in detail the POM cell population in zebrafish, focusing on its heterogeneity as well as its origins within the neural crest. In Chapter 3, I utilize several transgenic lines for POM-related transcription factors to demonstrate the heterogeneity of the POM through distribution mapping, co-expression analysis, migration behavior, and single cell RNA sequencing. I provide the first large scale

evidence that the POM is a collection of subpopulations working in conjunction with one another to form the AS. In Chapter 4 I outline the role of the neural crest in POM formation and the consequences that loss of neural crest has on the development of the POM, as well as the AS. My findings provide a new lens with which to understand AS development and the cells responsible for it, and ultimately uncover new pathways for understanding the biological mechanisms involved in Anterior Segment Dysgenesis and AS-related blinding disorders.

KEYWORDS: Periocular Mesenchyme, Anterior Segment, Foxc1, Pitx2, Eye Development

Kristyn Van Der Meulen

April 12th 2021
Date

PERIOCULAR MESENCHYME HETEROGENEITY DURING MORPHOGENESIS OF THE VERTEBRATE OCULAR ANTERIOR SEGMENT

By

Kristyn L. Van Der Meulen

Dr. Jakub Famulski
Director of Dissertation

Dr. David Weisrock
Director of Graduate studies

April 12th 2021
Date

To Mom

ACKNOWLEDGMENTS

Six years in graduate school has been nothing short of a wild and crazy ride. Every day brought new adventures and challenges, even before factoring in the world outside our lab doors. Adventures in life like these rarely take place without a little anxiety, a lot of complaining, and irreplaceable good company though, so I'd like to offer my sincere thanks to a group of people without whose support, encouragement, and friendship I would not have been able to succeed.

First, to my mother Teri, to whom I owe more thanks than I could ever put into words. She has always strived to instill in me a desire to learn and grow, no matter how much I resisted when I was young! She taught me the value of hard work and that there is always value in the things we experience, especially those experiences which scare us. But getting through those experiences is made easier by the relationship we form with one another. Life has not been easy for her or our family, but she has shown amazing strength and determination in these difficult times and I am unbelievably proud of her! I was able to complete my undergraduate and graduate studies because of her dedication, guidance, and friendship. Thank you, mom!

I would like to offer my deepest gratitude to my doctoral advisor Dr. Jakub Famulski. He took a chance on me when I was just a scared first year student who didn't want to rotate out of his lab and I am immensely thankful for that decision. He has always been open to discussions on everything from my research to classes to the future and even just the news of the day. His enthusiasm, positive attitude, and encouragement helped to foster a comfortable working environment where I felt secure enough to try out my ideas without fear of making mistakes or being reprimanded. He has always

encouraged all of us to reach for every opportunity and to always aim higher with every submitted abstract, grant, and paper. He was always willing to read my work or watch my presentations and provided endless amounts of helpful feedback and critiques. He has recognized every achievement and celebrated it, no matter how big or small (A special thank you to Kathy, who has provided us with endless snacks, treats, pumpkins, decorations, and party supplies over the years!). Jakub, thank you for guiding me through these past 6 years, for helping me grow as a scientist and a professional. Thank you for letting me work through my ideas and problems myself, but for also being ready in the wings to jump in and save me when I got in over my head. Thank you for your respect towards us as graduate students and human beings, who sometimes have bad days and just need to walk away to reset. Thank you for recognizing those moments and not simply ignoring them or pushing us past our breaking points. Thank you most of all for making me a better and more confident scientist.

I would like to thank the members of my committee: Dr. Ann Morris, Dr. Jeramiah Smith, and Dr. Jessica Blackburn. Thank you to Dr. Morris for your knowledge about eye development, for always being available to discuss your scientific insights, and for your words of encouragement over the years. To Dr. Smith, thank you for your help from the very beginning, from my very first semester in Bioinformatics. Both in and out of the classroom you have been willing to help me with the sequencing data for my work and I am unbelievably appreciative. Thank you too, for your advice on rotations, classes, and future employment. And thank you to Dr. Blackburn, for your words of encouragement and friendly discussions on my research.

Thank you to the entire Biology department for their help throughout the years. Thank you to everyone who watched my presentations and asked such insightful questions. Thank you to Dr. Cooper, who was so welcoming to me when I first applied to UK and gave me a personal tour of the city during recruitment. And thank you most of all, to Jacquie Burke! Life in graduate school is hard, but there is no one more willing and able to help than Jacquie. I couldn't thank you enough for all your help, both professionally and personally. Even before I started in grad school Jacquie was there to help in any way she could. Where would any of us be without her?

Thank you to my amazing lab mates who quickly became my friends and family, making day to day life so much more exciting. Megan, Warlen, and Nick, you guys were the best lab mates I could've asked for and being co-workers with you guys is more than I ever could've dreamed of. Megan, thank you for being my first friend in graduate school and for working together with me as the first official grad students of the Famulski lab! Thank you for all your help with my research, especially the bioinformatics, but thank you in particular for all the conversations. Whether it was about work, the world, stories of our lives, gossip, or just plain complaining about life, you were always there to talk to, and I am so grateful for that. Warlen, we've been through it all together. You and I took every one of our classes together and attended every conference together too. For every experience in grad school, major or minor, you were there with me. I will never forget the countless conversations with you and Megan and the endless stories we told. You are such an amazing friend, and I can't thank you enough for your friendship, support, and encouragement. Nick, my bench neighbor! Thank you for all the study sessions and adventures we shared. You are a great friend and I am happy to have shared

so much of my formative grad school years with you. Thank you to my undergraduate mentee Paige for your hard work and dedication to your project. Thank you to all the past undergraduate students of the lab: Amy, Sydney, Cassie, Reed, Austin, Chase, Darrington, Dylan, Grace, Aaron, and Megha for all your work and support. I would also like to thank members of the Morris lab: Kayla, Laura, Becky, Jess, and CC for being such great neighbors and for always sharing reagents and expertise with us.

Life outside of the lab is just as important as life inside of it during grad school, so I would like to thank some of the people in my personal life who helped me on my journey. First to my boyfriend Brandon, who I met during my 3rd year of grad school. He has been my support through countless rough times, always giving me encouragement when I felt like I wasn't good enough for a Ph.D., always making me laugh when I wanted to cry. Even though I don't study "the rods and cones" as you like to say, I thank you for listening to my struggles anyway and helping me to always smile and breathe. I would like to thank all my friends from my hometown, Wittenberg, and Lexington for pulling me away from my work and reminding me to have fun. I'd like to thank them also for understanding when I had to cancel plans or couldn't come to visit because my work needed to take precedent. Ellie, Melissa, Athena, Taylor, Leah, Sami, Lauren, Kara, Sam…you guys are the best friends a girl could ask for! Thank you for always being there for me whenever I need to vent!

Finally, I would like to thank my family. Not only my mom, but also my father and brother. You guys have always encouraged my studies and fostered a love of science in me. I wanted to be important like my dad when I grew up, and that determination has paid off. And thank you to my extended family, for their unwavering support and

willingness to brag about even my most minor accomplishments to their friends and other family. Their joy drives me to always try my hardest and be better, so they always have something to be proud of.

TABLE OF CONTENTS

LIST OF TABLES

LIST OF FIGURES

LIST OF ADDITIONAL FILES

CHAPTER 1: EYE DEVELOPMENT, NEURAL CREST, AND THE PERIOCULAR MESENCHYME

1.1 Introduction to Vision

A hallmark feature of all living organisms is the ability to perceive cues from their surroundings and act upon them accordingly, thus allowing for obtaining resources and avoiding harm. This perception is achieved through a number of senses, some of which are relied upon more than others depending on the organism. They include olfaction, auditory, and somatosensory perceptions. However, chief among these senses for many organisms is vision, the collection, processing, and interpretation of light cues either reflecting, emanating, or absorbing from objects in the surrounding environment. It is such a critical function to our everyday lives that many of us simply cannot imagine living without sight. A study published in JAMA Ophthalmology in 2016 found that 47% of adults in America surveyed listed vision loss as the worst possible health outcome on their daily life and rated it as equal to or worse than losing a limb or their memory (Scott et al., 2016). We understand the importance of vision even as children, as fear of the dark is a common concern, when we can no longer effectively position ourselves in an area or understand how things are moving around us.

Continuing in line with its critical function for survival, visual development and function are complex processes involving multiple tissues, cellular connections, and timing events. In vertebrates, the process of forming an eye and maintaining it over time involves an army of genes, cells, and tissues from multiple specified structures of the eye, through the optic nerve, and all the way to the visual cortex of the brain. Failures during

development or damage to any of the tissues involved in visual processing can lead to impaired vision or blindness. According to the World Health Organization (WHO), an estimated 285 million people globally were living with some kind of visual impairment in 2010 (WHO). In 2014, the National Eye Institute estimated 2.9 million Americans were living with low vision and an estimated 1.3 million were blind (NEI). Furthermore, more than 48 million Americans were living with a visual refractive error requiring the use of glasses or contacts to fix (NEI). All of these numbers are expected to increase significantly by 2050. In today's technologically advanced world, it is possible to live a long life in spite of visual impairment or blindness. However, losing vision can physically and mentally reduce the quality of life for those suffering from it, just as restoring it can improve life for those affected. Eighty percent of causes of visual loss can be treated, resulting in improved or restored vision, including cataracts and glaucoma (NEI, WHO). However, in 2014 the estimated total cost of diagnosing and treating visual impairment or disorders was estimated to be $145 billion in the U.S. alone, with that number expected to more than quadruple by 2050 (AAO). By understanding how the vertebrate eye develops, it may be possible to develop novel treatments and preventive measures to reduce the number of people who suffer from visual impairments.

In this chapter, the proper development of the eye and the visual system will be discussed including the retina and anterior segment, in particular its role in light direction and eye maintenance, with emphasis placed on its multiple structures and their development. In this regard, the discussion will focus heavily on neural crest cell contributions and genes relevant to their specification.

1.1.1 Eye Field Specification and Budding

The process of vertebrate eye development is highly conserved process in which, simply, a spherical shaped organ extends out from the brain to the peripheral edges of the organism, allowing for optimal positioning to capture light. The presumptive eye primordium is a mixture of all future neural eye cells, as it is an extension of the central nervous system. The primordium boundaries are established via a reduction of extrinsic signaling molecules such as BMP, FGF, and WNT at the anterior of the neural tube (Sinn and Wittbrodt, 2013; Chuang and Raymond, 2002; Fuhrmann, 2010; Holly et al., 2014). During gastrulation, the eye primordium establishes itself with these boundaries. Within this segregated eye field, Eye Field Transcription Factors (EFTF) such as *otx2, pax6, tbx3, six3* and *six6*, and *rx* begin to be expressed (Cavodeassi et al., 2005; Cavodeassi, 2018; Looslie et al., 2003; Sinn and Wittbrodt, 2013). Once established, the eye field will split into two distinct fields, the presumptive eyes. Hedgehog (Hh), another important morphogen, is a critical factor during eye field segregation (Lupo, 2005). In short, key signals within the midline mesoderm will activate the expression of Hh, thus splitting the eye field and reducing the expression of EFTFs like *pax6* within that midline region and restricting them to the bilateral eye fields instead (Lupo, 2005; Looslie et al., 2003; Sinn and Wittbrodt, 2013; Fuhrmann, 2010). The newly established eye fields then begin to evaginate, or bud out, from the midline towards the overlaying surface ectoderm. This budding action forms the bilateral Optic Vesicles (OVs) that continue to express EFTFs such as *rx3* (Fuhrmann, 2010; Looslie et al., 2003). The evagination of the OVs is dependent upon the migration of cells within the lateral regions of the OV (Cavodeassi, 2018; Looslie et al., 2003).

1.1.2 Vertebrate Eye Morphogenesis

As the OV continues its evagination and comes closer to the surface ectoderm, a series of crucial morphological movements take place in rapid succession (**Figure 1.1**). The OV invaginates along the anterior-posterior and dorso-ventral axes to form a bi-layered optic cup (Kwan et al., 2012; Fuhrmann, 2012; Lupo, 2005). The inner-most layer will become the neural retina containing the light sensitive photoreceptors and support cells while the outer layer will become the Retinal Pigmented Epithelium (RPE). The folding of this tissue into a 3D spherical structure creates a fissure along the ventral edge of the eye and through the presumptive optic stalk known as the optic fissure. This opening allows neural crest-derived cells to migrate into the eye and form blood vessels which will form the hyaloid vasculature (Sedykh et al., 2017; Gestri et al., 2018; Cavodeassi, 2018). This embryonic vasculature network will supply blood and nutrients to the retina, lens, and anterior segment structures during development (Skarie and Link, 2009). Later in development, the optic fissure will undergo a complete and complex epithelial fusion event driven by the expression of regulators like *pax2* and *vax1,* thus closing off the eye from its surrounding environment (Weaver et al., 20202; James et al., 2016; Gestri et al., 2018; Alsomiry et al., 2019; Gregory-Evans et al., 2004). Briefly, fusion occurs through the breakdown of the basement membrane, likely initiated by the migrating neural crest-derived endothelial cells entering into the eye (Weaver et al., 2020; James et al., 2016). Loss of the basement membranes allows the lamellipodia and filopodia of the actin cytoskeleton on opposing epithelial sheets to connect with one another and stitch the fissure into one continuous sheet of cells (Weaver et al.,2020; Bernstein et al., 2018). Failures in this fusion process lead to Coloboma, a congenital

blinding disorder often characterized by a keyhole shaped pupil (Weaver et al., 2020; Alsomiry et al., 2019; Gregory-Evans et al., 2004). It is estimated that about 10% of all pediatric blindness is related to Coloboma (Alsomiry et al., 2019; Weaver et al., 2020). The spectrum of blindness severity in Coloboma cases is directly related to the degree of fissure fusion completed and the amount of ganglion cell axons lost within the optic stalk as a result (Gregory-Evans et al., 2004; Alsomiry et al., 2019). In essence, the more the optic fissure remains open, the poorer the patient's vision will likely be.

As the optic cup is forming, the proximal edge of the optic cup that connects the tissue back to the forebrain will reduce its thickness, forming a thin rod-like structure called the optic stalk (Fuhrmann, 2012; Fuhrmann et al., 2000; Cavodeassi, 2018). This structure houses the axons of retinal ganglion cells and allows electrical signals to be sent from the eye to the brain. Simultaneously, the anterior most portion of the OV comes into contact with the outer surface ectoderm and lens induction occurs (**Figure 1.1**). The surface ectoderm immediately in contact with the OV specifies into the lens placode which will thicken and invaginate into the OC before pinching off from the surface ectoderm and becoming the independent lens vesicle (Cavodeassi, 2018; Fuhrmann, 2012; Soules and Link, 2005; Lang, 2004). The surface ectoderm reestablishes above the lens vesicle and becomes the first layer of the eye's outer protective surface, the corneal epithelium (Soules and Link, 2005).

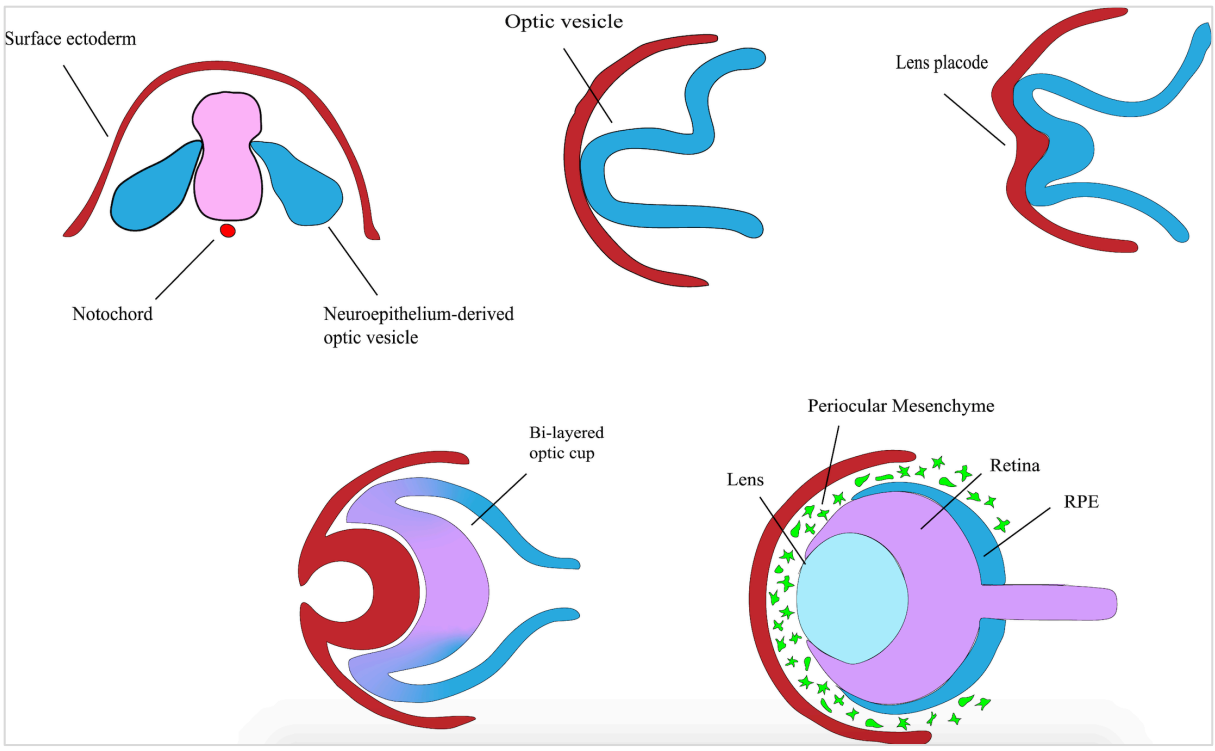

Figure 1.1: Vertebrate Eye Morphogenesis. Schematic representation showing a lateral view of vertebrate eye developmental, starting with the budding of the optic vesicle from the neuroepithelium out towards the surface ectoderm. As the optic vesicle reaches the surface ectoderm, a series of morphological changes occurs causing the thickening of the surface ectoderm to form the lens placode and lens vesicle, as well the folding of the optic vesicle into the bi-layered optic cup, creating the internal retina and the external RPE. In the final stages of eye development, the transient periocular mesenchyme population migrates around the optic cup and into the negative space between the outer most surface ectoderm layer (corneal epithelium) and the lens and anterior most portion of the optic cup.

1.1.3 Eye Maturation

Upon completion of the OC the building blocks of the eye are now present. From here, different areas of the OC begin to differentiate into key cell types. These cell types will contribute to two functionally diverse sections of the eye: the neural retina and the anterior segment. Vertebrate eye development and visual processing are known as a "camera-type" system, meaning that the eye, similar to a modern camera, works by manipulating and focusing light via a lens that will project that light onto a processing system which, in turn, will record and process that light-based image. In a camera, these two functions are carried out by the telephoto lens and the digital detector. In a vertebrate eye it is the anterior segment and the photosensitive retina. As a highly specialized extension of the central nervous system, the retina is able to capture and manipulate photons of light, convert them into electrical signals, and send the information via the optic stalk into the visual cortex of the brain for interpretation.

After establishment of the OC, maturation of these two areas begins to occur. The inner layer of the OC will begin to differentiate into distinct cell layers of the neural retina, including photoreceptors and ganglion cells. Meanwhile, the outer layer of the OC, which will become the RPE, begins to express melanin and darken. In the anterior segment, the peripheral edges of the OC, forming around the lens vesicle, will become the iris and ciliary body. Simultaneously, mesenchymal cells will migrate into the anterior portion of the eye to form several structures of the anterior segment including the cornea and the iridocorneal angle.

1.2 The Eye in Two Functionally Diverse Sections

1.2.1 The Retina and the RPE

The retina is derived from the inner layer of the OC; however, its progenitors are established during the evagination of the OV. Cells expressing *vsx2* are fated to become retinal progenitor cells, while those expressing *mitf* will become RPE cells (Graw, 2010). When the OV invaginates and folds into the OC, these progenitor cells will be positioned onto the inner and outer layers, respectively. The retinal progenitor cells found in the presumptive neural retina will specify into six types of retinal neurons: retinal ganglion cells (RGC), amacrine cells, horizontal cells, bipolar cells, and rod and cone photoreceptors. One additional cell type, the Müller glia, is also found in the retina. These unique cell types are further organized into a complex multilayered system with three major subgroups, here listed from the most peripheral layer inward towards the RPE: the Ganglion Cell Layer (GCL), the Inner Nuclear Layer (INL), and the Outer Nuclear Layer (ONL) (Graw, 2010). The GCL contains the cell bodies of the Retinal Ganglion Cells; the INL contains the cell bodies of the Amacrine, Bipolar, Horizontal, and Müller glia; and the ONL houses both photoreceptor types (Goldman, 2014; Graw, 2010). Unlike the other cell types, the Müller glia cellular projections extend throughout all three cell layers (Goldman, 2014). The Müller glia, however, is not a cell type involved in light transduction. It has the unique classification of being a support cell for the various retinal neurons, similar to all glial cells, and is involved in maintaining retinal homeostasis, providing neuroprotective properties, and functioning as scaffolding for structural integrity (Goldman, 2014). In some species, like teleosts, the Müller glia can reprogram to a stem cell-like fate following injury to regenerate retinal tissues and repair vision

(Goldman, 2014). This function is not seen in mammals. In between the three major retinal subgroups are two plexiform layers, which contain the synaptic connections between cell types. Developmentally, the differentiation sequence of the retina is also highly conserved with RGCs differentiating first, followed by Horizontal cells, Amacrine cells, and Cone photoreceptors, then Bipolar cells and Rod photoreceptors, and ending with the Müller glia (Goldman, 2014).

Failure during the development of the retina and its cell types can lead to a number of defects and disorders, many of which cause visual impairment or blindness. Retinitis Pigmentosa and cone-rod dystrophies are two such examples wherein the photoreceptor cells either fail to develop properly or fail to maintain themselves over time. However, not all mechanisms of retinal development are currently understood, so the genetic underpinnings of these disorders are not always identifiable.

Phototransduction is the process by which vertebrate retinas are able to convert light waves into electrical signals. When light waves enter into the eye, rhodopsin, a G-protein coupled receptor found in the outer segments of photoreceptor cells, activates (Fu, 2010). This triggers a cascade of events that activates the photoreceptor cells and causes them to become hyperpolarized and release less of the neurotransmitter glutamate (Fu, 2010). Less glutamate signals that light is present and the electrical signal is passed downstream to the bipolar cells and eventually transmitted via the ganglion cells through the optic stalk and into the brain (Fu, 2010).

The RPE, located between the retina and the choroid, is a vital structure for visual acuity, serving as a means of scattered light absorption as well as retinal nourishment and protection (Strauss, 2005; Fuhrmann et al., 2014; Graw, 2010). It is easily visible in

tissue samples at the back of the eye due to its abundance of melanin. The RPE is of neuroepithelial origin, similar to the retina and, when mature, consists of a single cell layer (Fuhrmann et al., 2014; Simó et al., 2010). The RPE is vital as it constitutes a portion of the blood-retinal barrier (BRB), forming tight junctions between RPE cells and endothelial cells in order to regulate macromolecule transport in and out of the retina (Simó et al., 2010; Graw, 2010). In addition, the RPE also functions as a waste removal system by removing the continuously shed outer discs of photoreceptor cells (Strauss, 2005; Simó et al., 2010). Specification of RPE cells during development relies on expression of *otx2, mitf,* and *Pax6*, as well as the migration of periocular mesenchyme cells, though the mechanism for this interaction remains unclear (Fuhrmann et al., 2014). Loss of RPE genes like *otx2* and *mitf* or the RPE itself can lead to microphthalmia, Coloboma, and RPE trans-differentiation into neural retina (Fuhrmann et al., 2014).

1.2.2 The Anterior Segment

The anterior segment (AS) of the eye is a broad term for the various structures of the front third of the eye residing in front of the posterior surface of the lens or the face of the anterior vitreous (**Figure 1.2**). These structures include the cornea, lens, iris, ciliary body, and iridocorneal angle. Together, these structures work to focus light onto the retina and maintain homeostasis of the eye, in particular through the regulation of intraocular pressure. To focus light, the cornea and lens work to refract light waves into the eye and onto the retina, while the iris controls the amount of light that can enter the eye through manipulation of pupil size. In regard to maintenance of the eye: the ciliary body continuously generates and deposits aqueous humor into the anterior chamber, providing

nutrients and generating intraocular pressure. Appropriate levels of pressure are maintained through the drainage networks of the iridocorneal angle, which consists of the trabecular meshwork and Schlemm's canal.

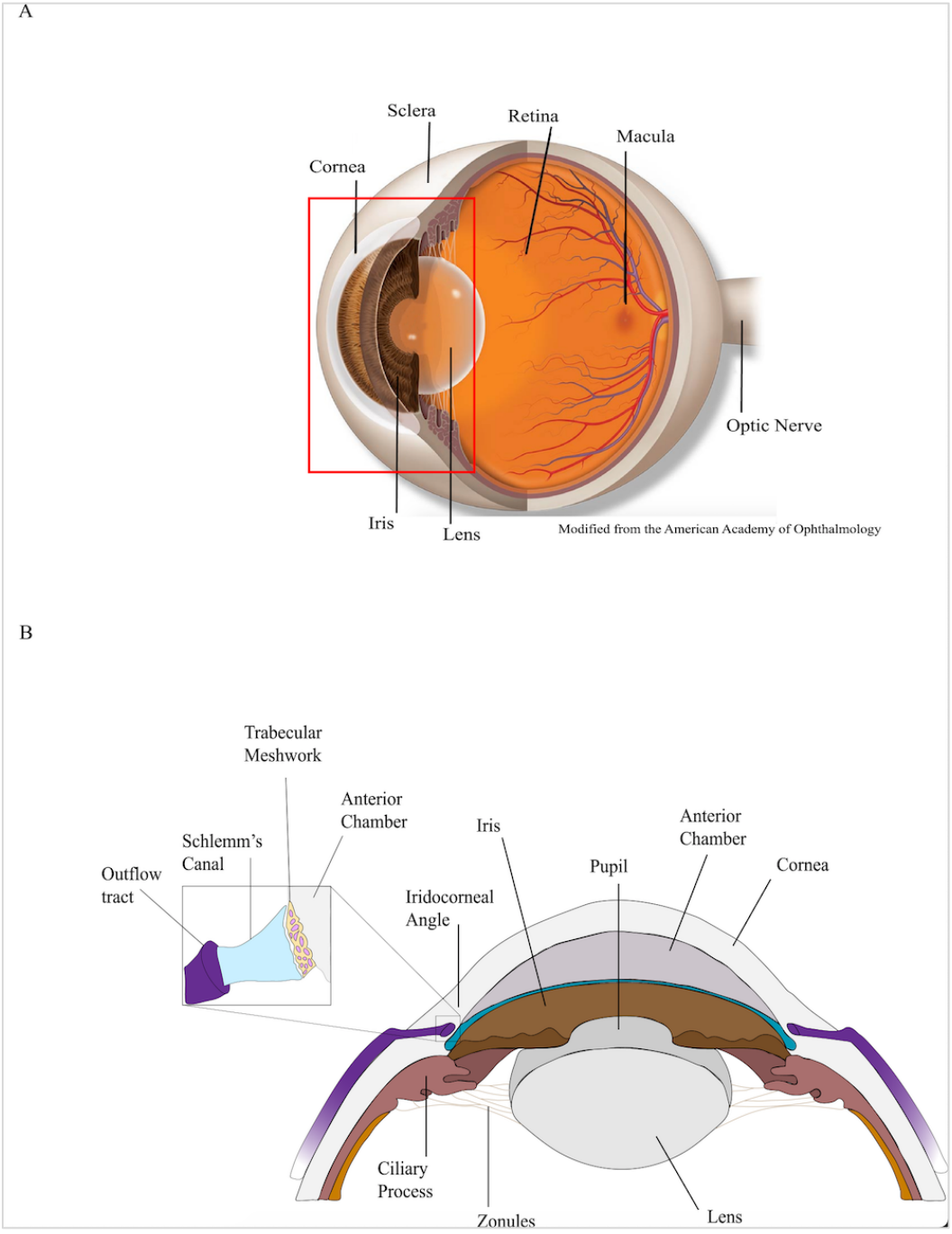

Figure 1.2: Key Structures of the Vertebrate Eye and Anterior Segment. Schematic diagrams of the mature human eye and anterior segment in cross section. **(A)** Lateral cross section of the eye as it is pointing to the left. Important structures like the cornea, lens, and retina are labeled. The anterior segment is highlighted by the red rectangle. **(B)**

Lateral cross section of the anterior segment as it is looking anteriorly. Moving distally to proximally, the first structure is the cornea, followed immediately by the negative space of the anterior chamber which houses the aqueous humor. Next is the iris and iridocorneal angle, located in the posterior of the anterior chamber. The iridocorneal angle is composed of the porous Trabecular Meshwork that filters and drains aqueous humor into Schlemm's Canal and eventually, into the bloodstream via multiple outflow tracts. Just beneath the iris sits the lens, which is manipulated by the zonules and attached to the ciliary processes on either side.

1.2.3 The Cornea

The cornea is the anterior most surface structure of the eye, providing vital protection for the eye from the outside environment and funneling light towards the retina. Concave or dome-shaped to refract light into the eye, a majority of refractive errors in vision (nearsightedness, farsightedness, astigmatism) are due to an improper curvature of the cornea (NEI). The cornea is very thin (< 1 mm at its thickest point) and completely devoid of blood vessels to maintain clear tissue layers for optimal light penetration (Graw, 2010; Gage et al., 2014). In order to get nutrients without a blood supply, a process of diffusion is utilized via both sides of the cornea. Oxygen is sourced from the outside environment, absorbed by the tear film that is always present on the outer surface, and diffused inwards to the rest of the corneal cells (Gage et al., 2014; Sridhar, 2018). Meanwhile, the inner most layers of the cornea absorb nutrients from the aqueous humor in the anterior chamber (Gage et al., 2014; Sridhar, 2018).

The cornea is divided into three main layers: the epithelium, stroma, and endothelium. These layers are formed in two main processes: 1) As a result of lens induction and 2) from the colonization of migrating cells. During lens formation, the lens will be momentarily suspended from the surface ectoderm via a lens stalk. As the lens makes its final detachment from the stalk, the surface ectoderm will fuse back together to form a new continuous layer of cells which will mature into the corneal epithelium (Cavodeassi, 2018; Fuhrmann, 2012; Soules and Link, 2005; Lang, 2004). Soon after this event, a population of neural crest-derived cells known as Periocular Mesenchyme cells (POM) will migrate into the space between the new corneal epithelium and the anterior of

the OC. These cells contribute to a remarkable number of tissues within the anterior segment, including the corneal stroma and endothelium.

The outer most layer of the cornea is the epithelium. This layer is responsible for protecting the rest of the cornea as well as the eye from the outside environment when the eye is open. Cells in this layer are of a non-keratinized stratified squamous nature, meaning that the cells are living, and must be kept moist by a continuous production of a tear film from the tear ducts (Graw, 2010; Sridhar, 2018). The epithelium averages 5-7 layers thick depending on the species. The two outermost layers are flat epithelial cells that are constantly being shed and replaced. The next 2-3 cell layers are elongated wing cells and the final layer is the basal columnar-shaped cell layer (Sridhar, 2018). This final cell layer is mitotically active and produces the new epithelial cells for the corneal surface, which is continuously replaced in humans approximately every 7-10 days (Sridhar, 2018; Graw, 2010).

The next layer immediately below the epithelium is called the corneal stroma. This is the thickest layer of the cornea, contributing 85%-90% of the total corneal thickness (Sridhar, 2018). Unlike the epithelium, the stromal layer is formed from a mixture of deposited extracellular matrix (ECM) proteins and POM cell derivatives. The first layer of the stroma is called Bowman's layer or Bowman's membrane and is a thin, acellular layer comprised of tightly compacted ECM proteins like collagen laminin, nidogen, and perlecan (Graw, 2010: Sridhar, 2018)). This layer is deposited via the epithelial cells and is thought to help the cornea maintain its shape (Sridhar, 2018). The next layer is the stroma itself, which consists of thickly woven collagen fibrils (predominately type I) and cells including keratocytes and fibroblasts (Graw, 2010). Collagen fibers have a lamellar

structure that runs parallel to the corneal surface allowing for compaction of lamella, strength of the stromal layer, and transparency of the cornea (Sridhar, 2018). Keratocytes in the stroma stay in the G0 phase which allows them to replicate and differentiate in response to wounds if necessary (Graw, 2010). These cells are involved in maintaining the ECM in the stroma by synthesizing new collagens and matrix metalloproteinases (MMPs), keeping the stromal components in balance (Sridhar, 2018). Both the keratocytes and the fibroblasts derive from the migratory POM cells. The final layer of the stroma is called Descemet's membrane. This acellular membrane serves as another basement membrane layer similar to Bowman's layer and is mostly composed of collagens and laminins. This layer is produced by the endothelial cells below it.

The final layer of the cornea is the corneal endothelium, a monolayer that separates the cornea from the anterior chamber. These squamous cells are needed to exchange nutrients between the corneal layers and the aqueous humor. Another major function of the endothelium is to prevent fluid flow up into the stroma using a combination of tight junctions and $Na^+ K^+$ ATPase pumps (Graw, 2010; Sridhar, 2018). This cell layer cannot regenerate and often thins out with age.

Directly behind the layers of the cornea and in front of the iris lies the anterior chamber. This fluid-filled cavity holds the aqueous humor, a clear gel-like fluid that provides nutrients to the several tissues of the AS and maintains the intraocular pressure of the eye (Graw, 2010; Sridhar, 2018; Borges-Giampani and Giampani Jr, 2013). Proper intraocular pressure is vital for the overall spherical shape of the eye and firmness of the cornea (Sridhar, 2018). The thickness of the anterior chamber can often be seen using slit lamp microscopy and its overall depth can be used as an indicator for glaucoma risk.

1.2.4 The Lens

Located immediately posterior to the iris directly below the pupil, this transparent structure is responsible for our ability to focus on objects near or far. The lens adjusts its shape via muscles from the ciliary body in order to accurately refract light onto the retina, a process known as accommodation (Lang, 2004). It is an oblong structure with a flattened anterior surface and a more rounded posterior that is held in place by zonule fibers that attach it to the ciliary body (Graw, 2010). Its transparent nature is vital to its function, with any clouding or opaqueness blurring vision. Like the cornea, the lens does not contain vasculature and therefore is deprived of the nutrients it requires. Instead, the lens uses diffusion to extract necessary resources from the aqueous humor and vitreous humor that surrounds it (Graw, 2010; Lang, 2004; Fuhrmann, 2012).

There are three distinct layers to the lens: the lens capsule, lens epithelium, and lens fibers. The outermost layer is the lens capsule, which is a transparent basement membrane made predominantly of collagen (Graw, 2010). This layer protects the lens and helps it to maintain its shape when not actively focusing. This layer is generated by the layer immediately below it: the lens epithelium. This middle layer contains the only mitotically active cells in the lens and is important for generating not only the capsule layer, but also the lens fibers themselves (Graw, 2010; Lang, 2004). Additionally, the epithelium is the active diffusion layer, working to maintain the environment and regulate nutrients for the fiber cells. It is found only on the anterior and lateral regions of the lens, not the posterior (Graw, 2010). The final, inner most layer of the lens makes up the bulk of the lens itself: the lens fibers. These are elongated, transparent cells packed tightly within the center of the lens (Graw, 2010; Lang, 2004). They are generated by the

epithelium layer and stretch anteriorly to posteriorly. New fiber cells are generated at the equator of the lens and pushed inwards, meaning that the youngest fiber cells are on the periphery of the lens, while the oldest ones are located towards the center (Graw, 2010). As these cells mature, they lose both their nuclei and their mitochondria (Graw, 2010; Lang, 2004). The process of new lens fiber production continues throughout life.

The lens, while located within the anterior segment does not, at least in some part, originate from migratory POM cells. All other structures in the anterior segment have some components differentiated from the POM. However, the lens develops exclusively from the surface ectoderm. When the OV comes into proximity to the surface ectoderm, it induces a thickening of the surface ectoderm into the lens placode, which will then invaginate. During invagination, the surface ectoderm will knit back together above the hollow lens vesicle and, after detachment of the lens vesicle, will form the corneal epithelium (Cavodeassi, 2018; Fuhrmann, 2012; Soules and Link, 2005; Lang, 2004). After vesicle formation, lens cells in the posterior of the lens (closest to retina) begin to elongate to form the first lens fibers (Graw, 2010; Lang, 2004). Meanwhile, the cells in the anterior will begin to differentiate into lens epithelium cells. After this initial elongation, new fiber cells will grow out from the epithelium and surround the original fibers.

1.2.5 The Iris

The iris is the pigmented portion at the center of the eye and is crucial for light control. Structurally, it is located at the posterior edge of the anterior chamber and the anterior edge of the OC just above the neural retina. The iris is critical for vision as it

dictates the amount of light allowed to reach the retina via the pupil. The pupil is nothing more than a hole in the center of the iris. The inner edge of the iris that surrounds the pupil is known as the pupillary zone and expands or contracts relative to the amount of light in the surrounding environment (Davis-Silbermann and Ashery-Padan, 2008; Cvekl and Tamm, 2004). The outer rim of the iris, known as the ciliary zone, is rigid and does not change size. Furthermore, the ciliary zone is responsible for anchoring the iris to the sclera and ciliary body (Davis-Silbermann and Ashery-Padan, 2008).

Similar to the cornea, the iris can be broken up into distinct layers: the stroma and the iris pigmented epithelium (IPE). These layers, again like the cornea, come from two different cell sources as well. Following the formation of the OC and the breaking off of the lens vesicle from the surface ectoderm, the anterior edges of the OC begin to undergo a change. The bi-layered edges of the OC, often referred to as the OC margins, begin to proliferate and extend themselves inward towards the newly established lens (Graw, 2010; Davis-Silberman and Ashery-Padan, 2008; Cvekl and Tamm, 2004). These cells will establish the base of the iris in the form of the IPE. Concurrently, POM cells begin to migrate into this area between the corneal epithelium and the lens. While the mechanism remains unclear, it is believed that some of these POM cells will differentiate into the fibroblasts and melanocytes of the iris stroma (Graw, 2010; Cvekl and Tamm, 2004).

The most anterior layer of the iris (in contact with the anterior chamber) is the stroma. This layer contains the cells, connective fibers, blood vessels, and muscles of the iris (Graw, 2010; Cvekl and Tamm, 2004). Two involuntary muscles work together to adjust pupil size. The circular sphincter pupillae contracts to shrink the pupil, while the dilator pupillae pull the iris outward to increase light onto the retina (Davis-Silberman

and Ashery-Padan, 2008). The second layer of the iris is the IPE layer, which is found posterior to the stroma. It is 2 cells thick and contains the majority of the melanin that determines eye color (Davis-Silberman and Ashery-Padan, 2008). The IPE is the root of the iris that is continuous with the ciliary body and anchors it in place. The pigmentation of the IPE is vital for blocking light waves from reaching the retina through the iris itself, instead restricting its path to the pupil alone. While the pigmentation of the iris is found mostly in the IPE, individuals with darker colored eyes often have some melanin in their iris stroma as well.

1.2.6 The Ciliary Body

The ciliary body resides in the posterior chamber of the AS, between the anterior most portion of the lens and posterior edge of the iris. The ciliary body is a structure providing a number of functions for vision and eye homeostasis, chief among them being accommodation or focusing of the lens and aqueous humor production (Graw, 2010). The two main structures of the ciliary body include the ciliary muscles and the ciliary processes.

The ciliary processes, found in the anterior region of the ciliary body, is where the aqueous humor is produced. These processes are a number of large and small sized finger-like projections that push out into the posterior chamber. The various sizes and large number of projections are necessary to create a large surface area for optimal aqueous humor production (Cvekl and Tamm, 2004; Borges-Giampani and Giampani Jr., 2013). Each of the projections contain two epithelial layers, a thin stroma, and a blood vessel. The outer epithelial layer is composed of non-pigmented columnar cells, is

continuous with the neural retina, and is in contact with the aqueous humor in the posterior chamber (Borges-Giampani and Giampani Jr., 2013). The inner epithelial layer is a pigmented cuboidal cell layer that is continuous with the RPE and iris and is separated from the stroma by a thin layer of basement membrane proteins. The epithelial layers together are only two-cells thick. The stromal layer is thin, surrounds the vasculature, and contains a large amount of connective tissues for permeability (Borges-Giampani and Giampani Jr., 2013).

The ciliary processes produce the aqueous humor, a thin and transparent fluid crucial for eye health. It is responsible for nourishing the avascular components of the anterior segment and works to maintain the spherical shape of the eye (Cvekl and Tamm, 2004; Graw, 2010). It is composed of mostly water but carries vital nutrients like glucose and amino acids to the cornea and other structures (Graw, 2010). Once produced, the aqueous humor flows out of the processes, through the posterior chamber, and up through the pupil into the anterior chamber. The fluid will eventually be drained out of the anterior chamber via the iridocorneal angle. Importantly, the ciliary processes have the same developmental origins as the iris (Cvekl and Tamm, 2004; Graw, 2010). The epithelium of the processes is formed by proliferation and extension of the OC margin, while the stroma is likely formed from differentiated POM cells that migrated into the area.

The posterior portion of the ciliary body contains the ciliary muscles. There are two main muscles that make up this collection: the longitudinal and circular muscles. The longitudinal muscle is the most external muscle, attaching to the trabecular meshwork of the iridocorneal angle and sclera, and is used to open the drainage of the angle (Borges-

Giampani and Giampani Jr., 2013). The circular fiber muscle is an anterior muscle that works to focus the lens by delicately adjusting its thickness or curvature. This is also the position in the Ciliary Body where the Zonular fibers attach (Borges-Giampani and Giampani Jr., 2013). These fibers are what anchors the lens in its proper position.

1.2.7 The Iridocorneal Angle

The iridocorneal angle is a crucial set of tissues vital for maintaining homeostasis of the inner eye by continuously draining the aqueous humor from the anterior chamber and controlling intraocular pressure. Without the outflow tract provided by the angle, aqueous humor would not be able to drain out of the anterior chamber. The increase in fluid would cause an increase in intraocular pressure, damaging the sensitive cells of the optic nerve and retina in a disorder called glaucoma (Goel, 2010; Gould et al., 2004; Rausch et al., 2018). The angle is located at the point where the edge of Descemet's membrane or the corneal endothelium and the outer edge of the iris meet on the periphery of the eye (Sridhar, 2018; Abu-Hassan, 2014). This placement is ideal as it creates a funnel like shape that allows the aqueous to drain from the anterior chamber. The iridocorneal angle is the last of the AS tissues to fully develop (Stamer and Clark, 2017; Abu-Hassan et al., 2014). In both mice and zebrafish, the foundation of the angle is established during embryonic stages, but its full maturation continues postnatally in mice and has been documented to continue for up to 30 days post fertilization in zebrafish (Raush et al., 2018; Soules and Link, 2005). There are two main structures within the drainage network: the trabecular meshwork (TM) and Schlemm's Canal (SC).

The TM functions as a porous filtration system for the aqueous humor as it flows out of the anterior chamber. This filtration not only provides resistance and prevents a rapid drainage for the aqueous humor, but it also works to systemically trap any debris in the fluid that may block the canal and remove it (Abu-Hassan et al., 2014). The complex tissue of the meshwork is derived once again from the POM cells that migrate into the anterior area between the lens and the corneal epithelium. However, the mechanism that drives the POM into TM cells remains elusive. Invading cells somehow begin to separate, elongate, and form into tube or beam-like structures, the defining characteristics of the meshwork (Rausch et al., 2018; Abu-Hassan et al., 2014; Gould et al., 2004). These flattened cells are separated by very small openings that are partially filled by ECM. After birth in most vertebrates, the trabecular meshwork matures by remodeling these small openings into larger intertrabecular spaces, thus generating a thick, porous tissue through which the aqueous humor can flow (Abu-Hassan et al., 2014). The TM also contains smooth muscle cells for contraction and increased drainage when necessary.

The TM is composed of 3 unique layers: the uveal meshwork, the corneoscleral meshwork, and the juxtacanalicular region. The first, the uveal meshwork, is the first layer located at the opening of the angle at the edge of the anterior chamber. It is comprised of 3 layers of connective tissue arranged in a crossing beam-like pattern with each beam being encased in flattened TM cells (Stamer and Clark, 2017; Rausch et al., 2018; Goel, 2010). This pattern leaves a patchwork of intratrabecular spaces between the beams, allowing fluid to flow through without much resistance. The beams are composed of ECM components like collagen, laminin, fibronectin, and elastin (Rausch, et al., 2018). The cells of this layer are highly phagocytic, indicating that they easily trap and

remove debris from the extracellular space (Abu-Hassan et al., 2014). The next layer, the corneoscleral layer, has a similar connective tissue, beam-like pattern to it. However, this layer is much thicker, 8-15 layers thick, and becomes more restrictive as you progress deeper into the layer with the intratrabecular spaces becoming tighter and tighter (Goel, 2010; Stamer and Clark, 2017). This serves to catch smaller debris artifacts that may have been missed by the more superficial layers above. The final layer, the juxtacanalicular region, is very thin and sits just above the opening of Schlemm's canal. This tissue is the most resistant to the aqueous humor as it is made up of irregularly shaped cells loosely connected to one another over a randomized ECM (Abu-Hassan et al., 2014; Goel, 2010; Stamer and Clark, 2017). This serves as the final filter to the fluid. Furthermore, the ECM of the Juxtacanalicular region forms tight junctions with the endothelial cells of the SC, thus allowing for a sealed pathway for the fluid into the canal (Goel, 2010).

While the porous TM filters the aqueous fluid, Schlemm's canal leads it from the eye out to the blood vessels for reabsorption. This canal is a large endothelial-lined tube covered by the TM at one end and emptying into the blood stream at the other via the episcleral blood vessels (Goel, 2010). SC itself never carries blood though, existing purely for aqueous humor. While Schlemm's canal is important for the overall drainage network, unlike the TM, it is not believed to be of POM cell origin. Instead, it is created from endothelial cells and vasculature remodeling within the corneoscleral transition area below the influence of migrating POM (Abu-Hassan et al., 2014; Goel, 2010).

1.3 The Neural Crest

1.3.1 Evolutionary Origins of the Neural Crest Cells

One of the great mysteries of the anterior segment lies in the complex dynamics of its beginnings. The exact molecular mechanisms and cellular relationships that allow for the development of these structures are poorly understood. However, Neural Crest Cells (NCCs) play a key role as the cell type of origin for POM derivatives and therefore, the AS. The evolutionary development of NCCs was pivotal to the divergence of vertebrates from invertebrates. Vertebrates have hinged jaws, larger brains, and expanded sense organs when compared to other chordates (Creuzet et al., 2005; Simões-Costa and Bronner, 2015). This is largely due to the evolution of the NCC, a multipotent and highly migratory stem cell-like embryonic cell population. This particular cell population is thought to have evolved approximately 450-550 million years ago in sync with the "new head" theory of vertebrate development hypothesized by Gans and Northcutt and focusing on the development of the hinged jaw and predation behaviors (Martik et al., 2019; Meulemans Medeiros, 2013). The NC itself, first characterized in 1868 in the chick, was quickly identified as a key source for derivatives for much of the peripheral nervous system and facial skeleton structures (Bronner and LeDouarin, 2012). With the advent of transplantation experiments to generate chick/quail chimeras and various labeling techniques, it became possible to mark NCCs and track them throughout the vertebrate body, allowing our understanding of NCC contributions to greatly expand to include further cell derivatives, as well as migration behaviors, cellular interactions, and possible defects (Bronner and LeDouarin, 2012).

The importance of the NCCs to the evolution, function, and development of vertebrates remains an extensive field of study amongst biologists. Sometimes referred to as the "fourth germ layer," NCCs are critical to the development of the vertebrate head structure as well as numerous other features throughout the body (Hall, 2000). Mechanical mechanisms and behaviors of these cells continue to be elusive, and the NC remains a large field of interest in the scientific community.

1.3.2 Characteristics of Neural Crest Subgroups

The highly migratory and multipotent nature of the neural crest (NC) and their importance to the development of key vertebrate features cannot be understated. Being such a complex population of cells as the NC is, they can be furthered divided into smaller subpopulations with distinct genetic makeups, differentiation abilities, and migratory behaviors. The populations of NC can be distinguished based on their location of origin along the anterior-posterior axis of the neural tube. These groups consist of cranial, cardiac, vagal, and trunk subtypes (Bronner and LeDouarin, 2012; Noisa and Raivio, 2014; Abzhanov et al, 2003; Snider et al.,2007; Zhang et al., 2014). All cells that migrate out from the neural tube can be classified as NC, however, each subtype of NC has specific capabilities and unique transcriptomic profiles. For example, not every NCC throughout the developing embryo has the same differentiation capabilities as the others (Le Douarin and Teillet, 1974). Cranial NCCs (cNCCs), when transplanted from the head into the trunk of an embryo, can differentiate into all necessary subtypes needed. However, when trunk NCCs are likewise transplanted into the head region, they are incapable of creating all necessary derivatives typically produced by cNCCs, specifically

cartilage and bone (Le Douarin and Teillet, 1974). While some NC derivatives are specific to certain subtypes of NC, others are not. All NCCs are capable of differentiating into melanocytes (pigment cells) and peripheral glia cells (Noisa and Raivio, 2014; Bronner and LeDouarin, 2012).

The most anterior population of NCCs is the cranial NC (cNC). This population is one of the most extensively studied populations as it gives rise to the most diverse cell types and is associated with the most congenital defects. cNC differentiates into facial skeleton, facial cartilage, glia cells, neurons of the sensory ganglia, pharyngeal arches which in turn give rise to the jaw and hyoid support, connective tissues, bones of the semicircular canal, dental components, ocular muscles, and portions of the ocular anterior segment (Cordero et al., 2011; Zhang et al., 2014; Trainor and Tam, 1995; Bronner and LeDouarin, 2012). cNCCs typically originate in the sections of the neural tube corresponding to the forebrain, midbrain, and first pharyngeal arches. For instance, cells that contribute to the frontonasal process and periocular regions will be sourced from the forebrain and parts of the midbrain (Williams and Bohnsack, 2015; Langenberg et al., 2008; Cordero et al., 2011). As the most diverse NC subtype, cNC have the largest differentiation capabilities and, in the early stages, are capable of reversing their fates between mesenchymal and neuronal fates in transplantation experiments (Mayor and Theveneau, 2013; Simões-Costa and Bronner, 2015; Abzhanov et al., 2003). However, approximately 24 hours after the onset of migration, cNCCs do become committed to their fates in chick models (Mayor and Theveneau, 2013; Simões-Costa and Bronner, 2015; Abzhanov et al., 2003).

Moving posteriorly from the head, the next subtype of NC is the cardiac NC. As their name implies, cardiac NC give rise to specific portions of the cardiac system. These structures include the cardiac outflow tract (forms cardiac ganglia and aorticopulmonary septation complex), the proximal outflow tract (closure of the ventricular outflow septum), and ectomesenchyme (create the asymmetric arteries of the thorax) (Kirby and Hutson, 2010; Snider et al., 2007). These cells originate from rhombomeres 6-8 in the neural tube before traveling through the posterior pharyngeal arches and into the cardiac muscle (Kirby and Hutson, 2010; Snider et al., 2007).

The vagal NC and trunk neural crest both originate from the posterior half of the embryo (Noisa and Raivio, 2014; Abzhanov et al., 2003). The vagal NC gives rise to the enteric glia of the digestive tract, allowing for regulation and movement of nutrients and waste through the large intestine. The trunk NC originates from the same area of the neural tube, but these NCs will differentiate into the dorsal root and sympathetic ganglia of the peripheral nervous system, as well as pigment cells and fins in relevant species (Noisa and Raivio, 2014; Kulesa et al., 2003; Abzhanov et al., 2003). Following migration, NCCs of all subgroups will begin or continue on their differentiation path based on signaling cues from their environment as well as neighboring cells.

1.3.3 Neural Tube Closure and EMT

The process of NC formation begins at neurulation in the developing vertebrate embryo. After gastrulation, a rod-like structure derived from cells of the primitive node called the notochord has developed along the anterior-posterior axis of the embryo (Copp et al., 2003). This rod induces the formation of the neural plate from ectoderm directly

above it. Between the peripheral edges of the neural plate and the epidermal ectoderm lies the neural plate border region, the cells of which are NC progenitor cells induced by BMP, as well as increased levels of Wnt, FGF, and RA (Mayor and Theveneau, 2013) (**Figure 1.3 A**). These various inductive morphogen signals originate from the neural ectoderm, epidermal ectoderm, and the paraxial mesoderm in some species (Simões-Costa and Bronner, 2015; Zhang et al., 2014; Mayor and Theveneau, 2013; Noisa and Raivio, 2014). In a process called primary neurulation the neural plate bends toward the notochord and folds the neural plate border regions upward, converging the two edges together at the newly established dorsal aspect of the neural tube (Simões-Costa and Bronner, 2015; Mayor and Theveneau, 2013; Bronner and LeDouarin, 2012; Zhang et al., 2014) (**Figure 1.3 B**). As this folding process is occurring, the cells within the neural plate border region specify into a more defined NCC identity through the expression of key transcription factors such as *Foxd3* and *Sox10* (Simões-Costa and Bronner, 2015; Zhang et al., 2014; Bronner and LeDouarin, 2012).

With the morphological movements of neural tube completed, the NCCs are located between the dorsal edge of the neural tube and the epidermal ectoderm layer. It is here, where they will undergo a rapid cellular change which will give them their hallmark feature of high motility: the epithelial-to-mesenchymal transition (EMT). This cellular process allows the NCCs to break their cellular connections to one another in the epithelial sheet, delaminate, and assume a mesenchymal cellular identity (Clay and Halloran, 2010; Theveneau and Mayor, 2012; Scarpa et al., 2015; Simões-Costa, 2015). Within the epithelial sheet, NCCs are attached to one another via E-cadherin at adherens junctions which must be broken down by downregulating cadherins (Scarp et al., 2015;

Theveneau and Mayor, 2012) (**Figure 1.3 C**). In addition to complete downregulation of E-cadherin, N-cadherin and cadherin-6B are also downregulated, while cadherin-7 is induced under the control of *snail1/2* (Cordero et al., 2011; Theveneau and Mayor, 2012; Clay and Halloran, 2010; Scarpa et al., 2015). While the various junctions and adhesion complexes are being disassembled, the cells must also lose their apico-basal polarity, assume a more rounded "blob-like" morphology, and create gap junctions between cells (Clay and Halloran, 2010; Mayor and Etienne-Manneville, 2016). Once separated from one another, the cells extend bleb protrusions towards the outer edge of the neural tube and promptly exit (Clay and Halloran, 2010). When they leave the neural tube, NCCs will switch from bleb protrusions to F-actin-based filopodia and lamellipodia as they begin targeted migration (Clay and Halloran, 2010; Scarpa et al., 2015). While some NCCs may immediately make the switch from exit-based migration to targeted migration, other cells may delay their migration for up to an hour after exiting (Clay and Halloran, 2010). With the completion of the EMT, NCCs now possess their full capabilities.

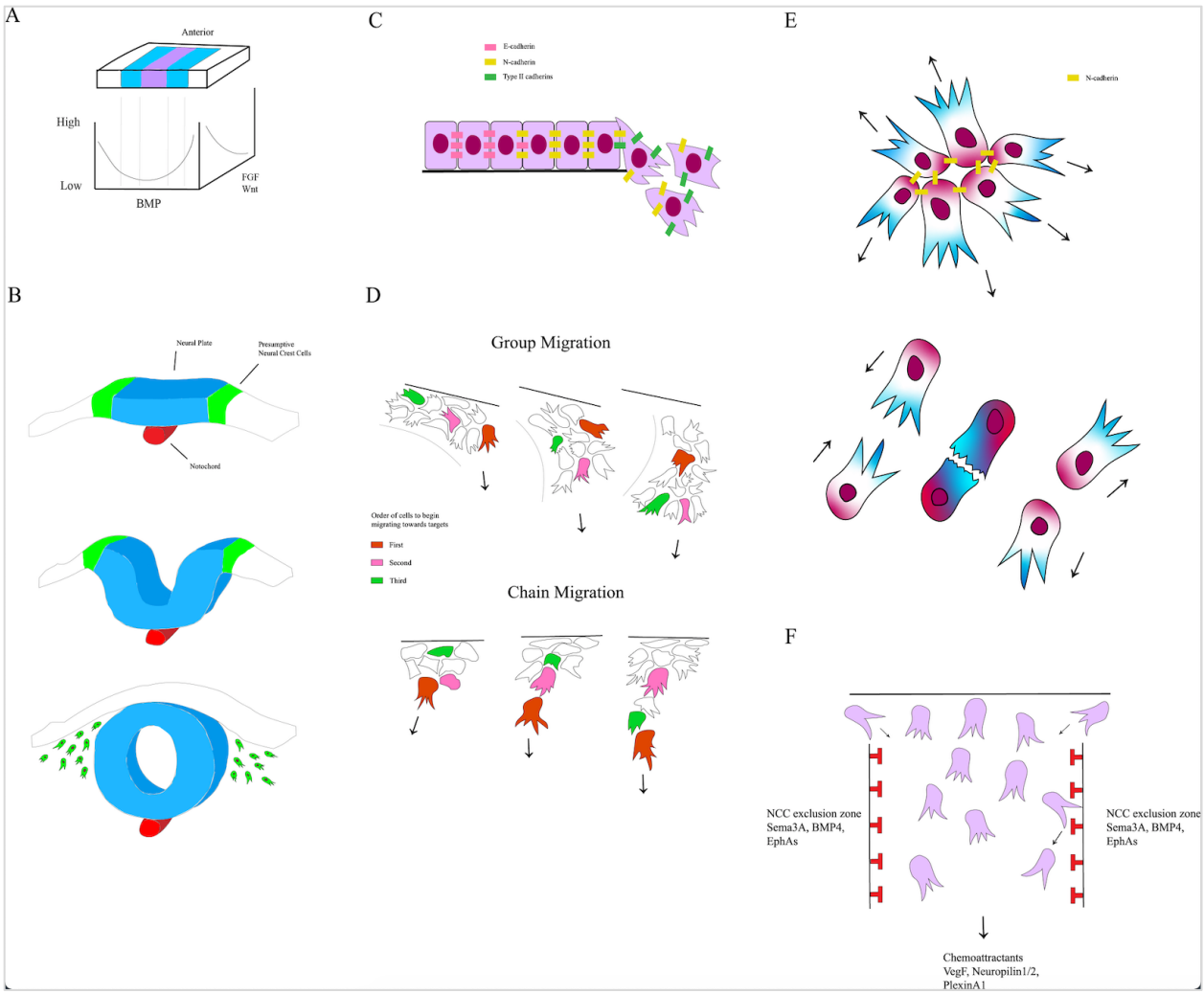

Figure 1.3: Neural Crest Cell Origins and Characteristics. (A) Neural crest cells are induced along the borders of the neural plate by moderate levels of BMP and high FGF and Wnt, resulting in the activation of a series of transcription factors like Sox10, Snail2, and Foxd3. **(B)** As the neural plate (blue) folds the neural plate border regions (green) come together at the anterior of the tube just below the surface ectoderm. The cells of the presumptive neural crest in the border regions will undergo an epithelial-to-mesenchymal transition (EMT), losing their epithelial connections to one another and becoming independent migratory cells. **(C)** During EMT, cells that are tightly connected within an epithelial sheet by E-cadherins will begin to undergo a large-scale change in cell

adhesion, eventually leading to the loss of cell connections and freely migrating cells. **(D)** Neural crest cells are known to have differing migratory behaviors depending on their place of origin within the neural tube. With cranial neural crest, cells migrate collectively within a group towards the target, with no leader cells, no defined hierarchy, and constant cell rearrangement. Cells each possess their own independent migratory capabilities and are not influenced by the cells around them. Trunk neural crest cells, however, move via chain migration, with defined leader and follower cells, with the entire chain ceasing to migrate when the leader cell is no longer functional. **(E)** Neural crest cells migrate away from one another via contact-inhibition of locomotion generated by cell polarization of one another on contact. Neural crest cells express Rac1 (blue) in their leading edges and RhoA (red) in their trailing edges. When two cells come into contact with one another, they collapse filopodia in the leading edge and repolarize themselves to express RhoA at the site of contact and Rac1 leading away from the site of contact, resulting in cell dispersal. **(F)** NCCs are directed towards their targets by positive and negative signals within their environments. Positive signals like Vegf and neuropilins lead NCCs to their target areas while negative signals like Sema3A and EphAs prevent NCCs from entering into neighboring neural crest streams or off-target areas.

1.3.4 The Neural Crest Gene Regulatory Network

The genetic control of induction and specification of NCC pathways is a complex and widely studied field made all the more difficult by the sheer number of genes involved. The NC has been studied in a large number of different organisms, the data from which has been summarized in a vast system of connecting genes known as the Gene Regulatory Network (GRN). The cranial neural crest cell network (cNCC GRN) is the most studied and highly conserved network and will be the focus of this discussion. The GRN can be summarized in four distinct, but heavily intertwined sections: inductive signals, neural plate border specifier genes, neural crest specifier genes, and finally neural crest migration. Each new iteration within the GRN network allows the cells to undergo extensive and radical changes to their regulation and specification.

The network begins at the induction of the presumptive NCCs in the neural plate border region. Extracellular signals from the neural ectoderm and non-neural ectoderm such as Wnts, FGFs, and BMPs form gradients within and around the neural plate, activating transcription factors and pathways at the border region, priming the cells for a NCC fate (Bronner and LeDouarin, 2012; Simões-Costa and Bronner, 2015; Mayor and Theveneau, 2013). This competence (the second phase of the cNC GRN known as the neural plate border specification genes) is achieved through the activation of genes such as *Msx1, Zic1, Dlx5/6, Tfap2a*, and *Pax3/7* (Bronner and LeDouarin, 2012; Simões-Costa and Bronner, 2015; Mayor and Theveneau, 2013; Hoffman et al., 2007). These genes are expressed in a broad section of the neural plate and surrounding tissues, and only where the expression of these genes overlap are the progenitor NCCs established in the border region (Bronner and LeDouarin, 2012; Simões-Costa and Bronner, 2015). Current

research indicates that these transcription factors are upstream activators of neural crest specifier genes, such as *Msx1* which induces expression of *Foxd3* (Simões-Costa and Bronner, 2015). The next stage of refinement (the neural crest specifiers) involves the coordination of both the genes of the border specification phase and the extracellular morphogens of the inductive phase. Genes turned on at the specification of cNCCs include *cMyc, Foxd3, Ets-1, Twist, Sox8/9/10, AP2α,* and *Snail1/2* (Bronner and LeDouarin, 2012; Simões-Costa and Bronner, 2015; Mayor and Theveneau, 2013; Zhang et al., 2014). While not all are activated simultaneously, these genes help to give NCCs their identity by maintaining a multipotent state, controlling proliferation, migration, and survival through regulation of cell adhesion and motility, and initiating EMT and delamination (Bronner and LeDouarin, 2012; Simões-Costa and Bronner, 2015; Mayor and Theveneau, 2013; Noisa and Raivio, 2014; Zhang et al., 2014). Many of these genes continue to be active throughout migration until cellular differentiation into specific derivatives, while also controlling a number of lineages derived from the NC. Furthermore, there is growing evidence of feedback loops within the GRN, especially within the neural crest specifier subnetwork, indicating continuous activation throughout induction and migration (Simões-Costa and Bronner, 2015). The expansive network of the cNC GRN continues to be studied to this day.

1.3.5 Cellular Migration and Communication

With the completion of the EMT, NCCs now possess the necessary genetic identities and migratory capabilities to begin to spread throughout the developing organism. The ability of the NC to migrate is one of their greatest features, as they travel the farthest

distances out of almost all other cells in the developing embryo (Simões-Costa and Bronner., 2015). The exact timing of migration initiation is dependent upon the species. In mice for instance, NCC migration begins around the 4-5 somite stage in the rostral hindbrain (Trainor and Tam, 1995). In zebrafish, migration of NCCs in the cranial regions begins between 12 and 14hpf (Klymkowsky et al., 2010). The process of migration is complex, with key differences seen between each of the different NC subtypes, but can be broken into two main categories: the long, single file chain migration of trunk NC or the randomized, large group migration of cNC (Clay and Halloran, 2010; Theveneau and Mayor, 2012; Kulesa et al., 2010; Richardson et al., 2018; Mayor and Etienne-Manneville, 2016).

Trunk NC cells follow distinct paths from their points of origin to their targets, migrating in a chain like fashion where cells with full migratory capabilities are called Leader cells and those who must rely on Leader cells to travel to their targets are called Follower cells. Migratory identities are established in trunk NC during the early neural crest specification phase of the GRN, prior to complete closure of the neural tube and delamination (Cordero et al., 2011; Abzhanov et al., 2003). After the completion of EMT, Leader cells become polarized and begin to migrate towards their targets, remaining at the front position of the chain for the entirety of the migration process (Jesuthasan, 1996; Richardson et al., 2016; Mayor and Etienne-Manneville, 2016) (**Figure 1.3 D**). Follower cells, however, do not possess the same capabilities as Leader cells and are incapable of migrating on their own. Instead, Follower cells, arrange themselves in a single file line behind the Leader cells, receiving directions from the Leader cells using cell-to-cell contact via filopodia (Jesuthasan, 1996; Cordero et al., 2011; Richardson et al., 2016).

Because no Follower cells have independent migratory abilities and they must extend filopodia to the Leader cell, they cannot receive signals from fellow Follower cells. Ablation of the Leader cell during chain migration will halt the progress of the entire chain of NCCs (Richardson et al., 2016; Cordero et al., 2011). The Follower cells of the chain will retain their cell motility, but they are unable to adopt a Leader cell identity to restart the migration process and will remain at the site of ablation.

cNCCs have no Leader/Follower cell identities established for their migration. Instead, all cells within the group migrate collectively, each possessing the same independent migratory capabilities and behaviors as the others with no regard to the origination of the cell or the sequence of delamination from the neural tube (Clay and Halloran, 2010; Kulesa et al., 2010; Cordero et al., 2011; Theveneau and Mayor, 2012; Richardson et al., 2016). The group will, together, target to the same general location, but the cells within the groups will migrate randomly within it (Richardson et al., 2016; Clay and Halloran, 2010; Cordero et al., 2011) (**Figure 1.3 D**). Similar to trunk NCCs, cNCCs will use filopodia to communicate with each other during the migration process, sometimes drastically changing their direction within the group (Cordero et al., 2011; Teddy and Kulesa, 2004). This stochastic manner of mobility means that cells located at the leading edge of the group are constantly turning over and being replaced by other cells (Clay and Halloran, 2010; Mayor and Etienne-Manneville, 2016). Additionally, ablation of the leading edge of this group will not hinder the migration of the rest of the cells (Richardson et al., 2016).

Despite differences in the overall migration behaviors of different subtypes of NCC, similarities in migration also exist. For instance, all NCCs use ECM components,

such as laminin and fibronectin as a secure footing during the migration process (Cordero et al., 2011; Kulesa et al., 2003; Carmona-Fontaine et al., 2008). After acquiring mesenchymal properties following EMT, NCCs must become polarized to begin migration. This most often starts through a process known as Contact-inhibition of locomotion (CIL), which allows the cells to disperse away from one another on contact, thus preventing overcrowding in an area (Clay and Halloran, 2010; Kulesa et al., 2010; Carmona-Fontaine et al., 2008; Maj et al., 2016; Scarpa et al., 2015; Teddy and Kulesa, 2004) (**Figure 1.3 E**). This is controlled via a cascade known as non-canonical Wnt planar cell polarity (PCP). In amphibians, birds, and fish, once the N-cadherin is broken and delamination at the dorsal edge of the neural tube occurs, cells are often within close proximity to one another. When cells come into contact with one another, the PCP pathway is activated and RhoA is upregulated at the point of contact (Clay and Halloran, 2010; Mayor and Theveneau, 2013; Carmona-Fontaine et al., 2008; Scarpa et al., 2015). This activation of RhoA in the area of upregulation causes any cellular protrusions in the area to collapse, halting migration in that area and preventing further cellular contact. Simultaneously, the PCP pathway also upregulates Rac1 on the side of the cell opposing the active area of RhoA (Clay and Halloran, 2010; Kulesa et al., 2010; Mayor and Theveneau, 2013; Carmona-Fontaine, 2008; Scarpa et al., 2015). Activation of Rac1 stimulates the cell to mobilize F-actin to create filopodia and lamellipodia in the opposing area, creating a leading edge of the cell that will actively pull the cell away from the previous point of contact (Clay and Halloran, 2010; Kulesa et al., 2010; Mayor and Theveneau, 2013; Teddy and Kulesa, 2004). This pathway provides clear evidence that migratory cells can change direction upon interactions with other NCCs in their

immediate vicinity indicating a fine-tuned mechanism for ordered and directed migration. However, cells also receive migratory signals from their environment which greatly influences their behaviors and targeting.

All varieties of NCCs migrate through very distinct paths, or streams, using strong communication amongst themselves, as well as their surrounding environment. These streams are designed to segregate groups of NCCs from one another, with each group being targeted to a specific area of the developing organism. For example, cells originating from the anterior forebrain and parts of the midbrain are all targeted to the nasal process and periocular regions (Williams and Bohnsack, 2015; Langenberg et al., 2008). Signaling molecules within the environment that NCCs will travel through are designed to prevent different streams of cells from intermingling with one another. These signals may include substrate binding, chemotactic, and cell-to-cell interactions (Kulesa et al., 2010; Kulesa et al., 2003; Yu and Moens, 2005; Theveneua and Mayor, 2012; Clay and Halloran, 2010). NCCs in the hindbrain migrate in streams based on their positions along the rhombomeres, or specific sections of the neural tube, while actively avoiding other rhombomeres (Casazza et al., 2007; Clay and Halloran, 2010). In birds and mice, it has been shown that NCCs migrate from rhombomeres 2, 4, and 6 with distinct NCC free zones located in rhombomeres 3 and 5 (Casazza et al, 2007; Yu and Moens, 2005; Kulesa et al., 2010; Teddy and Kulesa, 2004; Clay and Halloran, 2010; Kulesa et al., 2003). Cells that originate in these two rhombomeres will, upon initiating their migration and encountering negative signals, quickly move rostrally or caudally to join a neighboring stream. There may also be some evidence of apoptosis in these rhombomeres in some species (Kulesa et al., 2010; Casazza et al., 2008; Yu and Moens, 2005).

These streams of NCCs are able to segregate themselves based on cues in their immediate environment. While it is not known just how many different signals NCCs may be responsive too, there are several cues that have been well documented in the cNC and trunk NC. Within the NC free zones of rhombomeres 3 and 5, several ephrins are expressed, which repulse the NC away from the neighboring rhombomeres and prevent the integration of differing NC groups (Teddy and Kulesa, 2004; Yu and Moens, 2005; Kulesa et al., 2010; Mayor and Theveneau, 2013; Casazza et al., 2007) (**Figure 1.3 F**). Another negative signal comes from semaphorins, including semaphorin3A and 3F (Sema3A/F) and their receptors neuropilin 1/2 (Nrp1/2) (Yu and Moens, 2005; Casazza et al., 2007; Mayor and Theveneau, 2013; Clay and Halloran, 2010). Nrp1/2 are expressed by the NCCs themselves, while Sema3A/F are expressed with the NC free zones (Casazza et al., 2007; Yu and Moens, 2005). When a NCC begins to cross the boundaries of its stream, the Sema3A/F will bind to Nrp1/2 receptors causing cellular protrusions to collapse and forcing the cell to polarize in the opposite direction (Kulesa et al., 2010; Yu and Moens, 2005; Casazza et al., 2007; Clay and Halloran, 2010). Evidence suggests that each NC stream has its own unique Semaphorin and Neuropilin gene expression levels indicators allowing the cells within the various streams to know when they are coming into contact with a cell from a neighboring stream (Yu and Moens, 2005; Casazza et al., 2007). In extreme circumstances, such as the loss of a large number of NCCs in a stream, it is possible for cells from a neighboring stream to target to the area and repopulate another stream (Clay and Halloran, 2010). These attractive and repulsive signals can be found on varying degrees in both the cranial and trunk NC (Mayor and Theveneau, 2013; Casazza et al., 2007).

While repulsive signals keep NCCs in line during migration, it is equally if not more important to attract these cells to their intended targets. This is a process that is much less understood as each target throughout the developing organism is likely to have its own unique set of attractive cues. cNCCs, as previously stated, travel together in a large group and despite the effects of CIL, do not continuously disperse farther away from each other as time goes on. This is due to co-attraction principles opposing the dispersal forces. In *Xenopus,* cNCCs secrete C3a during migration, while simultaneously expressing its receptor as well, C3aR (Mayor and Theveneau, 2015). This dual expression allows cells to both attract one another and keep them contained with the rest of the group. Should a cell become separated from the group, the upregulation of C3a produced can attract the cell back by activating Rac1-mediated protrusions in the direction of the group (Theveneau and Mayor, 2012; Theveneau and Mayor, 2013). This allows for a continuous balance of repulsive and attractive forces between cells throughout the duration of migration.

In addition to attractive signals from other NC, cells must also respond to signaling that directs them where in the embryo to target in the first place. Since all NCCs originate in the dorsal neural tube, these chemical cues must be specific to their corresponding tissues and some must be sent over significant distances (Clay and Halloran, 2010; Cordero et al., 2011; Kulesa et al., 2003; Teddy and Kulesa, 2004). Tissue specific guidance cues are still investigated to this day, but several possible signals have been identified. For instance, VEGFA has been identified as a positive attractant to NCCs migrating to the second branchial arch in chicks (Mayor and Theveneau, 2015; Clay and Halloran, 2010; Teddy and Kulesa, 2004). While Glial cell Derived

Neurotrophic Factor (GDNF) is an attractive signal for enteric NC within the developing gut and FGF-2 and FGF-8 are likely positive cues within the cardiac muscle and cranial space (Cordero et al., 2011; Mayor and Theveneau, 2015; Clay and Halloran, 2010). With regard to eye development, however, the picture is less clear. The developing eye is an attractive signaling cue to NCCs of the forebrain and midbrain, but the exact nature of those signals has yet to be defined (Creuzet et al., 2005; Langenberg et al., 2008; matt et al., 2008; Zhang, et al., 2014). There is evidence that the ECM components around the eye are more permissive to migration overall, enticing the cells to migrate into and around the eye (Langenberg et al., 2008; Clay and Halloran, 2010). It has also been suggested that the eye secretes one or more attractive signals to the cells, such as Sdf1 or PDGF (Mayor and Theveneau, 2015; Theveneau and Mayor, 2013). Additional work remains to further understand these eye-based signals. However, without the eye to provide these attractive cues, NCC migration cannot proceed. In *Rx3* mutant zebrafish (a gene necessary for eye development), NCCs normally destined to occupy the periocular regions failed to migrate with appropriate directionality, lacked organization, and traveled much more slowly overall (Langenberg et al., 2008). Importantly, this was seen only in cells that were slated to migrate into the ocular region, and had not affected other NCCs from other regions of the embryo. This suggests some signal from the eye is necessary for NCC migration from the forebrain (Langenberg et al., 2008).

1.3.6 Neurocristopathies and a Defective Neural Crest

NCCs play a pivotal role in the development of key vertebrate systems and are highly studied in the field of developmental biology, due in no small part to the extensive

number of defects and diseases associated with their improper development. First characterized by Robert Bolande in 1974, neurocristopathies entail a broad range of phenotypic abnormalities associated with deviations in NC development, including their delamination, population size, migration, gene expression, and differentiation into various derivatives (Noisa and Raivio, 2014; Trainor, 2013). Neurocristopathies are one of the most common birth defects in the world with the most common kind of neurocristopathy, craniofacial defects or anomalies, accounting for approximately one third of all congenital birth defects globally (Trainor, 2013). These disorders can include isolated, single tissue abnormalities, such as albinism, or can present as multi-tissue syndromes like CHARGE syndrome (discussed below). To date, there are more than 700 different syndromes listed as neurocristopathies, many of which share similar phenotypes (Trainor, 2013).

One of the most familiar neurocristopathies in the modern world is cleft lip or cleft palate, classified together as orofacial clefts. Both defects occur as a failure of two opposing epithelial sheets to fuse during early morphological events of the head, leaving a gap where the fusion did not occur (Cox, 2004; Trainor, 2013). In cleft lip, this is a failure of three different facial prominences to fuse at the upper lip, causing a visible gap in the upper lip which may extend into the nose. In cleft palate, the fusion fails in the palatal shelves, creating a gap in the roof of the mouth which cannot be seen without opening one's mouth (Trainor, 2013, CDC). Cleft lip and palate may each occur individually or appear together. Orofacial defects are very common with cleft lip seen in 1 in 1,600 births and cleft palate seen in 1 in 1,700 births in the US with both defects accruing a lifetime treatment cost of $697 million in the US each year (CDC; Trainor,

2013). These defects have a number of genetic and environmental causes including alcohol and smoking consumption during pregnancy however, a few genetic mutations identified in patients with orofacial defects seen within syndrome cases have shown a promising link to NC development, with mutations seen in BMP4, SHH, and Msx1, all genes vital to the establishment of NCC identity during neural tube closure (Cox, 2004; Bronner and LeDouarin, 2012; Simões-Costa and Bronner, 2015; Nieminen, 2003; Mayor and Theveneau, 2013). Mutations in Msx1 in particular have shown delayed or absent proliferation of the NC, leading to clefting of the lip (Nieminen, 2003). When appearing in a syndrome, orofacial defects can often present with malformations or abnormalities seen in other NC-derived tissues including middle ear and dental defects, resulting in difficulties eating, speaking, and hearing loss (Nieminen, 2003; Trainor, 2013). Cleft lip or palate is seen in other neurocristopathy syndromes like Treacher Collins Syndrome as well.

Waardenburg Syndrome and Hirschsprung disease are another two neurocristopathies that can present either separately or together. Waardenburg Syndrome is a collection of defects that often include deafness or hearing loss and discoloration or lack of pigmentation in the skin, hair, and eyes (albinism) (NIH; Pingault et al., 2010). Additional symptoms may include facial abnormalities such as wide set eyes, and flattened nasal bridge, and Hirschsprung disease (NIH; Pingault et al., 2010). Genetic mutations leading to Waardenburg syndrome can be used to identify which subtype of the disease a patient has. The most common mutations are in Mitf, Pax3, Snail2, and Sox10 (Pingault et al., 2010; NIH). All mutations seen disrupt the NCCs ability to specify into NCC off the neural tube and/or migrate to the appropriate targets (Pingault et al., 2010).

Pax3, Snail2, and Sox10 work to maintain NCCs in their multipotent state and migrate effectively, while Mitf is involved in migration capabilities and differentiation (Pingault et al., 2010).). There is no cure for Waardenburg Syndrome.

Hirschsprung disease is a defect wherein significant portions of the lower enteric nervous system are missing or nonfunctional. Without regulation from the nervous system, the intestines are not able to control the movements and activity of the colon (NIH, Emison et al., 2010). Symptoms of Hirschsprung disease include abdominal pain, constipation, obstructed bowel, diarrhea, vomiting, and slowed growth (NIH). Hirschsprung disease is most often caused by mutations in the genes Ret or EDNRB (Emison et al., 2010). Ret is a signaling gene and is important for NCC motility through the developing digestive tract to the space between the intestinal wall and the smooth muscle (Emison et al., 2010). Without Ret, NCCs fail to migrate to their intended target. EDNRB (endothelin receptor type B) interacts with endothelin cells to transmit the nerve signals to the intestines (NIH). Without these proteins, nerve signaling cannot reach its intended target. Some evidence suggests that mutations in Sox10 have also been associated with Hirschsprung disease in a small number of patients, likely suggesting additional ways the migration of NCCs may be affected (Emison et al., 2010). There is no cure for Hirschsprung but is usually treated with surgery to remove the affected intestine.

A final neurocristopathy to discuss is perhaps the most comprehensive of the listed syndromes because of how many tissues are affected: CHARGE syndrome. CHARGE syndrome stands for Coloboma, Heart defects, Atresia of the nasal choanae, Retardation of growth/development, Genital abnormalities, and Ear abnormalities (NIH; Zentner et al., 2010; He et al., 2016). Despite the name, not all listed features need to be

present for a person to be diagnosed with CHARGE syndrome. The most common phenotypes seen include ocular colobomas (a failure of the optic fissure to fuse, resulting in vision impairment or blindness) and semicircular canal hypoplasia (a malformation or absence of the bones of the inner ear, resulting in hearing impairment or deafness) (Zentner et al., 2010). CHARGE is most often caused by a mutation in the CHD7 gene, a chromatin remodeler gene (NIH; Zentner et al., 2010; He et al., 2016). While much remains to be studied, recent evidence suggests that Sox10 and Sox11 may be downstream targets of CHD7, without which NCCs are unable to migrate to target areas or proliferate appropriately (He et al., 2016). Like the other syndromes listed, there is no known cure or treatment for CHARGE syndrome.

In addition to craniofacial defects, neurocristopathies may also include serious heart defects, specifically of the outflow tract, and multiple defects of the ocular anterior segment (discussed in detail below). Many more neurocristopathies exist than can be listed here including Fetal Alcohol syndrome which may cause major disruptions to not only the NC but the neural tube as well. Certain cancers have also been associated with neurocristopathies including neuroblastomas and carcinoids (NIH). In cancers, malignant cell growth may be aided by the reactivation of developmental signals and processes, including EMT and migration capabilities of NCCs (Mayor and Theveneau, 2013). The extensive phenotypes and wide-reaching effects of these neurocristopathy disorders emphasize the need to understand the role of the NC and its associated GRN in development in order to engineer more targeted and efficient treatments for patients suffering from these disorders.

1.4 Periocular Mesenchyme

1.4.1 Characteristics of POM

Loosely defined, Periocular Mesenchyme (POM) cells are migratory cells located within the periocular space. This terminology is intentionally vague and as such has, in past literature, been used to identify cells that not only contribute to the eye and its relevant tissues (including extraocular muscles and the lid), but also facial cartilage, components of the ear, and craniofacial structures. This broad definition has resulted in confusion within the literature about the exact context of POM cells, thus leading to the question "What is a POM cell?" The field of developmental biology and eye development has been working diligently to refine that definition.

POM cells are a migratory population of cells composed largely of NC-derived cells, but also including a small proportion of mesoderm cells, that populate the space immediately surrounding the eye and are essential for the proper development of the ocular anterior segment (Creuzet et al., 2005; Fuhrmann et al., 2000; Langenberg et al., 2008; Williams and Bohnsack, 2015; Akula et al., 2018; Gould et al., 2004). The POM are a relatively small population of cells that maintain close proximity to the developing retina during the morphogenetic stages. Though not currently well understood, evidence suggested that POM play a key role in signaling development in other areas of the eye, such as the optic stalk, RPE, and vasculature (Evans and Gage, 2005). As lens induction occurs, these cells migrate into the space created between the neuroectoderm of the retina and the thin surface ectoderm that remains after lens induction (Soules and Link, 2005; McMahon et al., 2004; Creuzet et al., 2005; Langenberg et al., 2008; Lovett et al., 2018; Trainor and Tam, 1995). Any tissues formed from so called 'periocular mesenchyme

cells' that are not directly related to the formation of the AS are not considered true POM cells but are rather other cNCC/mesoderm derivatives that happen to traverse the periocular space but are not specifically targeted to the AS (Lovatt et al., 2018; Williams and Bohnsack, 2015; Langenberg et al., 2008).

Though the exact mechanisms and transcriptomic profiles of POM cells remains unclear, it is understood that true POM cells eventually give rise to crucial portions of various specialized structures of the AS. POM cells can essentially be thought of as one step further specified than their NCC origin cells: still highly migratory with the capability of differentiating into several different cell types, but lacking the broad pluripotency of their cNCC counterparts. If cNCCs are multipotent stem cell-like cells contributing to numerous different cranial structures, than POM cells are slightly more refined, able to differentiate into a number of different cell and tissue types, but not as expansively as a NCC. Similar to NCCs, any disruption in the specification or migration of these cells can give rise to ASD phenotypes and disorders (Akula et al., 2018; Gould et al., 2004; McMahon et al., 2004; Reis and Semina, 2011). With the information presently available, the only difference between the NCC that contribute to the sclera, blood vessels of the hyaloid vasculature, and cartilage and bone of the orbital area and true POM is that the POM is specifically targeted to the AS and the other NCCs are not. Extensive work in a multitude of model organisms is needed to further elucidate the exact molecular mechanics that define a POM cell. The truth remains that the exact, concrete definition of what exactly constitutes a POM cell remains unclear at the present time.

1.4.2 Genes involved in the specification, migration, and function of POM cells

Critical to the understanding of POM cell molecular machinery, interactions with their surrounding environment, and unique identity is knowing their exact genetic compositions. In other words, what genes are active during the brief window of POM identity between cNCC and further specification? In the following sections, we will discuss the genes known to be associated with the POM and AS development. The first 3 genes listed (FoxC1, Pitx2, and Lmx1b) are the 3 most often identified as large-scale regulators of proper AS formation. Next, the NCC genes that remain active in the POM will be discussed, and finally a few additional, more precise genes of interest will be outlined.

1.4.2.1 FoxC1

The first major regulator of AS formation is a transcription factor called Forkhead Box C1 or FoxC1. As a transcription factor, FoxC1 remains in the nucleus of a cell and regulates the expression of other downstream targets. The forkhead family of transcription factors are named after their distinct forkhead or winged shaped DNA binding domain consisting of 3 loop helices (McMahon et al., 2004; Gould et al., 2004; Seo et al., 2017; Seo et al., 2012; Aldinger et al., 2009). FoxC1 is a duplicated gene in the zebrafish genome, consisting of FoxC1a and FoxC1b, though they are redundant to one another (Seo et al., 2017; Seo et al., 2012). It is located on chromosome 6 in humans, while FoxC1a is located on chromosome 2 and FoxC1b is located on chromosome 20 in zebrafish (NIH Genetics Home Reference; Zfin). During eye development, FoxC1 is highly expressed within the surrounding POM cells, consisting of mainly cranial NCCs

but also a small proportion of mesenchymal cells (Langenberg et al., 2008; Williams and Bohnsack, 2015; Gould et al., 2004; McMahon et al., 2004). In mice, as development continues, FoxC1-expressing cells begin to restrict down until they are only visible in the presumptive trabecular meshwork region, suggesting that FoxC1 may play a role in the maintenance of the mature structure (Gould et al., 2004; McMahon et al., 2004). Though it remains unclear, some evidence suggests that FoxC1 expression in the adult AS may be necessary for the eye to control oxidative stress levels (Aldinger et al., 2009). In addition to its expression within POM cells, FoxC1 is also expressed or involved with the formation of the cardiac outflow tract, blood vessels, somites, brain, and kidneys (Aldinger et al., 2009; Seo et al., 2012; Skarie and Link, 2009; Berry et al., 2006).

Heterozygous and null mutants for FoxC1 have both shown defects in AS development in zebrafish and mice. While null mice die at birth with multiple systemic defects including moderate to severe ASD, hydrocephalus and skeletal deformities, heterozygous mice show milder ASD phenotypes (Gould et al., 2004). These AS defects may include thickened corneal epithelium and no endothelium, corneal opacity, thinned or absent anterior chamber, iridocorneal adhesions including missing Schlemm's canal and compressed meshwork, iris malformations, and an increased risk for developing glaucoma (Gould et al., 2004; Berry et al., 2006; Reis et al., 2012; Seo et al., 2017) (**Table 1.1**). However, not every individual with a FoxC1 mutation develops glaucoma in their lifetime, suggesting that FoxC1 may interact with other loci during either the development or maintenance of the iridocorneal angle and that interaction may be what leads some to develop glaucoma and others to remain healthy (McMahon et al., 2004). Alterations in FoxC1 gene dosage have also caused ASD and glaucoma in humans,

suggesting that AS development is very sensitive to overall FoxC1 transcription factor levels (McMahon et al., 2004; Gould et al., 2004; Berry et al., 2006). Haploinsufficiency in FoxC1 is seen in many ASD patients (McMahon et al., 2004). Interestingly, FoxC1 and FoxC2, another transcription factor, have largely overlapping expression and functions in eye development (Seo et al., 2012). While neither a single mutation in FoxC1 or FoxC2 results in defects within the ciliary body, a double heterozygous mutation does (Gould et al., 2004; Seo et al., 2012). This suggest that they have overlapping functions that one can compensate for in the absence of the other, but when both are defective, additional AS structures may become affected (Gould et al., 2004).

In addition to overall ASD phenotypes, mutations in FoxC1 have also been linked to several more disorders including but not limited to Axenfeld-Rieger Syndrome with or without systemic abnormalities (ARS), Peter's Anomaly (PA), and Dandy-Walker Malformation (DWM) (Aldinger et al., 2009; Reis et al., 2012; Berry et al., 2006) (**Table 1.1**). Interestingly, while mutations in FoxC1 and Pitx2 have both been linked to ARS, when ARS is seen with more systemic issues including the heart and the kidneys, it is more often associated with mutations in FoxC1 than Pitx2 (Reis and Semina, 2011).

FoxC1 works with other genes of interest in the establishment of the AS, chief among them in early development is Pitx2. Both transcription factors are considered to be major regulators of AS development and when one is not present, large scale abnormalities occur. In fact, evidence has shown that both FoxC1 and Pitx2 are responsive to retinoic acid signaling and, in fact, can bind to one another and regulate the others expression (Hendee et al., 2018; Berry et al., 2006; Chawla et al., 2018; Matt et al., 2005; Matt et al., 2008). FoxC1 and Pitx2, when co-expressed, can localize to the same

subnuclear compartments and interact with one another (Berry et al., 2006; Hendee et al., 2018). Specifically, the Pitx2 homeodomain can interact with a Pitx2 specific binding domain within the C-terminal activation domain in FoxC1 (Hendee et al., 2018; Berry et al., 2006). They are both necessary for establishing angiogenic privilege in the developing cornea, a system that prevents the formation of blood vessels in the cornea to keep it clear (Gage et al., 2014; Seo et al., 2012; Skarie and Link, 2009). Though many downstream targets of FoxC1 haven't been fully mapped and identified, a few genes have been identified. TGFβ1i4 is expressed predominantly in the conjunctival epithelium during normal development however, in the absence of FoxC1 in mouse models, the expression of TGFβ1i4 increases suggesting that FoxC1 may negatively regulate its expression (Sommer et al., 2006). FGF19 has been shown to be positively regulated in the POM and cornea in both zebrafish and human AS cells (Tamimi et al., 2006).

1.4.2.2 Pitx2

The second major regulator of AS formation is Paired-like homeodomain 2, or Pitx2. Similar to FoxC1 this gene is another transcription factor, binding to other pieces of DNA and regulating the activity of other genes. It is a member of the PITX homeobox family, a bicoid class of homeodomains (Evans and Gage, 2016; Hendee et al., 2018). Homeodomain genes are broadly defined as being involved in the regulation of development. In humans Pitx2 is located on chromosome 4, while in zebrafish it is on chromosome 14 (NIH Genetic Home Reference; Zfin). Vertebrate Pitx2 encodes for multiple isoforms of the gene, generated either through the use of different promoters or alternative splicing sites (Hendee et al., 2018; Ji et al., 2016). They all share the same C-

terminal and homeodomain sequences, but they have different N-terminals (Ji et al., 2016). These isoforms are listed as Pitx2a, Pitx2b, and Pitx2c. Pitx2a and Pitx2b are very similar in size and overlap in function, but Pitx2c is shorter with fewer exons and is exclusively involved in cardiogenesis (Ji et al., 2016; Berry et al., 2006; Chawla et al., 2016). In zebrafish, 2 isoforms exist that correspond to the human versions: Pitx2a and Pitx2c (Ji et al., 2016).

The expression and function of Pitx2 is highly conserved during vertebrate ocular and craniofacial development. Involved in the early development of the AS and many other craniofacial structures such as the teeth, Pitx2 is considered a key gene in cranial development. Evidence also suggests it may play a role in the left-right axis asymmetry of the heart and other abdominal organs (Ji et al., 2016; Lu et al., 1999; Kioussi et al., 2002). It is expressed in both the NCC and mesoderm-derived cells of the POM in early stages of development, transitioning to expression within mature murine AS structures including the cornea and iridocorneal angle, as well as vasculature, lens, and sclera (Evans and Gage, 2005; Chen and Gage, 2016; Strungaru et al., 2011; Chawla et al., 2016). Pitx2 may be involved in the overall function of the eye. In addition to monitoring intraocular pressure through the iridocorneal angle, some evidence suggesting its expression is involved in the maintenance of oxidative stress (Berry et al., 2006; Strungaru et al., 2011).

The exact molecular pathway involving Pitx2 has not been fully elucidated, however, several downstream targets of Pitx2 have been identified. Dickkopf 2 (Dkk2) is a member of a family of secreted glycoproteins which operate as antagonist of Wnt signaling and is important for NCC specification (Devotta et al., 2018; Gage et al., 2008;

Liu and Semina, 2012). Mutations in Hesx1, another member of the paired homeodomain family, have been identified in some instances of anophthalmia and pituitary conditions that also present with mild craniofacial defects, ASDs, and optic nerve dysplasia (Brickman et al., 2001). Other non-ocular downstream targets include Dlx2, activated within the dental epithelium (Ji et al, 2016). While the exact function of Pitx2 in AS development remains unclear, an abnormality in Pitx2 expression levels may lead to many ocular and systemic defects. Similar to FoxC1, proper human development appears to be highly sensitive to disruptions in the dosage of Pitx2 levels (Hendee et al., 2018; Berry et al., 2006; Bohnsack et al., 2012; Liu and Semina, 2012; McMahon et al., 2004; Reis and Semina, 2011; Devotta et al., 2018). Even small increases or decreases in the levels of Pitx2 protein at various points along the developmental pathway can lead to abnormalities, the severity of which is dependent on the level of disruption (Berry et al., 2006; McMahon et al., 2004; Reis and Semina, 2011; Liu and Semina, 2012). Previous mouse work has shown that Pitx2 is needed for the proper establishment of cell fates and angiogenic privilege within the stromal and endothelium layers of the cornea (Gage et al., 2014; Devotta et al., 2018; Liu and Semina, 2012). Common defects seen in the eye when Pitx2 is mutated include but are not limited to malformed or absent corneal stroma and endothelium, increased corneal thickness, reduced anterior chamber, iris hypoplasia, corectopia, polycoria, aniridia, loss of some extraocular muscles, and abnormal RPE and optic nerve development (Chen and Gage, 2016; Gage et al, 2014; Bohnsack et al., 2012; Hendee et al., 2018; Ji et al., 2016; Liu and Semina, 2012; Reis et al., 2012; Volkmann et al., 2011) (**Table 1.1**).

Pitx2 mutations typically present as heterozygous, as null mice are embryonic lethal (Gage et al., 2014; Chen and Gage, 2016). Mutations within the homeodomain often result in ARS, but both gain and loss of function mutations resulting in a truncated protein have been noted in ARS patients (Ji et al., 2016; Hendee et al., 2018; Evans and Gage, 2005; Volkmann et al., 2011). Pitx2 mutations are often the root cause of disorders including but not limited to Axenfeld-Rieger Syndrome (ARS) with or without systemic abnormalities, Peter's Anomaly (PA), and congenital glaucoma (Reis and Semina, 2011; Gould et al., 2004; McMahon et al., 2004; Reis and Semina, 2011). In addition to POM-related development, malformations in the establishment of the RPE have also been noted in NCC-specific Pitx2 knockouts in mice (Evans and Gage, 2005). In addition to developmental defects, overexpression of Pitx2 has been noted in some cancers, particularly ovarian and colon cancers (Hirose et al., 2011).

Table 1.1: Table of genes commonly associated with an ASD phenotype. Several of these genes are specifically related to the development of the POM. D = autosomal dominant, R = autosomal recessive, * inheritance unknown

Gene Name	Gene Type	Chromosome Location	Mode of Inheritance	ASD Phenotypes/Disorders
Pitx2	Transcription factor	4q25	D	Iris hypoplasia, polycoria, corectopia, Axenfeld-Rieger Syndrome. Glaucoma, Peter's Anomaly
Foxc1	Transcription Factor	6p25	D	Posterior Embryotoxin, corectopia, polycoria, glaucoma, aniridia, Axenfeld-Rieger Syndrome
Lmx1b	Transcription Factor	9q33	D	Glaucoma, Nail-Patella Syndrome
Foxd3	Transcription Factor	1p31	*	Aniridia, craniofacial defects, Peter's Anomaly
Sox10	Transcription Factor	22q13	D	Iris heterochromia, wide set eyes, Waardenburg
Cyp1B1	Monooxygenase enzyme	2p22-p21	R	Congenital Glaucoma, abnormal iridocorneal angle tissues, aniridia, Peter's Anomaly
Foxe3	Transcription Factor	1p32	D or R	Congenital cataracts, microphthalmia, iridocorneal adhesions, cataracts, Peter's Anomaly
Pax6	Transcription Factor	11p13	D	Aniridia, congenital cataracts, keratitis, Peter's Anomaly
B3GLCT	Glycosyl Transferase	13q12	R	Peter's Plus Syndrome
Tfap2a	Transcription Factor	6p24.3	D	Coloboma, microphthalmia, Branchio-oculo-facial syndrome

1.4.2.3 Lmx1b

The last major player in AS development is another transcription factor LIM homeobox transcription factor beta 1, or Lmx1b. This gene has 2 LIM domains that allow it to facilitate protein-to-protein interactions, plus a homeodomain for DNA binding purposes (McMahon et al., 2004). Because of a duplication event in teleosts, zebrafish have two copies of Lmx1b, known as Lmx1b.1 and Lmx1b.2. In humans, Lmx1b is located on chromosome 9, while in zebrafish Lmx1b.1 is located on chromosome 8 and Lmx1b.2 is located on chromosome 5 (NIH Genetic Home Reference; Zfin).

Lmx1b was first identified as a transcription factor involved in the establishment of the dorso-ventral patterning in limb development, but further evidence has since supported its involvement in the development of podocytes in the kidneys, the midbrain-hindbrain organizer, neuronal subtypes of the CNS, and AS formation (Liu and Johnson, 2010; McMahon et al., 2009; Pressman et al., 2000; Dunston et al., 2004). Additionally, Lmx1b works cell non-autonomously to pattern the ventral optic cup during eye morphogenesis and choroid fissure closure (McMahon et al., 2009). During early eye morphogenesis, the POM surrounds the forming optic cup and contributes key signaling genes for proper pattering, such as Lmx1b (McMahon et al., 2009; Liu and Johnson, 2010). Without these POM-derived signals, optic cup morphogenesis and the specification of key tissues like the RPE continues abnormally or halts entirely. This has been shown to occur in Lmx1b knockouts via apoptosis of the POM cell population, but the phenotype can be rescued by blocking apoptosis (McMahon et al., 2009; Pressman et al., 2000). It has been shown that Lmx1b is required in many NC-derived cells, especially POM, for their survival, maintenance, and migration (Liu and Johnson, 2010; McMahon

et al., 2009). In the established murine AS, Lmx1b plays an essential role in the postnatal maturation of the trabecular meshwork, maintenance of corneal transparency and prevention of corneal neovascularization (Liu and Johnson, 2010). There is some evidence to suggest that Lmx1b plays a role in overall eye size and growth as well, as Lmx1b mutants often have smaller eye sizes when compared to controls (McMahon et al., 2009). Evidence in mice suggests that different AS tissue types may have different Lmx1b level requirements (Liu and Johnson, 2010; McMahon et al., 2009). Lmx1b regulates the specification, differentiation, and overall survival of cells in general, but different tissues have different levels of need for it (Liu and Johnson, 2010). Despite knowing the detrimental effects a lack of Lmx1b has on the development of the AS and eye, the specific role Lmx1b provides for eye development remains poorly understood at this time.

Loss of function of Lmx1b severely impacts AS development with common phenotypes observed being decreased thickness of the anterior chamber, thin cornea, abnormal corneal fiber arrangements, and an absence of the ciliary body and iris stroma (Liu and Johnson, 2010; McMahon et al., 2009; Pressman et al., 2000; Dunston et al., 2004) (**Table 1.1**). Abnormal expression of Lmx1b often leads to the development of Nail Patella Syndrome (NPS), a systemic disorder characterized by misshapen or absent nails, knee, joint, and hip malformations, kidney dysfunction, and a 50% increased risk of developing glaucoma (McMahon et al., 2009; McMahon et al.,2004; Liu and Johnson, 2010; Gould et al., 2004; Dunston et al., 2004). Surprisingly, NPS patients rarely have obvious ASD-like phenotypes or any ocular abnormalities (Dunston et al., 2004; Liu and Johnson, 2010). The AS, and especially the angle of the iridocorneal angle structures,

appears normal in development, yet they are likely to develop glaucoma anyway. This suggests that these patients do not have a form of congenital glaucoma but rather, they are likely seeing elevated intraocular pressures over time and eventually glaucoma due to decreased Lmx1b activity in maintaining the outflow of the trabecular meshwork (Liu and Johnson, 2010). Interestingly, not everyone with a Lmx1b mutation develops glaucoma, suggesting that Lmx1b interacts with other loci during development and maintenance that leads to glaucoma (McMahon et al., 2004).

NPS in humans is caused by a haploinsufficiency of Lmx1b during development, while null mutant mice show NPS-like phenotypes, though they die shortly after birth (McMahon et al., 2004). Heterozygous mice, however, appear normal (McMahon et al., 2004). Like the other major players of AS development, Lmx1b expression levels do have an impact on other POM and AS-related genes. Previous work has shown that Lmx1b can negatively regulate the expression of FoxC1 (Pressman et al., 2000). In zebrafish studies, when Lmx1b has been knocked out, the expression patterns of both FoxC1 and Pitx2 have also been disrupted, further illustrating that these 3 genes are intimately linked and an abnormality in one can have major negative effects on the process of AS development as a whole (McMahon et al., 2009; McMahon et al., 2004; Reis and Semina, 2011; Akula et al., 2018; Liu and Johnson, 2010). These first 3 genes listed, Pitx2, FoxC1, and Lmx1b, are considered the most critical genes for the formation and maintenance of the POM and ultimately, the AS. Numerous studies have shown that model organisms such as zebrafish, chick, and mice that are deficient in either Pitx2, FoxC1, or Lmx1b will present with profound ocular abnormalities and other possible systemic defects (Akula et al., 2018; Lovatt et al., 2018; Liu and Johnson, 2010;

Pressman et al., 2000; Lu et al., 1999; McMahon et al., 2004; Reis and Semina, 2011; Evans and Gage, 2005; Berry et al., 2006).

1.4.3 Neural Crest Transcription Factors in POM

In addition to the POM specific genes discussed above, there are also several NC specific genes that remain active in POM cells and have been shown to effect AS development. The molecular mechanisms surrounding the transition between cNCC and POM cell remain inconclusive. It has been speculated that, in general, genes associated with a NC identity slowly fade out or are shut off entirely within the POM as they approach the AS. However, a small handful of the NC-specific genes have been shown to have an effect on AS development and within the ASDs, with and without other systemic issues that would be indicative of a large-scale NC defect and not something POM specific. This relationship with the POM may be the result of NC-specific genes remaining active to keep the migration capabilities, survival, and pluripotency of NCCs active within the POM until their migration is complete and their differentiation begins. Here we will highlight two of these NC genes: Foxd3 and Sox10.

Forkhead box D3 (FoxD3) is a transcription factor of the forkhead gene family. Like FoxC1, FoxD3 contains a forkhead domain allowing it to bind to DNA and regulate the expression of other genes (Drerup et al., 2009). In humans it is located on chromosome 1, while it is found on chromosome 6 in zebrafish (NIH Genetic Home Reference; Zfin). FoxD3 is a vitally important gene of the cNC gene regulatory network, broadly expressed throughout the pre-migratory NC and needed for the induction, survival, migration, and pluripotency of NCCs (Lister et al., 2006; Volkmann Kloss et al.,

2012; Stewart et al., 2006; Hanna et al., 2002). FoxD3 is first activated during the neural crest specifier gene stage of NC development, as the cells become specified, undergo the EMT and delamination, and begin their migratory journeys (Wang et al., 2011; Bronner and LeDouarin, 2012; Simões-Costa and Bronner, 2015; Mayor and Theveneau, 2013; Noisa and Raivio, 2014; Zhang et al., 2014). FoxD3 in zebrafish is active at the neural plate border during gastrulation and continues to be expressed throughout the pre-migratory stages (Volkmann Kloss et al., 2012; Wang et al., 2011; Stewart et al., 2006). However, as differentiation begins, expression decreases in most cells, with only a subset of cells establishing the neural glia (Volkmann Kloss et al., 2012). Like other NC genes, FoxD3 remains active during the process of migration until further differentiation can occur and has been shown to be required for many, but not all, derivatives of the cNC (Wang et al., 2011; Lister et al., 2006; Simões-Costa and Bronner, 2015; Mayor and Theveneau, 2013; Lister et al., 2006; Hanna et al., 2002). It is not currently known exactly when FoxD3 expression downregulates or ceases in the POM population. Not many downstream targets of FoxD3 are known, so it cannot be currently speculated what targets of FoxD3, if any, are involved in the development of the AS, though it is known that FoxD3 regulates itself (Lister et al., 2006; Volkmann Kloss et al., 2012).

In mice, FoxD3 has been shown to be required for the continued pluripotency of stem cells (Hanna et al., 2002). A heterozygous FoxD3 mouse may appear normal and healthy, but homozygous mutants are embryonic lethal (Volkmann Kloss et al., 2012). In zebrafish lacking FoxD3, craniofacial defects, cardiac abnormalities, and embryonic lethality are often seen (Volkmann et al., 2012; Lister et al., 2006) (**Table 1.1**). In chick,

FoxD3 overexpression results in an inability to differentiate NCCs (Volkmann Kloss et al., 2012).

In regard to eye development, the influence of FoxD3 itself within the POM and throughout the AS are not widely understood at this time. However, FoxD3 variation has been identified in human ASD patients in the past. Several families with Peter's Anomaly or aniridia have variations in the conserved region of FoxD3, a mutation enriched in those patients with ASDs when compared to the general population (Volkmann Kloss et al, 2012). While the FoxD3 mutations in these cases were not the primary cause of the ASD phenotypes, it is believed that they increase the general risk of ASD phenotypes (Volkmann Kloss et al., 2012)

The second NC-related gene involved in POM and AS development is SRY-box 10, also known as Sox10. It is a member of the SOX family of transcription factors and is a major specifying gene in the NC, critical for early embryonic development (Dutton et al., 2001; Kulesa et al., 2003; Bronner and LeDouarin, 2012; Simões-Costa and Bronner, 2015; Mayor and Theveneau, 2013; Noisa and Raivio, 2014). It is located on chromosome 22 in humans and chromosome 3 in zebrafish (NIH Genetic Home Reference; Zfin).

Sox10 is critical for the specification, and migration of NCCs throughout the body, laying the foundation for numerous tissues, organs, and cell types during the early stages of development. Sox10 is a member of the expansive Gene Regulatory Network of NCCs and is involved in specifying many different genes within the NCC population (Seen Section 3: Neural Crest for more detail). It is essential for the formation of anything that is derived from the NCC including, but not limited to, blood vessels, enteric

nerves, melanocytes, craniofacial cartilage, the inner ear, and the AS (Simões-Costa and Bronner, 2015; Mayor and Theveneau, 2013; Dutton et al., 2001). Originally, Sox10 was thought of exclusively as a NCC gene. Cells expressing Sox10 in the AS region were found to be exclusive to the ventral regions of the eye, entering into the AS via the choroid fissure as invading endothelial cells establishing the transient hyaloid vasculature (Creuzet et al., 2005; Williams and Bohnsack, 2015). As this is not a structure necessary for the function of the adult eye, it is not considered AS. As a NCC marker, naturally, when levels of specifying genes like Pitx2 and FoxC1 become more prominently expressed in the differentiating POM, genes like Sox10 begin to rapidly decline in expression (Lovatt et al., 2018; Kelsh, 2006). If Sox10 expression is lost as cranial NCCs begin to approach the AS, that would suggest a normal developmental step from NCC to POM cell. Work presented in this dissertation suggests that a small number of Sox10-lineage marked cells do populate throughout the AS, suggesting that perhaps they do have some small contribution to one or more tissues (Van Der Meulen et al., 2020).

1.4.4 Other genes of interest

Many more genes currently identified have linked to POM or AS development in a much smaller way than the previously discussed regulators and NC genes. Additionally, many more genes have yet to be identified. The following are other POM related genes.

1.4.4.1 Eya2

A possibly lesser-known POM gene of interest is Eyes Absent Homolog 2, known as Eya2. Eya2 is thought to be involved in DNA repair and may work as a transcriptional

coactivator (Clark et al., 2002; Lupo, 2011). As such, Eya2 has been implicated in organogenesis, DNA repair, and limb regeneration (Xu et al., 1997; Clark et al., 2002; Matt et al., 2005; Lupo, 2011). It is located on chromosome 20 in humans and chromosome 6 in zebrafish (NIH Genetic Home Reference; Zfin). Within the eye, it is expressed in the POM, neural retina, sclera, lens, and optic nerve sheath (Lupo, 2011; Matt et al., 2005; Matt et al., 2008). Expression of Eya1 and Eya2 are dependent on Pax6 expression in lens development, however, it is unknown if this is the case with Eya2 expression in the AS (Xu et al., 1997). The exact role of Eya2 in the context of eye development is not currently fully understood. However, one role of Eya2 have been elucidated.

Although not thought to be a regulator of the same caliber as FoxC1, Pitx2, and Lmx1b, Eya2 still plays an important role in POM biology and AS development. Similar to FoxC1 and Pitx2, Eya2 in the POM is at least partially under the control of RA signaling (Lupo, 2011; Matt et al., 2008; Williams and Bohnsack, 2019; Chawla et al., 2018; Cvekl and Wang, 2009). RA signaling is needed to regulate the expression of FoxC1 and Pitx2 as they enter the AS (Lupo, 2011; Bohnsack and Kahana, 2013; Matt et al., 2005; Matt et al., 2008). Similarly, Eya2 is also activated by RA in the POM at this time, working to control the expression of Pitx2 and FoxC1, as well as programmed cell death within the POM and overall growth of the ventral retina (Xu et al., 1997; Matt et al., 2005; Matt et al., 2008; Clark et al., 2002; Williams and Bohnsack, 2019). Eya2 is prominently expressed in cells in high POM apoptotic areas, primarily the posterior dorsal region and the ventral anterior region (Matt et al., 2005). When RA signaling is reduced via the loss of RA producing Aldh1a1/3 in murine eyes, Eya2 expression and

apoptosis are also decreased in these two POM clusters (Matt et al., 2005). This suggests that Eya2 is somehow involved in the programmed cell death within the POM population, without which the number of POM cells in a specific area may be too great and remodeling of the population post-migration cannot occur, resulting in impaired eye development (Matt et al., 2005; Matt et al., 2008; Clark et al., 2002; Lupo, 2011).

1.4.4.2 Cyp1B1

Cytochrome P450 1B1 is a member of the large cytochrome P450 family of enzymes. It localizes to the endoplasmic reticulum and works as a monooxygenase enzyme, adding an oxygen molecule to other molecules (Vasiliou et al., 2008; Achary et al., 2006; Vincent et al., 2006; Bejjani et al., 2002). In humans it is located on chromosome 2, while in zebrafish it is found on chromosome 13 (NIH Genetic Home Reference, Zfin). While it is involved in tissues all throughout an organism, our focus will be on its role in eye development.

The exact role of Cyp1b1 mechanics in eye development is not currently well understood, but it is believed that it is involved in metabolizing a molecule, possibly a steroid, critical to the development of the eye. This is especially relevant to the iridocorneal angle and drainage structures as Cyp1B1 is heavily implicated in primary congenital glaucoma or PCG (Bejjani et al., 2002; Achary et al., 2006; Vincent et al., 2006; Vasiliou et al., 2008; Williams et al., 2017) (**Table 1.1**). PCG is a rare disease wherein the trabecular meshwork and/or anterior chamber angle are abnormally formed, resulting in an increased IOP from a very young age without the presence of other eye or ASD related defects (Visiliou et al., 2008; Williams et al., 2006). In order to be diagnosed

with a PCG, a person must be diagnosed with glaucoma prior to 5 years of age however, most diagnoses come before the age of 2 years old (Achary et al., 2006; Vasiliou et al., 2008). Roughly 20-40% of all PCG cases with a genetic cause have been linked to mutations in Cyp1B1 with over 140 different genetic mutations catalogued so far (Achary et al., 2006; Williams et al., 2017; Vasiliou et al., 2008). These mutations likely lead to an unstable or improperly folded enzyme, rendering it ineffective. In addition to PCG, Cyp1B1 mutations have also been linked to some cases of Peter's Anomaly (Vincent et al., 2006; Williams et al., 2006). Previous work in mice has showed severe loss or atrophy of the trabecular meshwork in individuals lacking Cyp1B1 (Bejjani et al., 2002). In zebrafish, work with heterozygous or null mutants have shown that Cyp1B1 may indirectly have an effect on NC-derived POM migration to the AS and choroid fissure closure, affecting the openness of the angle (Williams et al., 2017). Although the mechanisms of its involvement are poorly understood, given its association with PCG and PA, Cyp1B1 is likely heavily involved in the development of the iridocorneal angle and/or the regulation of aqueous humor production as well. It remains unclear if POM cells generate Cyp1B1 themselves.

1.4.5 Retinoic acid signaling

Attractive cues involved in guiding cNCCs towards the eye and perhaps helping to initiate their specification into POM cells remain largely unknown. However, one targeting signal has been shown to be a key influence on eye morphogenesis: Retinoic Acid (RA). A metabolite of vitamin A, RA is instrumental for the overall development of the eye as it is critical for the proper, directed migration of cNCCs and the specification

of AS tissues (Lupo, 2011; Matt et al., 2005; Matt et al, 2008; Bohnsack and Kahan, 2013; Liu and Johnson, 2010; Chawla et al., 2018). In short, RALDHs (RA-synthesizing enzyme retinaldehyde dehydrogenases) are expressed in a gradient throughout the eye, specifically in high concentration in the retina, cornea, RPE, and lens (Matt et al., 2005; Matt et al., 2008; Lupo., 2011). RA produced in these areas diffuses out towards the anterior space of the eye which will shortly be populated by POM cells (Lupo, 2011). This RA signaling is activated through its heterodimer receptors RARα/RARβ and RARα/RARγ, which are expressed within the migrating POM cells (Matt et al., 2005; Matt et al., 2008; Lupo, 2011). RA signal activation is a vital determinate of AS development, with proper cues regulating several genes of AS development.

RA acts in a paracrine manner to regulate eye development in two ways: through the activation of critical POM identification genes like Pitx2 and FoxC1, but also as an attractive signaling cue to guide these cells towards the area of AS formation between the surface ectoderm and the anterior edge of the neural retina (Lovatt et al., 2018; Matt et al., 2005; Ittner et al., 2005). As such, POM cells are very responsive to RA (Liu and Johnson, 2010). Both FoxC1 and Pitx2 expression and signaling within the POM are dependent on RA signaling with both having RA response elements located within their promoters (Cvekl and Wang, 2009; Matt et al., 2005). In a crucial feedback loop, Pitx2 and FoxC1 expressing POM cells help to mediate overall RA signaling within the rest of the POM population as well as within the AS developmental region (Matt et al., 2005; Gage et al., 2008). Eya2-dependent apoptosis within the POM is also regulated through RA signaling (Matt et al., 2005; Matt et al., 2008; Clark et al., 2002). NCC-specific deactivation of the RA receptors RARα, RARβ, and RARγ results in a complete loss of

Pitx2 in the POM and developing AS, while an increase in RA signaling leads to increase in expression of Pitx2, FoxC1a, and Lmx1b.1 in the ventral eye region (Matt et al., 2008; Lupo., 2011). RA signaling may play a role in coloboma phenotypes as well. When fewer POM cells contain RAR receptors, or fewer RA ligands are generated, fewer POM cells enter into the choroid fissure and fusion fails to occur completely (Lupo, 2011). It is currently hypothesized that migrating POM traveling through the choroid fissure trigger the extracellular matrix remodeling necessary for fusion to occur (Lupo, 2011; Weaver et al., 2020). Several models have been proposed attempting to explain the complicated role of RA in the expression levels of so many POM genes. In one proposed model, RA expression activates FoxC1a in early NC, which works with additional RA signaling to activate Pitx2 and Eya2 (Lupo, 2011). In turn, Pitx2 activates Lmx1b (Lupo, 2011). Further work needs to be conducted in order to understand the exact mechanisms of RA influence in the POM population.

1.4.6 POM identity Remains a Contentious Issue

The field of eye development requires some much-needed clarity on POM biology. Very little information exists illustrating where exactly POM cells come from and how exactly they are incorporated into the AS. Presently, we simply know that, somehow, these transient cells appear from the cNCCs and eventually become key components of the AS. Little detail about how they get from point A to point B exists, while even less exists on the specification required to get from point B to point C. We do not understand when or how POM cells specify out from the NC or what targets them to the developing eye. Nor do we know when, where, or how each POM cell differentiates

into one or more of the specific AS structures. Crucial to our knowledge of how POM cells are derived from NCCs, or how they become AS cell types, is determining the full transcriptomic profile of POM cells during different stages of development, thus allowing us to see how their profiles change as they move from pluripotent NC to POM to AS cell to their final specifications. Understanding when and how these key elements in POM cell life occur is absolutely critical to our understanding of proper AS development. This transient population between pluripotent NCC and AS tissue lays out the critical foundation of the AS, without which the AS does not form and leaves patients with visual impairments or even blindness. How these critically relevant structures arise *in vivo* will help scientists and clinicians generate novel therapies for the prevention, treatment, and one day, cure, of ASDs.

With the number of POM genes associated with AS development, one essential question that still remains is "What role does each gene play in this process?" While we know the loss of a gene like Lmx1b can lead to an increase in glaucoma risk, we do not yet know what exactly the Lmx1b gene actually does during the development of the AS or its function in the adult eye. Furthermore, we do not know many of the downstream targets associated with large-scale regulators like Pitx2. What genes are in the molecular pathway of Pitx2 or FoxC1 and how do they lead to a functioning iridocorneal angle, for example. We have already seen that a loss of some of these POM genes, especially Pitx2 or FoxC1, leads to widespread defects in several AS structures. But what we don't yet understand is how these genes and the cells that express them interact with one another. Is every POM gene activated in every POM cell at the same time, or is there a pathway that activates them in succession depending on where in the development the organism is

at? Or are genes active at the same time, but in different cells within the broader POM population, in which case, how do these different groups of POM cells behave with one another? The developmental progression of POM cells, their interaction with one another, and their immediate environment could be a key feature in some AS abnormalities.

No one POM gene has been specifically and exclusively linked to just one tissue within the AS. As laid out extensively in the sections above, many different POM genes have been linked to various structures within the AS, but no one gene has been conclusively linked to any one AS disorder. Furthermore, it has been widely shown that POM genes are highly connected to one another, with one gene affecting multiple AS structures and multiple gene mutations resulting in the same kind of defects. This suggests that the POM are highly connected to one another and that AS development is not as simple as one gene being needed for the development of one specific structure. What is more likely with the present information, is that each POM gene is needed in a specific proportion relative to other POM genes and that any manipulation to these dosages sends all the other genes out of balance, causing ASD phenotypes. Therefore, it remains poorly understood how exactly these cells work in conjunction with one another to form these different tissues and which genes, if any, are capable of forming a structure independently, or if coordination amongst multiple different genes and cell populations is necessary. More broadly, why does this lack of uniformity exist within the POM population at all? What is the evolutionary advantage of all of these different regulatory genes? Interestingly, the POM represent a multipotent population of cells. Can we use this fact, and stem cell techniques, to help us generate new POM cells as a method of repairing or completely replacing AS tissues that were damaged or malformed? The

opportunity to greatly advance our understanding of NCC derivatives and AS development lies with our understanding of POM biology. These unique cells have an incredible impact on arguably one of the most important senses we as humans have: our sight. Without the POM, we may diminish or lose a critical way of interacting with our world. This section is simply for the broad questions about POM biology facing the field right now. For more specific future directions that have arisen as a direct result of the research discussed today, please see the "Discussion" section.

1.5 Anterior Segment Dysgenesis

1.5.1 Hallmark Features of ASD

While neurocristopathies can lead to a number of different birth defects throughout the body, perhaps the most interesting amongst them is those with ocular phenotypes. Anterior Segment Dysgenesis (ASD) is a collection of defects and disorders associated with a failure of the normal development of one or more of the structures of the AS and that present with a spectrum of severity that may include vision problems or even blindness (Todorova et al., 2014; Williams, 1993; Akula et al., 2018; Gould et al., 2004). Broadly, it is believed that these abnormalities are the result of improper migration and/or specification of NC-derived POM cells specifically. Every tissue within the AS is susceptible to ASD anomalies and, because of the number of structures possibly affected and the spectrum of severity associated with each genetic mutation, classifying ASDs is often quite complex (Williams, 1993; Espinoza et al., 2002; Sowden, 2007). Many abnormalities can be stand-alone defects or seen repeatedly within larger system-wide syndromes (Reis and Semina, 2011; Soules and Link, 2005; Gould et al., 2004; Sowden,

2007; AAO). The first half of the 20th century saw the identification and characterization of a number of ASD phenotypes. This was often confusing, with complex symptoms, poor description of phenotypes, and often overlapping defects seen amongst different patients (Williams, 1993). Finally, ASD was originally coined "anterior chamber cleavage syndrome" in the 1950s in order to bring all AS defects under one umbrella term, from simple, single tissue anomalies, to multiple ocular defects, to multi-tissue complex syndromes, in order to more readily arrive at a diagnosis and begin attempts at treatments (Williams, 1993). In 1975 when chick-quail chimeras showed the extensive nature in which NC-derived POM contribute to the AS, it was established that AS congenital defects, or even predispositions later in life, are neurocristopathies in origin (Williams, 1993). These various tissue abnormalities seen in ASD may be different in presentation and precise origin in regard to genetic mutations but are likely linked by their overall outcome to the organism (Williams, 1993; Alward, 2000). Owing to the varying classifications of ASDs and the complexities of diagnosis, it is hard to estimate the number of people living with ASD or the number of affected births.

An ASD diagnosis can be made in infancy and throughout childhood, depending on the number and severity of the abnormalities and how they affect overall vision. Anatomical defects most often associated with ASD include corneal opacity (cloudy or scarred cornea), iris hypoplasia (underdeveloped iris), posterior embryotoxon (visible white ring in the iris that demarcates where the Schwalbe Ring has been displaced and Descemet's membrane terminates prematurely), corectopia (displaced pupil), polycoria (multiple pupils), maldeveloped anterior chambers (thinned anterior chamber), and persistent iris strands (strands of iris tissue attaching to the cornea or other structures)

(Gould et al., 2004; Volkmann et al., 2011; Akula et al., 2018; Bohnsack et al., 2012, Ji et al., 2016; Davis-Silberman and Ashery-Padan, 2008; McMahon et al., 2004; Reis and Semina, 2011; NEI, AAO). Other symptoms associated with ASD may also include congenital or juvenile glaucoma, enlarged eyes, and vision problems (Gould et al., 2004; Volkmann et al, 2011; McMahon et al., 2004; NEI). While the cause of each individual tissue abnormality and systemic syndrome associated with ASD has been loosely tied to defects in POM-derived NCC migration and differentiation, the exact genetic mutations of each defect are not currently known. However, great progress has been made in unraveling the mutations most often associated with ASD systemic syndromes, whether they are inherited, or sporadic mutations. Several transcription factors such as Pitx2, FoxC1, Lmx1b, Pax6, and Cyp1B1 have all been linked to cases of Axenfeld-Rieger Syndrome (ARS) and Peter's Anomaly (PA). For a more comprehensive discussion of POM related genes in AS development, please see Section 4: Periocular Mesenchyme.

1.5.2 Glaucoma

One of the most common outcomes associated with ASD defects and syndromes is an increased risk for developing glaucoma (Gould et al., 2004; McMahon et al., 2004). Glaucoma is a collection of disorders that, over time, cause progressive damage to the optic nerve via a buildup of intraocular pressure (NEI; Chak et al., 2014; Stamer and Clark, 2017; Rausch et al., 2018). This increased pressure is most often caused by an inability to drain the aqueous fluid out of the anterior chamber through irideocorneal angle (Rausch et al., 2018; McMahon et al., 2004; Gray et al., 2009; Gould et al., 2004; Gray et al., 2009). Glaucoma is a leading cause of blindness globally, with an estimated 3

million people affected by it in America alone (WHO; Quigley and Broman, 2006; NEI). Furthermore, it is predicted that by 2050, the number of Americans affected by glaucoma is expected to double from just under 3 million to over 6 million (Quigley and Broman, 2006; NEI). Though the exact cause of glaucoma is not known in many cases, there are genetic factors in disease manifestation with glaucoma being particularly prevalent in African American and Hispanic communities (NEI).

Glaucoma is often described as a silent disease because of its slow progression and relative lack of noticeable symptoms in its early stages, making it a dangerous disease. When not treated, it causes progressive and irreversible damage to the optic nerve. Most patients can not feel the increase in intraocular pressure if it is a slow build over time. Oftentimes, the first problem a patient may notice is a reduction in peripheral vision (AAO; NEI; Quigley and Broman, 2006). When this occurs, there has already been substantial damage to the optic nerve, which cannot be reversed. Additionally, once diagnosed with glaucoma, the disease cannot be cured; the symptoms can only be managed. There is no way to restore vision that has been lost, but medications and surgeries can be used to lower intraocular pressure and prevent further damage and vision loss from occurring (Mannino, 2016; NEI). The only way to diagnose and treat glaucoma before permanent damage to the nerve occurs is by having routine eye exams, where an ophthalmologist can measure intraocular pressure and examine the retina and optic nerve for signs of stress or damage.

Many different forms of glaucoma exist, not all of which are caused by genetic mutations. Secondary glaucoma can be caused by an injury directly to the eye or as a result of an eye surgery or disease (Quigley and Broman, 2006; CDC; NEI). The most

common form is open angle glaucoma, which occurs when the trabecular meshwork or Schlemm's Canal in the iridocorneal angle becomes blocked and fluid can no longer be drained properly (McMahon et al., 2004; NEI; Quigley and Broman, 2006). However, glaucoma can also present in children, called congenital glaucoma, as a result of missteps in the development of the AS (Gould et al., 2004). While statistics are unclear about the number of children born with any form of an ASD condition, it is estimated that 1 in 10,000 babies born in the United States have some sort of defect in the AS causing a problem with normal fluid drainage and therefore greatly increasing their chances of developing glaucoma (NEI). Children and infants with congenital glaucoma show more visible signs of trouble than adults, possibly exhibiting larger than normal eyes, cloudy or foggy eyes, excessive tears, red eyes, or light sensitivity (NEI; AAO). Surgery to correct aqueous humor flow is often used to treat congenital glaucoma, if possible.

1.5.3 Axenfeld-Rieger Syndrome and Peter's Anomaly

ASD can often present as part of a larger systemic issue within an organism. These larger scale syndromes are excellent points of research to study NCCs and key genes and the different effects they have on multiple tissues throughout the body at once. Two widely researched syndromes studied with large ASD components are Axenfeld-Rieger Syndrome (ARS) and Peter's Anomaly (PA). These two syndromes also provide an example of the complexities of diagnosing ASDs as they present as multiple combinations of different ASDs with a range of severities for the patient.

ARS is a rare autosomal dominant disorder seen in approximately 1 in every 200,000 live births that encases a wide array of ASD phenotypes (Alward, 2000; Hendee

et al., 2018; Liu and Semina, 2012). It was first characterized in the 1920s when a man named Axenfeld documented posterior embryotoxon and iris strands attachments in his patients (Williams, 1993). In 1935, a man named Rieger characterized different patients with congenital iris hypoplasia, corectopia, and polycoria (Williams, 1993). The two syndromes were distinct from one another until physicians and researchers began to document the overlap between the two diseases, eventually combining the two into one overarching syndrome that can present with a spectrum of anatomical abnormalities (Williams, 1993). Other eye phenotypes include ectropion uveae (iris pigment epithelium on the anterior surface of the eye) and increased IOP and iris strands (Liu and Semina, 2012; Ji et al., 2016; Evans and Gage, 2005). However, the single defining characteristic of ARS patients is that they have a 50% increased risk of developing glaucoma (AAO; Alward, 2000; Bohnsack et al., 2012; Chen and Gage, 2016; Tümer and Bach-Holm, 2009). There are many other anatomical abnormalities outside of the AS that present in ARS, almost all of which are related to NCCs and their derivatives. These can include dental defects and malformations (including microdontia, hypodontia, and oligodontia), craniofacial defects like a flattened and broad nasal bridge and maxillary hypoplasia, excess umbilical skin, hearing loss, developmental delays, heart defects, and possible pituitary defects (Tümer and Bach-Holm, 2009; JI et al., 2016; Bohnsack et al., 2012; Hendee et al., 2018; Liu and Semina, 2012).

Peter's anomaly shares many of the same characteristics as ARS, however it is a distinct syndrome. The distinction between the two syndromes lies in corneal defects seen in all PA cases, but not is ARS (Bhandari et al., 2011; Williams, 1993). It is characterized by corneal opacities often caused by an absence of Descemet's membrane and the

endothelial layer of the cornea (Bhandari et al., 2011). It also has variable adhesion of the iridocorneal angle to the cornea (Bhandari et al., 2011). Systemic issues with Peter's anomaly can also include heart defects, hearing loss, genitourinary defects, CNS defects and delayed development (NEI; Bhandari et al., 2011). It remains challenging to this day to diagnose ASD syndromes like ARS and PA because of their strong similarity to one another in phenotype (Williams, 1993).

Defects in the migration and specification of NCCs are considered the underlying cause of ARS and PA as the NC are not only responsible for the POM-derived AS tissues, but also play a significant role in the development of many of the other tissues throughout the organism (Creuzet et al., 2005; Zhang et al., 2014; Akula et al., 2018). The vast majority of documented cases of ARS have been linked to mutations in Pitx2 and FoxC1, but mutations in other genes like Pax6 and FoxO1a have also been mutated in much fewer cases (Reis and Semina, 2011; McMahon et al., 2004; Berry et al., 2006; Sowden, 2007; Liu and Semina, 2012; Seo et al., 2012). Interestingly, ARS cases that include dental defects are more commonly associated with mutations in Pitx2 than cases that do not include dental defects (Sowden, 2007). PA, however, while sharing many of the same anatomical abnormalities, is most often associated with mutations in Pax6, but it too has documented cases involving Pitx2, Cyb1B1, or FoxC1 (Bhandari et al., 2011). While some genetic mutations have been identified as causes for certain ASDs, like Pitx2 being strongly associated with Axenfeld-Rieger syndrome (ARS), they do not account for all patients with ARS, indicating that one gene is not the sole cause of ARS. This is common with many different ASDs; Many different genes can lead to the same clinically

relevant phenotypes. This result is one of the many reasons that the study of POM and their influences on one another are so relevant.

1.6 Zebrafish

Zebrafish (*Danio rerio*) are a small, freshwater teleost fish native to the Ganges network of rivers and streams located in India and Bangladesh (Fadool and Dowling, 2008; Kimmel et al., 1995; Parichy et al., 2009). Teleosts are small, bony ray-finned fish identifiable by the enhanced jawbone and surrounding musculature that allows them to protrude their lower jaws past their heads, thereby enhancing their feeding capabilities. A well-known and popular fixture among pet store and fish enthusiasts, the zebrafish has also gained ground as an impressive model organism for a wide array of scientific research, particularly amongst developmental biologists and eye researchers.

1.6.1 Zebrafish Maintenance and Molecular Techniques

The zebrafish possesses many characteristics desirable in a model organism. Chief among these traits is its high fecundity, or clutch size. A single mating pair of one male and one female has the potential to produce more than one hundred viable embryos per breeding session, with an upper limit of several hundred (Fadool and Dowling, 2008; Gross et al., 2005; Chhetri et al., 2014). Zebrafish can also breed with more frequency than other model organisms, with the capability of mating once a week all year round, easily giving researchers large sample sizes. Embryos are also fertilized and develop external to the mother, allowing researchers to directly observe the developmental process from fertilization through adulthood. These embryos are naturally transparent for

the first 24hpf when pigmentation begins, however, this pigmentation can easily be halted with the use of noninvasive chemicals (Chhetri et al., 2014; Kimmel et al., 1995). The importance of transparent and external embryos cannot be understated, as this allows for a multitude of imaging techniques to be utilized with minimal effect on natural development, a benefit to zebrafish not seen in most other model organisms. The timeline between embryo and larvae is quite short, with an embryo becoming a free swimming and food seeking larvae just five days post fertilization (Kimmel et al., 1995; Parichy et al., 2009; Fadool and Dowling, 2008). Between 30 and 60 minutes after fertilization the first cell division occurs and at just 24hpf the head, eye, tail, and beating heart are all visible under a basic microscope (Kimmel et al., 1995). Three days post fertilization (72hpf), large scale development has completed. At 5dpf, the embryo's swim bladder gives its buoyancy for swimming and it begins food seeking behavior (Kimmel et al, 1995; Parichy et al., 2009). By 14dpf the larvae take on more characteristics associated with adult fish including more prominent fins, scale development, and sexual characteristics, with full sexual maturity achieved by 8-12 weeks post fertilization (Parichy et al., 2009).

Zebrafish are a desirable model organism not only for their biological traits, but also for the ease of genetic manipulation and wide array of molecular techniques available to researchers. This is due in no small part to their fully sequenced and annotated genome. The zebrafish has been a popular organism to use for large scale forward genetic screens made possible by chemical mutagenesis, which allowed for the identification of many genes, especially in relation to eye development (Gross et al., 2005). With the identification of many genes through these genetic screens, as well as

sequencing, more targeted genetic approaches can be utilized. Reverse genetic screen targeting specific genes have greatly expanded with the continued introduction of a number of new techniques over the years. Knockdown experiments often use translation blocking or splice site modifying morpholinos or employ chemical mutagenesis. Several gene knockout techniques are also frequently implemented in zebrafish studies for genome editing, including zinc finger nucleases (ZFN), transcription activator-like effector nucleases (TALENs), and clustered regularly interspaced short palindromic repeats (CRISPR/Cas9).

1.6.2 Similarities and Differences in Zebrafish Eye Development

As with all vertebrates, eye development in zebrafish is a highly conserved process. At approximately 12hpf the optic primordia evaginates out towards the surface ectoderm on either side of the forebrain and by 18hpf has reached the surface ectoderm and initiated invagination of the primordia into the optic cup (Kwan et al., 2012; Kimmel et al., 1995; Fadool and Dowling, 2008; Richardson et al., 2017). At 16hpf, lens induction begins. At one day post fertilization (24hpf), the bi-layered optic cup is formed with the lens fully detached (Richardson et al., 2017). The next major macro change observed is the closing of the choroid fissure in the ventral region of the eye, which occurs at approximately 48hpf (Weaver et al., 2020). After this step, large scale morphological changes to the eye are complete.

Several small but significant difference between the zebrafish eye and the human eye lie within the structure of the retina. Similar to most vertebrates, the zebrafish eye contains the inner and outer nuclear layer, two plexiform layers, and the ganglion cell

layer (Richardson et al., 2017; Chhetri et al., 2014). The zebrafish have both rods and cones in their outer nuclear layers, however, there are 4 subtypes of cone photoreceptors. Humans possess 3 cone photoreceptor subtypes: blue, red, and green, but zebrafish also have an ultraviolet cone, expanding the amount of the visual spectrum they can see and interpret (Soules and Link, 2005; Chhetri et al., 2014). Perhaps most fascinating about the zebrafish eye is their ability to undergo repair and regeneration of their retinas throughout their lifetime. In response to disease, injury, or routine growth, the zebrafish retina can undergo neurogenesis and replace damaged or missing cone and rod photoreceptors, as well as other retinal cell types. New cells are generated in the ciliary marginal zones on the peripheral edge of the retina and from reactivated stem cell-like Müller Glia cells located throughout the retina in the outer nuclear layer (Wan et al., 2016; Bernardos et al., 2007). Mammalian retinas, while also containing Müller Glia cells, cannot undergo the same neurogenesis due to currently unknown roadblocks preventing their response to environmental cues and reactivation of the cell cycle (Bernardos et al., 2007).

Subtle differences in anatomy between the human and zebrafish AS are also present. The first of these differences focuses on AS maturation. Generally, in mammals, the maturation of many tissues is temporally dependent, meaning that full maturation is reached by certain ages in the organism's life. In zebrafish eye development however, maturation is directly correlated with the organism reaching a certain size, not its age (Chhetri et al., 2014; Soules and Link, 2005). In general, AS maturation occurs around 1-month post fertilization, but may occur earlier or later than this point depending on resource availability and tank size. In the zebrafish embryo, like all vertebrates, portions of the cornea develop from POM cells. In both humans and zebrafish, these cells migrate

into the AS space in a large collective group, whereas in birds, POM cells migrate in distinct waves (Soules and Link, 2005). However, between fish and mammals, POM cells appear to behave in largely the same manner, though further study on this is needed.

In zebrafish, the middle corneal stroma layer and corneal endothelial layer are thinner when compared to mammals. While the stromal layer does become thicker with age, the endothelial layer remains a single layer of flat cells (Soules and Link, 2005). The lens, formed from the same surface ectoderm as the corneal epithelium, also has a few differences in the zebrafish, chief among them its shape. The mammalian lens is elliptical, with a flatter anterior and posterior edge and circular sides, while the zebrafish lens is much more spherical (Chhetri et al., 2014; Richardson et al., 2017; Soules and Link, 2005). This distinction in shape cause there to be a much smaller volume of aqueous humor within the AS (Chhetri et al., 2014; Richardson et al., 2017). In mammalian eye morphogenesis, the lens undergoes invagination when it is induced by the approaching optic vesicle. However, in fish, the lens will instead delaminate from the surface ectoderm, thus creating a solid mass of cells making up the lens as opposed to the hollow shape formed by invagination (Chhetri et al., 2014; Richardson et al., 2017). In zebrafish and mammals, zonules attach to the lens at the equator and the nonpigmented epithelium of the ciliary, anchoring it in place. In zebrafish, the dorsal zonules are thicker than the ventral ones (Soules and Link, 2005).

In all vertebrates, the iris and ciliary structures are formed from the anterior most regions of the neural retina and migratory POM cells. The differentiation of the iris stroma cells occurs more rapidly in the dorsal half of the eye when compared to the ventral half, a pattern that can be seen in many different AS structures in zebrafish

(Soules and Link, 2005). A key difference when comparing mammalian irises to zebrafish is the lack of iris musculature in zebrafish (Soules and Link, 2005; Richardson et al., 2017). This means that zebrafish eyes lack the ability to control the amount of light entering their eyes because they cannot control their pupil size. Zebrafish do not have a ciliary process like mammals do, rather, they have what is called a ciliary zone located immediately below the iris (Soules and Link, 2005). The nonpigmented epithelium of the dorsal ciliary zone, like other structures, is thicker than those found in the ventral area. Dorsal ciliary zones are secretory and contain vesicles for aqueous humor production, which are missing in the ventral regions (Soules and Link, 2005).

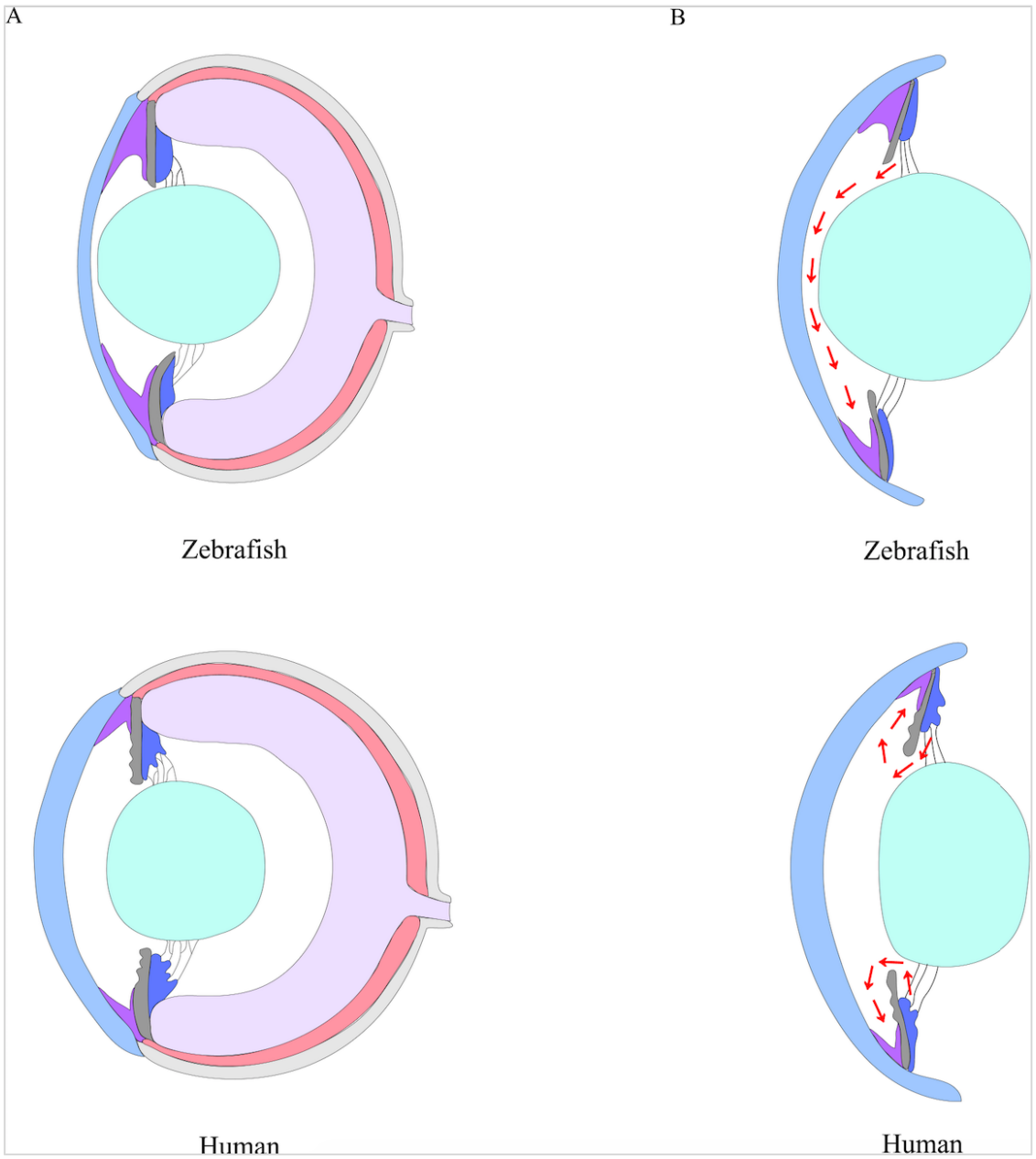

Figure 1.4: Structural Differences between the Zebrafish (*Danio rerio*) and Human Anterior Segment. (A) Cross section of whole mature eyes. Zebrafish have more elongated eye shape, with thinner corneas and more spherical lenses when compared to humans. Additionally, the ciliary zone and zonules located in the dorsal half of the eye are thicker than their ventral counterparts. Zebrafish lack iris musculature, making their irises incapable of dilating like humans. The zebrafish iridocorneal angle in the ventral

angle will develop into a mature structure containing porous openings and canals to drain aqueous humor, while the dorsal angle will not. **(B)** Aqueous Humor flow differences exist when comparing human and zebrafish eyes. Because of its structural differences between the dorsal and ventral AS regions, zebrafish will produce aqueous humor in the ciliary zone in the dorsal half of the eye, which will then flow into the anterior chamber, over the lens, and drain out through the canals of the ventral iridocorneal angle. In humans, the ciliary body produces aqueous humor around the entire eye. It flows up into the anterior chamber where it can be drain by the iridocorneal angle, also located around the entire circumference of the anterior. Image modified from Soules and Link, 2005.

The final differences in the zebrafish eye are related to the drainage structures of the iridocorneal angle, wherein fish have several differences when compared to mammals. Zebrafish possess a unique embryonic structure called the annular ligament that serves as a predecessor to the adult iridocorneal angle (Soules and Link, 2005). This ligament is a meshwork of fibrous tissues that runs the entire circumference of the anterior chamber. A thin layer of mesothelial cells separates the ligament from the iris surface (Chhetri et al., 2014; Richardson et al., 2017). In the dorsal half of the eye, the annular ligament is "U" shaped, while it is shaped more like a funnel in the ventral regions (Soules and Link, 2005). The funnel-like shape of the ventral region is an early indicator of the area's future drainage capabilities. With time, the ventral annular ligament will mature into the iridocorneal angle, creating a network of many porous openings and canals that lead to the angular aqueous plexus exterior to the sclera (Soules and Link, 2005). The main canals of the ventral angle can first be detected as early as 3dpf but take approximately one month to fully develop and begin draining fluids. While the dorsal region of the eye also contains the annular ligament during embryonic development, it does not mature in a similar manner to the ventral region and will lack both a canal network and absorptive tissues in adulthood (Soules and Link, 2005).

The flow of the aqueous humor is one of the major differences in zebrafish AS form and function when compared to mammals. In mammals, both the ciliary body and the iridocorneal angle have full 360 circumferential positions in the AS, allowing for both production and drainage of fluid around the entire eye. In general, mammalian aqueous humor is created by the ciliary behind the iris, the humor flows up through the pupil into the anterior chamber, where it is then drained by the iridocorneal angle located where the

cornea and iris meet at the edge of the angle (Richardson et al., 2017; Soules and Link, 2005) (**Figure 1.4**). In zebrafish, the humor instead is created and drained in one direction, dorsal to ventral. The aqueous humor is generated by the ciliary zone in the dorsal region, flows up into the anterior chamber via the pupil, and flows downward into the ventral angle region where drainage occurs (Chhetri et al., 2014; Richardson et al., 2017; Soules and Link, 2005) (**Figure 1.4**).

1.7 Hypothesis and Specific Aims

While previous work has identified a handful of genes expressed within the POM that are necessary for the proper development of different structures within the AS, little work has been done to determine the specification or identity of the POM themselves. Similarly, the timing or distribution of these cells as they enter into the ocular space, their transcriptional identity, nor their interactions amongst themselves or their environment has been comprehensively investigated. This lapse in knowledge of POM biology severely limits our ability to understand AS development and the delicate balance of gene expression and spatiotemporal marks. Furthermore, while genetic testing has determined the genetic cause of ASDs within a small fraction of affected individuals, the underlining cause in a vast majority of cases remain a mystery. The aim of this dissertation is to determine the early developmental underpinnings and molecular machinery of POM cell identity, its relationship to the neural crest, and its eventual role in the formation of AS components.

The hypotheses of this work and their individual specific aims are as follows:

I. Hypothesis: The Periocular Mesenchyme targeting to the developing anterior segment in zebrafish is heterogeneous in nature, comprised of several unique subpopulations.

-Characterize the existence of POM subpopulations, including their expression patterns and general arrival timing, using *in situ* hybridization.

-Using two-color fluorescent *in situ* hybridization, determine the amount of co-expression that exists between the subpopulations, taking note of locations within the AS where co-expression occurs and its persistence over time.

-Characterize and describe AS colonization of each POM subpopulation throughout eye development using transgenic reporter lines of well-known POM-related genes like *foxc1b*, *pitx2, foxd3,* and *lmx1b.1.*

-Analyze migratory behaviors over 24-hour periods of each POM transgenic line using 4D confocal live imaging.

-Identify genes with differing expression levels in the POM subpopulations denoted by our key transcription factors of interest. Validate genes with *in situ* expression data.

II. Hypothesis: Proper cNCC formation and migration is required for the proper development of the POM subpopulations and ocular anterior segment

-Determine the expression of POM-related genes in NC mutants including *Sox10, Tfap2a,* and *Foxd3* mutant embryos.

-Evaluate the expression levels of POM-related genes in wildtype and *Sox10* NC mutants by quantitative PCR (qPCR) at the height of POM colonization.

CHAPTER 2: MATERIALS AND METHODS

2.1 Zebrafish Maintenance

Zebrafish lines were bred and maintained in accordance with IACUC regulations (IACUC protocol 2015-1380) at the University of Kentucky. AB and ABix strains were used as wildtype. Transgenic lines used were: Tg[*foxc1b:GFP]* (Dr. Brian Link), Tg[*foxd3:GFP]* (Dr. James Lister), Tg[*pitx2C4:GFP]* (Dr. Elena Semina), Tg[*lmx1b.1:GFP]* (Dr. Brian Link), and Tg[*sox10:RFP]* (Dr. James Lister). Mutant lines used included: *Sox10CLS* (Dr. James Lister), *Tfap2a*^{sa24445} (Dr. Robert Cornell), and *Foxd3*$^{\Delta 537}$ (Dr. Robert Cornell). All embryos were raised for the first 24 hours post fertilization (hpf) in embryo media (E3) at 28˚C. After 24 hours, E3 media was replaced with embryo media containing 1-phenyl 2-thiourea (PTU) every 24 hours to maintain embryo transparency.

2.2 Whole-Mount *in situ* Hybridization (WISH)

Whole-mount *in situ* hybridizations were performed using a minimum of 20–25 embryos for each time point (12, 18, 24, 32, 36, 48, 54, and 72hpf). DIG and FITC labeled RNA probes were created using PCR incorporating T7 promoters in the primers and transcribed with T7 polymerase (Roche). Forward and Reverse primer sequences are listed in **Supplemental Table S3.1**. WISH protocol was performed as previously described (Thisse and Thisse, 2008). Embryos were fixed overnight at 4°C using 4% PFA. The following day, PFA was washed out with PBST 4x at 5 min each. Permeabilization with Proteinase K (10 µg/mL) was conducted at room temperature in the following manner: 12hpf = 2 mins; 18hpf = 3 mins; 24hpf = 5 mins; 32hpf = 12 mins;

48hpf = 20 mins; 54hpf = 28 mins; 72hpf = 40 mins). Permeabilization was washed out with PBST and then embryos were washed for a minimum of 2 hours at 65°C in hybridization buffer + tRNA before being incubated overnight in the desired probe (250µL) at 65°C. The following day, embryos were incubated in a series of solutions at 65°C to take them from a hybridization buffer to 2x SSC (5 min washes) before being incubated for 20 mins in 0.2 SSC+0.1% Tween. This was followed with 2x 20 mins washes in 0.1 SSC+0.1% tween at 65°C. Embryos were then washed in a series of solutions from 0.2 SSC to PBST (5 mins) at room temperature. For at least 1 hour, embryos incubated at room temperature on a shaker in blocking buffer (PBST, 2% sheep serum, 2mg/mL BSA). Finally, a 1/5000 concentration of anti-DIG or anti-FITC was added to fresh blocking buffer and the embryos were incubated overnight on a shaker at 4°C. On Day 3, the primary antibody was washed out with 4x 10 min washes of PBST and then washed in 4x 5 mins washes of coloration buffer. Coloration using NBT/BCIP was used at a concentration of 45µL/10mL and 35µL/10mL, respectively. Coloration protocols involving Fast Blue coloration (Sigma) were used at a concentration of 10µL/1mL for both NAMP and Fast Blue. Fast Blue colored embryos were also counterstained with DAPI at a concentration of 3µL/1mL. Dorsal, lateral, and ventral images of whole embryos stained with NBT/BCIP were captured using a Nikon Digital Sight DS-U3 camera and Nikon Elements software. Lateral 3D images of Fast Blue stained embryos were captured using a Nikon C2+ confocal microscope using a 20x (0.95 NA) oil immersion objective. All images were adjusted for brightness using Adobe Photoshop and assembled into figures using Adobe Illustrator.

2.3 Immunohistochemistry (IHC) for Distribution and Proliferation Analysis

Approximately 30 embryos were imaged for each transgenic line at each of the given time points (24, 26, 28, 30, 48, 54, and 72hpf). Embryos were fixed overnight at 4°C using 4% PFA. PFA was washed out with PBST 4 times for 5 min each. Embryos were permeabilized with Proteinase K (10 µg/mL) at the following times (24hpf = 5 mins; 26hpf = 6 mins; 28hpf = 7 mins; 30hpf = 9 mins; 48hpf = 20 mins; 54hpf = 25 mins; 72hpf = 40 mins), washed with PBST and then blocked with 5% goat serum (1 g/100 ml), 1% BSA in a solution of 1x PBST for at least 2 hours at room temperature. Primary antibody (Rockland rabbit anti-GFP) was diluted at 1/200 in blocking buffer and incubated overnight at 4°C on rotation. The following day, the primary antibody solution was washed out with PBST 5 times for 15 min each. Secondary antibody (Alexa Fluor 488 anti rabbit, 1/1000) and DAPI (1/2500) were diluted in blocking buffer and incubated for 1 hour on rotation in the dark at room temperature. Embryos were washed 2x for 15 min with PBST in the dark.

After staining, embryos were embedded in a 1.2% Low-gelling agarose in a 1-inch glass bottom cell culture dish (Fluorodish, World Precision Instruments) and visualized using a Nikon C2+ confocal microscope with a 20x (0.95 NA) oil immersion objective. The anterior segment of the eye was imaged in 3D in the lateral position as a 100µm z-stack using 3.50µm steps. All images were captured using Nikon Elements software, adjusted for contrast and brightness using Adobe Photoshop and assembled into figures using Adobe Illustrator. Images generated from IHC analysis were rendered in 3D using Nikon Elements Viewer software. Eyes were divided into 4 quadrants: dorsal nasal, dorsal temporal, ventral nasal, and ventral temporal. Nasal and temporal regions were

divided by a vertical straight line through the center of the lens, while dorsal and ventral were divided by a horizontal straight line through the center of the lens. For distribution analysis, GFP+ cells were manually counted based on their position within one of the four quadrants of a 3D constructed anterior segment. For each timepoint 25+ embryos from three independent trials were imaged for quantification.

2.4 Two-Color Fluorescent WISH

RNA probes were generated using the MEGAscript T7 transcription Kit (Ambion) in combination with RNA labeling mixes for both DIG and FITC (Roche). Double *in situ* hybridization was performed according to the protocol by Lauter et al. (2011) and Thisse (2008). WISH protocol was performed as previously discussed. Forward and reverse primers can be found in **Supplemental Table S3.1**. Both probes were added into embryo tubes to incubate at 65°C overnight (concentration dependent on probe), with the stronger probe used for Fast Red staining and the weaker one for Fast Blue staining. The WISH protocol for Day 2 was followed as previously described until the incubation step, in which anti-FITC (1/5000) was diluted in blocking buffer overnight at 4°C.

The following morning, anti-FITC was washed out 4-6x in PBST for 10 mins each. Coloration buffer was prepared with an adjusted pH of 8.2. Embryos are washed in coloration buffer 3x at 10 mins at room temperature on a shaker. While washing, NAMP and Fast Red solutions were brought to room temperature and made into the staining solution (1 NAMP tablet dissolved completely in 1mL ddH_2O, Fast Red tablet vortexed until completely dissolved in solution immediately before staining). Embryos were

incubated in the dark until proper staining was achieved after which embryos were washed 2x in PBST for 5 mins each and then incubated in 0.1M glycine (pH 2.2) for 10 mins at room temperature to inactivate the alkaline phosphatase. Embryos were washed 2x in PBST for 5 mins each and then incubated overnight at 4°C in blocking buffer + anti-DIG (1/5000) on a shaker. The following day embryos were again washed 4-6x in PBST for 10 mins each and then 3x in coloration buffer (adjusted to pH 8.2). During the washes, the staining solution was prepared by adding 10µL of NAMP to 1mL of coloration buffer and, in a separate tube 10µL Fast Blue was added to 1mL coloration buffer (pH 8.2) and kept in the dark. When embryos were ready to be stained, the NAMP solution was slowly added to the Fast Blue solution and vortexed before being added. Embryos were incubated in the dark until coloration was complete and washed 2x in PBST for 5 mins each. After successful *in situ* double staining, embryos were additionally stained using DAPI (3µL/1mL) and imaged using a NIKON C2+ confocal microscope. Images were adjusted for brightness and contrast using Adobe Photoshop and assembled into figures using Adobe Illustrator. 15–20 embryos were analyzed for each probe combination.

2.5 Time-Lapse Confocal *in vivo* Imaging

Embryos from each of the previously mentioned transgenic lines were collected and raised in E3 media at 28°C. Fluorescent embryos were placed in E3 PTU media including 3-amino benzoic acid ethyl ester (Tricaine) to prevent pigmentation and to anesthetize them, respectively. They were then dechorionated and embedded laterally in 1% low-gelling agarose in a 35mm glass bottom cell culture dish (Fluorodish, World

Precision instruments). Real-time imaging was conducted at 28°C using a Nikon C2+ confocal microscope and a 20× (0.95 NA) oil immersion objective. 3D *z*-stacks over a 75µm thickness with a slice size of 3.5µm were collected to encompass the entire developing anterior segment. *Z*-stack images were taken at 10 min intervals over a 24 hour period (embryos imaged: $n = 12$ *foxc1b:GFP*, $n = 9$ *foxd3:GFP*, $n = 13$ *pitx2:GFP*, $n = 10$ *lmx1b.1:GFP*, $n = 7$ *sox10:RFP*). Data were collected and rendered using Nikon Elements software. Images were adjusted for brightness using Adobe Photoshop and assembled into figures using Adobe Illustrator.

2.6 Cell Migration Tracking and Displacement Analysis

Completed 4D live imaging files were uploaded into FIJI software (https://fiji.sc) for analysis. Approximately 25 cells were manually tracked per video file using manual tracking tools. Tracked cells were measured for total distance traveled (µm), average velocity (µm/min), and total displacement (pixels). Tracked cells were randomly selected from all four eye quadrants to ensure all eye regions were represented, as well as all time frames. After tracking, data were exported to Microsoft Excel for statistical analysis. Displacement was measured using the line measurement tool in FIJI software. Previously tracked lines were identified as "completed" tracks in one of two ways: (1) at the end of the migration video or (2) the track was seen in the last frames of video before the specific track disappeared. Once the completed track was identified, the line measurement tool was used to measure the straight-line distance (in pixels) from the first point of the track to the last point of the track. Statistics were analyzed in Microsoft Excel and Graphpad Prism8.

2.7 Single Cell Transcriptomic Analysis

Embryos from each of the POM subpopulation transgenic lines were dechorionated and incubated in E3 media at 28˚C until 48hpf. At this time, embryos were anesthetized using 3-amino benzoic acid ethyl ester (Tricaine) and their eyes dissected and collected on ice. Eyes were incubated for 2 min in 0.25% Trypsin + EDTA at 37˚C. After incubation, a 20G needle and syringe were used to dissociate the tissue before the tube was placed back at 37˚C for 2 min. This process was repeated four times. After incubation, the dissociated cells were strained using a 40µm filter (VWR) and spun down for 10 min at 3,500 rpm at 4˚C. The supernatant was removed, and the pellet resuspended in 1x PBS + 2 mM EDTA and goat serum. Cells were sorted for GFP+ identity at the University of Kentucky Flow Cytometry and Immune Monitoring Core at the Markey Cancer Center. After sorting, cells were spun down and resuspended using PBS and goat serum. Approximately 1,000 cells from each transgenic line were then loaded onto the Chromium 10x V3 chip (10x genomics) and processed in the University of Kentucky Department of Biology Imaging Core to generate single cell barcoded cDNA. Sequencing was performed using NovaSeq SP, 2 x 150 bp paired ends to achieve 100,000 reads per cell at University of Illinois at Urbana-Champaign Roy J. Carver Biotechnology Center. Sequencing results were processed and subsequently aggregated (incorporating mapped normalization), using the Cell Ranger3.1 pipeline and results analyzed using Loupe Cell Browser 3.1.1 software (10× genomics).

2.8 Real-Time Quantitative PCR (qPCR)

Primers for POM and NC genes (*Foxc1a, Foxc1b, Foxd3, Pitx2, Lmx1b.1, Eya2,* and *Sox10*) as well as the endogenous control gene GAPDH were generated and validated (**Supplemental Table S4.1**). Total RNA was isolated from either AB control embryos or *Sox10CLS* mutant embryos at 36hpf using Trizol (Invitrogen). A total of 3 biological replicates were used for each treatment. cDNA was synthesized from the total RNA (1mg) using SuperScript reverse transcriptase (Invitrogen) and its concentration was quantified by Epoch Microplate Spectrophotometer (BioTek). cDNA was diluted to 100ng/mL. qPCR was performed in sets of three using 5µL of iTaq Universal SYBR Green Supermix (BioRad), 1µL total of Forward and Reverse Primers, 1µL of cDNA from either the control or *Sox10CLS* samples, and 3µL of ddH2O for a total sample volume of 10µL using the CFX Connect Real Time System (BioRad). Results were analyzed via the ΔΔCt standard method.

2.9 ALT-R CRISPR Injections

All gRNA, solutions, and protocols for ALT-R CRISPR experiments were obtained from Integrated DNA Technologies (IDT). Mutated sequences of *Sox10, Tfap2a,* and *Foxd3* crRNA:tracrRNA were predesigned by IDT to be nonfunctional knockouts for the zebrafish genome. The crRNA:tracrRNA work together to form a functional duplex wherein the crRNA contains the gene specific sequence and the tracr:RNA hybridizes to the crRNA to form a gRNA duplex that activates the Cas9. crRNA (100µm) was resuspended in 20µL of IDT Duplex Buffer (IDT) and incubated at 65°C for 10 mins. tracrRNA (100µm) was resuspended with 200µL of IDT Duplex

Buffer (IDT) and incubated at 65˚C for 10 mins. To form the duplex, 5µL of crRNA (50µM) was combined with 5µL of tracrRNA (50µM) in a PCR tube. The mixture was incubated at 95˚C for 5 mins before being rapidly cooled to 25˚C at a rate of 0.1˚C/sec. Once 25˚C had been reached, the solution was incubated for 5 mins.

The desired fish (WTs, *Sox10-CLS, Tfap2as*^{a24445}, *FoxD3*$^{\Delta 537}$) were released to breed and embryos were collected after 30 mins. Golden was used as an injection control. The final injection mix was as follows: 1.5µL of the Duplex mix (5µL of Duplex diluted in 5µL of IDT Duplex Buffer for a final concentration of 25µM), 1.5µL 25µM Cas9 protein, and 0.1µL dex red. 1-2nL of this mixture was injected into the cell of each embryo. After injection, embryos were stored at 28˚C in fresh E3 media. PTU media was not supplemented on these embryos to more easily identified mutants, which do not naturally pigment. Golden injected embryos were de-pigmented using 30% hydrogen peroxide until de-pigmentation had occurred.

2.10 Statistics

One-way ANOVA analysis (multiple point analysis) and unpaired *t*-tests (individual comparison analysis) were performed using Microsoft Excel and GraphPad Prism8 software. All graphs are shown with their respective means ± standard deviations. Values were considered significant by the conventional standard: *P*-value of 0.05 or less.

CHAPTER 3: SPATIOTEMPORAL CHARACTERIZATION OF ANTERIOR SEGMENT MESENCHYME HETEROGENEITY DURING ZEBRAFISH OCULAR ANTERIOR SEGMENT DEVELOPMENT

Kristyn L. Van Der Meulen, Oliver Vöcking, Megan L. Weaver, Nishita N. Meshram and Jakub K. Famulski

Previously Published in *Frontiers in Cellular and Developmental Biology;* May 2020

3.1 ABSTRACT

Assembly of the ocular anterior segment (AS) is a critical event during development of the vertebrate visual system. Failure in this process leads to anterior segment dysgenesis (ASD), which is characterized by congenital blindness and predisposition to glaucoma. The anterior segment is largely formed via a neural crest-derived population, the Periocular Mesenchyme (POM). In this study, we aimed to characterize POM behaviors and transcriptional identities during early establishment of the zebrafish AS. Two-color fluorescent *in situ* hybridization suggested that early AS associated POM comprise of a heterogenous population. *In vivo* and time-course imaging analysis of POM distribution and migratory dynamics analyzed using transgenic zebrafish embryos (Tg[*foxc1b:*GFP], Tg[*foxd3:*GFP], Tg[*pitx2:*GFP], Tg[*lmx1b.1:*GFP], and Tg[*sox10:*GFP]) revealed unique AS distribution and migratory behavior among the reporter lines. Based on fixed timepoint and real-time analysis of POM cell behavior a comprehensive model for colonization of the zebrafish AS was assembled. Furthermore, we generated single cell transcriptomic profiles (scRNA) from our POM reporter lines and characterized unique subpopulation expression patterns. Based on scRNA clustering analysis we observed cluster overlap between neural crest associated (*sox10*/*foxd3*), POM

(*pitx2*) and finally AS specified cells (*lmx1b*, and *foxc1b*). scRNA clustering also revealed several novel markers potentially associated with AS development and/or function including *lum*, *fmoda*, *adcyap1b*, *tgfbi*, and *hmng2*. Taken together, our data indicates that AS-associated POM, or Anterior Segment Mesenchyme (ASM), is not homogeneous but rather comprised of several subpopulations with differing colonization patterns, migration behavior, and transcriptomic profiles.

3.2 INTRODUCTION

Vertebrate cranial development has benefitted significantly from the evolutionary addition of the multipotent neural crest cells (NCC). Originating in the dorsal neural ectoderm of the folding neural tube, neural crest cells (NCC) undergo an epithelial-to-mesenchymal transition, detaching themselves from the epithelial sheet and migrating in distinct streams to invade regions all over the developing embryo. NCCs ultimately go on to form diverse mesodermal derivatives including cartilage, myofibroblasts, neurons, and glial cells (Trainor and Tam, 1995; Langenberg et al., 2008; Williams and Bohnsack, 2015). In the developing cranial region, migrating NCCs come together with lateral plate mesoderm to surround the developing optic cup and form the Periocular Mesenchyme (POM) (Trainor and Tam, 1995; Langenberg et al., 2008; Williams and Bohnsack, 2015). POM subsequently contribute to the development of the ocular anterior segment (AS) (**Supplementary Figure S3.1**) (Fuhrmann et al., 2000; Creuzet et al., 2005; Williams and Bohnsack, 2015; Akula et al., 2018). The AS, comprising of the cornea, lens, iris, ciliary body, and drainage structures of the iridocorneal angle, is essential for the function of the visual system. The AS focuses light onto the retina while maintaining intraocular

homeostasis.

Anterior segment development begins after the establishment of the optic cup, when POM cells migrate into the periocular space between the retina and the newly established corneal epithelium (Creuzet et al., 2005; Cavodeassi, 2018). These mesenchymal cells will eventually differentiate into the corneal stroma and endothelium, iris and ciliary body stroma, and the iridocorneal angle, amongst others. Mis-regulation of POM migration or function has been associated with congenital blinding disorders under the term anterior segment dysgenesis (ASD). ASD includes, alone or in combination, corneal opacity, iris hypoplasia, polycoria, corectopia, posterior embryotoxon, juvenile glaucoma, and disorders including Peter's Anomaly and Axenfeld-Rieger Syndrome (Gould et al., 2004; Volkmann et al., 2011; Akula et al., 2018). These rare autosomal dominant disorders, in addition to ASD phenotypes, also often exhibit systemic issues including dental malformations and craniofacial defects (Volkmann et al., 2011; Bohnsack et al., 2012; Ji et al., 2016). In addition to congenital diagnoses, failure of proper AS formation may also result in a predisposition to ASD later in life. Despite its fundamental role in the establishment of the AS, little is understood about the mechanisms governing POM specification, migration or differentiation.

The most common mutations seen in ASD patients involve the transcription factor *pitx2* (Paired-like homeodomain) (Ji et al., 2016), as well as *foxc1* (Forkhead Box c1) (Berry et al., 2006; Bohnsack et al., 2012; Reis et al., 2012; Chen and Gage, 2016; Seo et al., 2017). Loss of function of either *pitx2* or *foxc1* has been shown to result in ASD phenotypes in mice and zebrafish (Berry et al., 2006; Liu and Semina, 2012; Reis et al., 2012; Chen and Gage, 2016; Ji et al., 2016; Seo et al., 2017; Hendee et al., 2018). *Pitx2*

in particular has been associated with the survival and migration of NCCs, as well as the development of the optic stalk, establishment of angiogenic privilege within the cornea, and craniofacial development (Evans and Gage, 2005; Bohnsack et al., 2012; Liu and Semina, 2012; Gage et al., 2014; Chawla et al., 2016; Chen and Gage, 2016; Ji et al., 2016; Hendee et al., 2018). *Foxc1* and *pitx2* are also known to interact with one another, and their expression is regulated by retinoic acid signaling (Matt et al., 2005; Chawla et al., 2018). Not surprisingly, mutations in NCC regulatory genes have also been associated with ASD. *Foxd3* (Forkhead Box d3) has been implicated in ASD (Volkmann Kloss et al., 2012) and is known to regulate early NCC specification, migration and long-term cell survival (Lister et al., 2006; Stewart et al., 2006; Drerup et al., 2009; Wang et al., 2011). *Sox10* (SRY- Box 10), another key regulator of the NCC population (Dutton et al., 2001; Creuzet et al., 2005; Langenberg et al., 2008; Drerup et al., 2009; Williams and Bohnsack, 2015), is critical for NCC migration and viability during early development (Dutton et al., 2001). Finally, *lmx1b* (LIM homeobox Transcription Factor 1 beta) is associated with Nail-Patella syndrome and glaucoma predisposition (McMahon et al., 2009; Liu and Johnson, 2010). *Lmx1b* is expressed within the developing cornea, iris, ciliary bodies, and trabecular meshwork of the iridocorneal angle in mice (McMahon et al., 2009; Liu and Johnson, 2010) and is essential for POM migration in zebrafish (McMahon et al., 2009). While several genes have been linked to POM or ASD, few studies to date have shed light on how POM cells, migrate to and participate in AS formation.

One signaling molecule that is known to be involved in cranial neural crest cell migration and anterior segment specification is Retinoic Acid (RA). RA, a metabolite of

vitamin A, is instrumental for the overall development of the eye. RALDHs (RA-synthesizing enzyme retinaldehyde dehydrogenases) are expressed in a gradient through the eye, specifically in the retina, cornea, RPE, and lens (Matt et al., 2005, 2008; Lupo et al., 2011). RA produced in these areas diffuses out toward the anterior space of the developing eye, which will be populated by the POM. RA signaling is activated through the heterodimer receptors RARα/RARβ and RARα/RARγ expressed within the POM (Matt et al., 2005, 2008; Lupo et al., 2011). This signal is a vital determinate in eye morphogenesis. Activation of these receptors helps to control *eya2* dependent apoptosis in the POM as well as control the expression levels of *foxc1* and *pitx2* and therefore anterior segment development (Matt et al., 2005, 2008). NCC-specific deactivation of RARα, RARβ, and RARγ results in a complete loss of *pitx2* in the POM and AS, while increased RA signaling leads to an increase in *pitx2*, *foxc1a*, and *lmx1b.1* (Matt et al., 2008; Lupo et al., 2011). Though not explicitly explored in this study, RA signaling is a crucial component of cell migration and overall eye morphogenesis.

Although information about the anatomy of the anterior segment in vertebrates and anatomical consequences of POM regulatory gene mutations has been well documented, few studies have investigated the mechanism of development for AS structures overall. Specifically, little is known about when or how POM cells acquire their AS targeting, behave during migration, interact with one another, and finally, specify into various AS structures. Within this study, we aimed to characterize the developmental underpinnings that drive the formation of the AS. Using zebrafish embryos, we characterized the precise migration patterns and transcriptional profiles of AS associated POM cells (ASM). We specifically examined ASM gene expression as

well as cellular distribution by taking advantage of POM-associated transgenic lines; Tg[*foxc1b:*GFP], Tg[*foxd3:*GFP], Tg[*pitx2*:GFP], Tg[*lmx1b.1:*GFP], and Tg[*sox10:*GFP]. In doing so, we have cataloged distribution, migratory dynamics, and population size of ASM during early AS development. Furthermore, single cell transcriptomic comparison of isolated ASM cells revealed four specific clusters, each associated with potentially novel AS regulatory genes. Our findings indicate that AS-associated POM is composed of several subpopulations, each identifiable by their own distributions, migratory patterns, and gene expression profile.

3.3 RESULTS

3.3.1 POM-Associated Genes Exhibit Unique Expression Patterns During Early Establishment of the Anterior Segment

With several genes being implicated in regulating POM migration and identity, we first chose to carefully characterize patterns of their expression during zebrafish ocular morphogenesis (12–72hpf). Whole Mount *in Situ* Hybridization (WISH) using embryos aged 12, 18, 24, 32, 48, and 72hpf revealed that POM-related genes *foxc1a*, *foxc1b*, *eya2*, *foxd3*, *pitx2*, *sox10*, *lmx1b.1* and *2*, display both overlapping and individualized expression patterns within their originating neural crest streams and surrounding the AS (**Figure 3.1**). Several POM-related genes showed expression at 12hpf, the earliest time point we assayed, suggesting that POM acquire their identity early, perhaps immediately following their delamination from the neural tube. As the optic cup begins to take shape (18hpf), *foxc1a*, *foxc1b*, and *sox10* expressing POM cells

are already visible within the craniofacial space. At the same time, *pitx2* expression is absent from periocular regions and presents primarily in the lens. By 24hpf we observed various degrees of periocular expression of all the aforementioned POM-associated genes. *Foxc1a* displays the prototypical POM expression pattern with signal extending from the forebrain and into the surrounding periphery, and on top of, the retina by 32hpf (**Figure 3.1 A** and **Supplementary Figure S3.1**). Similar, albeit much weaker expression of *foxc1b* and *eya2* can be observed at 24 and 32hpf (**Figures 3.1 B,H**). Both *foxd3* and *sox10* display partial periocular patterns of expression, predominantly in the temporal regions at 24hpf and more homogenously by 32hpf (**Figures 3.1 C,G**). *Pitx2* also displays strong periocular expression staining at 32hpf but is also uniquely expressed in the lens (**Figure 3.1 D**). Periocular- like expression patterns become clearest by 48hpf for *foxc1a*, *foxc1b*, *eya2*, *pitx2*, and *sox10*. *Foxd3* periocular expression is significantly diminished by 48hpf. By 72hpf only *foxc1a*, *pitx2*, *sox10*, and *eya2* still exhibit strong periocular expression. In spite of the implicated role of *lmx1b* genes in pathogenic features of the Nail-Patella Syndrome (McMahon et al., 2009; Liu and Johnson, 2010), both *lmx1b.1* and *lmx1b.2* genes did not display classical AS expression patterns in our WISH assay at early timepoints, 12–48hpf, but are detected in the AS at later stages, 72hpf+ (**Figures 3.1 E,F**). Taken together, we observe that POM- associated genes are not uniformly co-expressed in POM cells during early AS formation. Early POM, 12–24hpf, express high levels of *foxc1a*, and only at later stages of AS colonization, 24–32hpf, do they initiate high levels of expression for *foxc1b*, *eya2,* and *pitx2*. POM cells which express *sox10/foxd3* display periocular patterns only after 24hpf, suggesting they may arrive as a second wave. At late stages of AS colonization, 48–72hpf, we observe the

persistence of strong *foxc1a* expression and an upregulation of *foxc1b*, *pitx2*, and *eya2*. Between 48 and 72hpf, *sox10* expression is detected throughout the AS but does not appear to increase significantly while *foxd3* expression is no longer detected in the AS after 48hpf. Based on our WISH observations, we therefore hypothesized that AS colonizing POM populations are likely heterogenous.

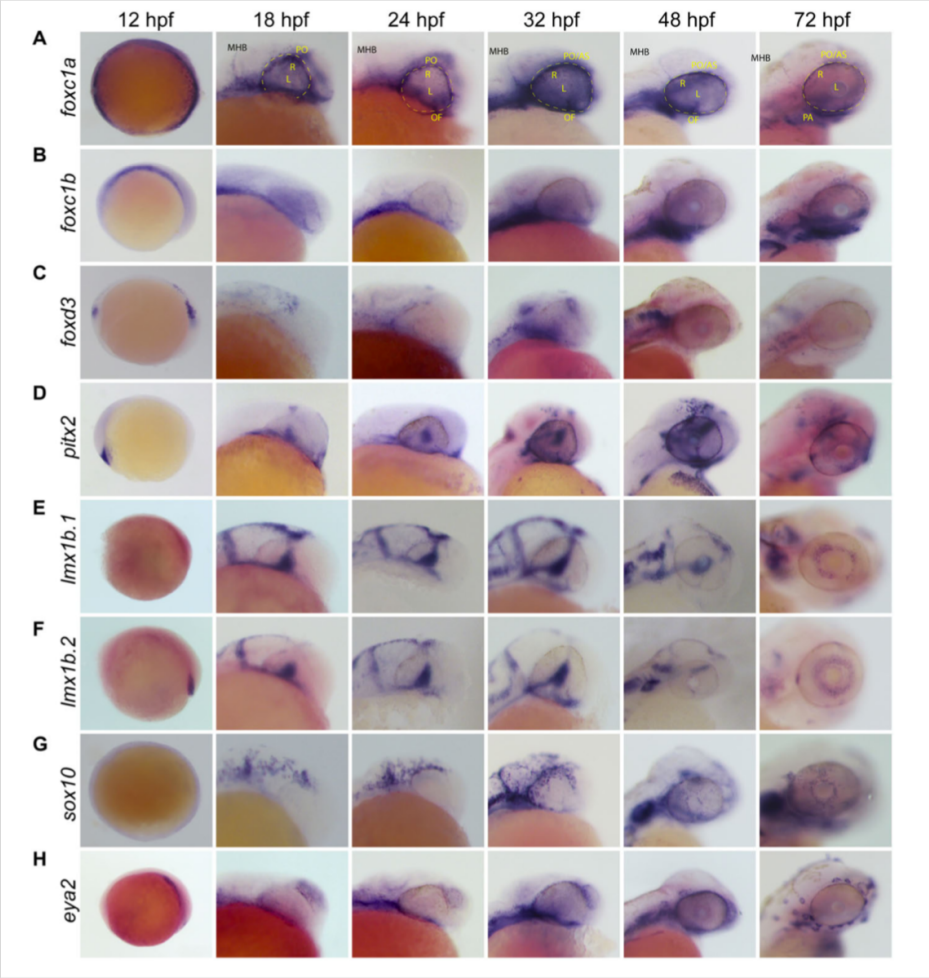

Figure 3.1: Whole Mount *In Situ* Hybridization (WISH) of known POM and neural crest-related marker genes. Whole-mount in situ hybridization for POM marker gene mRNA expression patterns were observed during early to late stage eye development in the lateral view. POM genes examined were **(A)** foxc1a, **(B)** foxc1b, **(C)** foxd3, **(D)** pitx2, **(E)** lmx1b.1, **(F)** lmx1b.2, **(G)** sox10, and **(H)** eya2. Foxc1a, foxc1b, pitx2, eya2, and sox10 in particular show strong expression surrounding the optic cup and on the surface of the anterior segment from 24 to 72hpf. Lmx1b.1 and lmx1b.2 expression is detected within the anterior segment, surrounding the lens by 48–72hpf. MHB, midbrain-hindbrain boundary; R, retina; L, lens; OV, optic vesicle; PO, periocular space (outlined with dashed line); OF, optic fissure; AS, anterior segment.

3.3.2 Co-expression Analysis Confirms Anterior Segment Mesenchyme Heterogeneity

Based on our WISH study, we next sought to determine the extent of co-expression between the POM associated genes. To study these relationships, we performed two-color fluorescent whole mount *in situ* hybridization (FWISH) at 32 and 48hpf. These timepoints represent early and intermediate steps of POM AS colonization. We focused our attention on the expression of *foxc1*, *foxd3*, *sox10*, and *pitx2* as they represent the best studied AS-associated POM marker genes. 3D confocal imaging qualitatively indicated that all these POM markers clearly exhibit both overlapping and individualized expression patterns at 32hpf (**Figures 3.2 A–F**). All of our described results are based on reproducible patterns observed in 12hpf+ embryos from two independent experiments. At 32hpf, *foxc1* expression appears restricted largely to the periphery of the AS while *sox10*, *foxd3*, and *pitx2* display varying degrees of expression throughout the dorsal, ventral, nasal, and temporal quadrants. *Pitx2* exhibited broad expression throughout the AS and a high degree of co- expression with *foxc1*, primarily in the dorsal quadrant, and *sox10*, throughout the entire AS, at 32hpf (**Figures 3.2 C,D**). *Foxc1* exhibited a high degree of co-expression with *pitx2* in the dorsal and ventro-temporal AS and partial co-expression with *foxd3* and *sox10* (**Figures 3.2 A,B,D**). The expression of *sox10* was most pronounced in the dorsal AS and had the highest degree of co-expression with *foxd3* (**Figures 3.2 B,C,F**). *Foxd3* expression was detected throughout the AS, albeit in fewer cells than the other markers, and exhibited a co-expression primarily with *sox10* and *pitx2* throughout the entire AS (**Figures 3.2 A,E,F**). By 48hpf, noticeably pronounced individualized expression patterns emerged (**Figures**

3.2 G–L). *Pitx2* expression became restricted to the dorsal and ventral quadrants of the AS, while *foxc1* expression expanded into the entire AS (**Figures 3.2 G– K**). Co-expression was still evident between *pitx2* and *foxc1*, but primarily in the dorsal and ventral quadrants. *Foxd3* and *sox10* maintained the same spatial pattern of expression as observed at 32hpf and continued to have a high degree of co- expression, particularly surrounding the lens (**Figure 3.2 L**). *Foxd3* and *sox10* continued to have only minor co-expression with *pitx2* or *foxc1* throughout the AS. We also analyzed expression of *eya2* and observed a high degree of co-expression with *pitx2* throughout the entire AS, and slight co-expression with all the other markers (**Supplementary Figure S3.2**). Taken together, we show that already at 32hpf AS-associated POM do not exhibit a homogenous expression pattern of POM-associated regulatory genes. This suggest that the AS is colonized as an already heterogenous population rather than undergoing later diversification from a common progenitor.

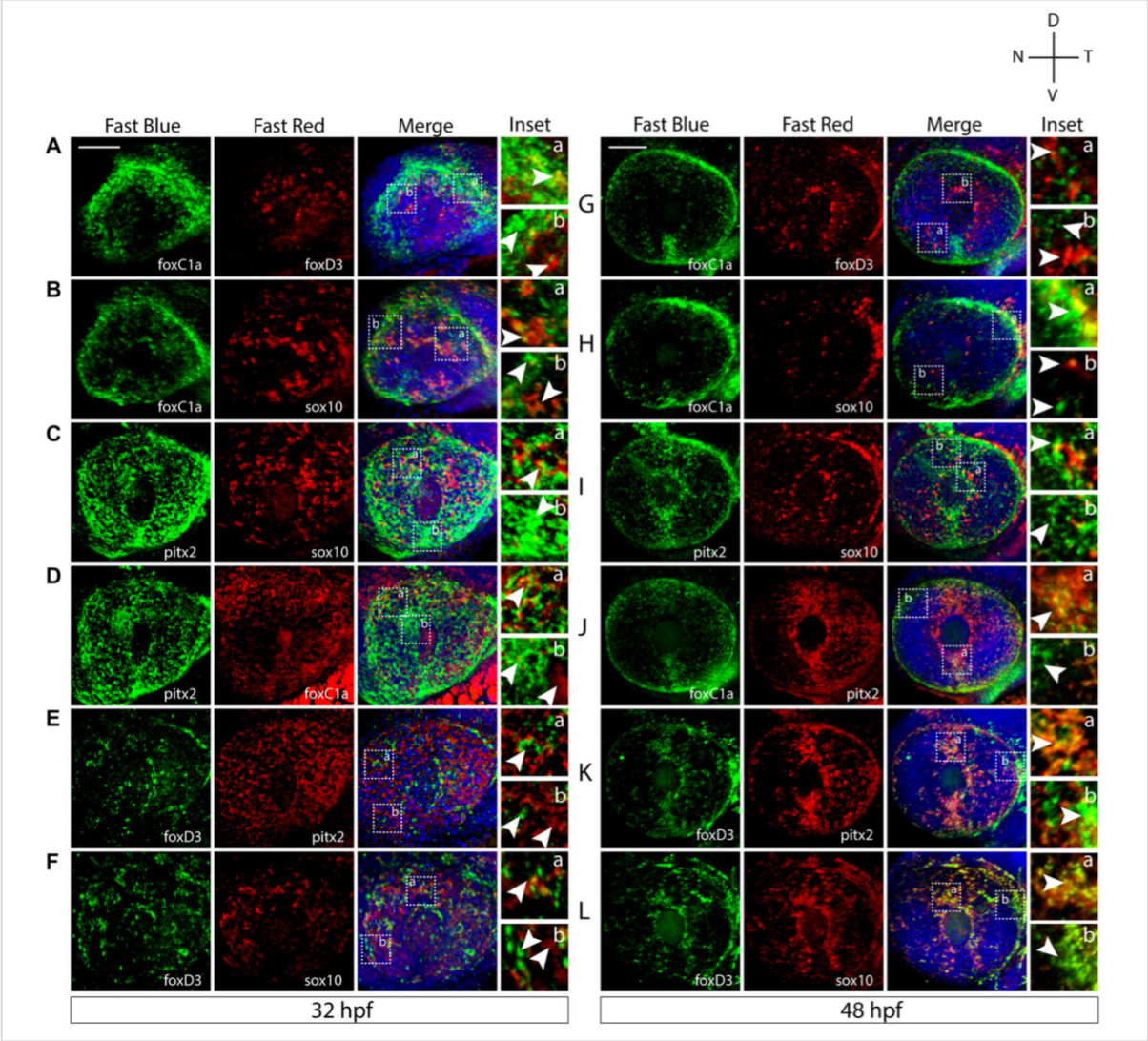

Figure 3.2: Two-color fluorescent in situ hybridization supports ASM heterogeneity. Two-color fluorescent WISH (FWISH) performed for all possible combinations of *foxc1a, foxd3, pitx2*, and *sox10* at 32 **(A–F)** and 48hpf **(G–L).** DAPI is in blue. Lateral images of 3D reconstructions are displayed. White arrows within inset panels (dashed squares) display instances of individual (b) and co-expression (a). Scale bar = 50µm.

3.3.3 POM Cells Display Distinct Targeting Patterns During Early AS Colonization

Based on our FWISH results we hypothesized that the heterogenous population of AS progenitors may display unique migration patterns and behavior. Furthermore, key to our understanding of AS formation will be the awareness of when and how the POM colonize. To begin characterizing this process, we first took advantage of available transgenic lines known to label POM: Tg[*foxc1b:*GFP], Tg[*pitx2:*GFP], Tg[*lmx1b.1:*GFP], or NCC: Tg[*foxd3:*GFP], Tg[s*ox10:*GFP] (Matt et al., 2005, 2008; McMahon et al., 2009; Volkmann et al., 2011). These reporter lines enable single cell distribution analysis while also delineating lineage specification. Due to persistence of GFP protein, these lines do not necessarily represent active expression of their reporter driven promoter but do mark the lineage of POM/NCCs that have, at some point, expressed the respective POM-associated gene. To analyze AS colonization, transgenic embryos were fixed at key AS developmental stages (24, 26, 28, 30, 48, 56, and 72hpf) and immunohistochemistry (IHC) was used to detect GFP. 3D confocal images of the AS were collected for each transgenic line at each timepoint and were employed to subsequently quantify distribution of the cells within the AS (**Figure 3.3 A**). In particular, 3D rendered images of the AS were subdivided into four quadrants (**Figure 3.3 A, top left panel**) and cells found in each were quantified at each timepoint.

Our assay revealed that initial colonization of the AS begins at approximately 22hpf (data not shown) with GFP+ cells of the *pitx2*-derived population occupying the temporal AS regions (**Figure 3.3 A**). At 24hpf *foxc1b*, *foxd3*, and *lmx1b.1* derived GFP+ cells have begun to enter the AS across the dorsal most periocular regions, while *sox10*-derived cells begin to occupy all four regions. By 28hpf all of the reporter lines, with the

exception of *pitx2*, exhibit GFP+ cells primarily in the dorsal half of the AS. Tg[*foxc1b*:GFP] signal is also observed in the developing lens region up to 32hpf, but was not considered for our analysis. Similarly, up to 32hpf Tg[*lmx1b.1*:GFP] non-AS signal is observed in the dorsal-nasal region but is not considered in our analysis because it does not contribute to the AS. *Foxc1b*, *foxd3*, and *sox10* derived cells continue to spread to the ventral regions with roughly equal distribution throughout the AS by 48hpf. Conversely, *pitx2*-derived cells remain exclusively associated with the temporal half of the AS while *lmx1b.1*-derived cells gradually re-distribute to occupy the nasal half of the AS. Starting at 54hpf and continuing to 72hpf, Tg[*pitx2:*GFP] expression turns off in POM cells and initiates in what is likely photoreceptor progenitor cells. Of note, our Tg[*pitx2*:GFP] transgenic line did not exhibit GFP signal in all regions of AS that were found to be positive for *pitx2* mRNA using FWISH (**Figures 3.2, 3.3 A**). We hypothesize this discrepancy arises from the fact that ASM progenitor cells induce *pitx2* expression upon arrival at the AS, while the GFP+ cells are a lineage mark of the early *pitx2*+ progenitors. The enhancer element driving the Tg[*pitx2*:GFP] line, C4, may be no longer responsive in ASM cells at the later time points and therefore explain the lack of GFP signal in all of the *pitx2* expressing cells.

All of our observations were subsequently validated by quantification of each GFP+ population (**Figure 3.3 B**). At 24hpf the majority of POM cells are located within the dorsal half of the AS, with the exception of *pitx2*-derived cells. By 30hpf we note a significant reduction in the proportion of *foxc1b*, *foxd3*, and *lmx1b.1*-derived cells in the dorsal half combined with significant increase of these cells in the ventral half. At 48hpf, we found equal distribution of *foxc1b*, *foxd3*, and *sox10* derived cells within all regions of

the AS, while *lmx1b.1*-derived cells become predominantly associated with the nasal half of the AS.

Overall, we observe an ordered pattern of AS colonization, as summarized in **Figure 3.3 C**. The majority of POM cells, *foxc1b*, *foxd3*, and *sox10:*GFP-derived cells, enter the AS along the dorsal retina and progress ventrally, while the *pitx2:*GFP sub-lineage enters the AS temporally and remains exclusively within the temporal AS. *lmx1b.1*:GFP cells enter the AS dorsally and initially migrate ventrally but by 48hpf become restricted to the nasal regions of the AS.

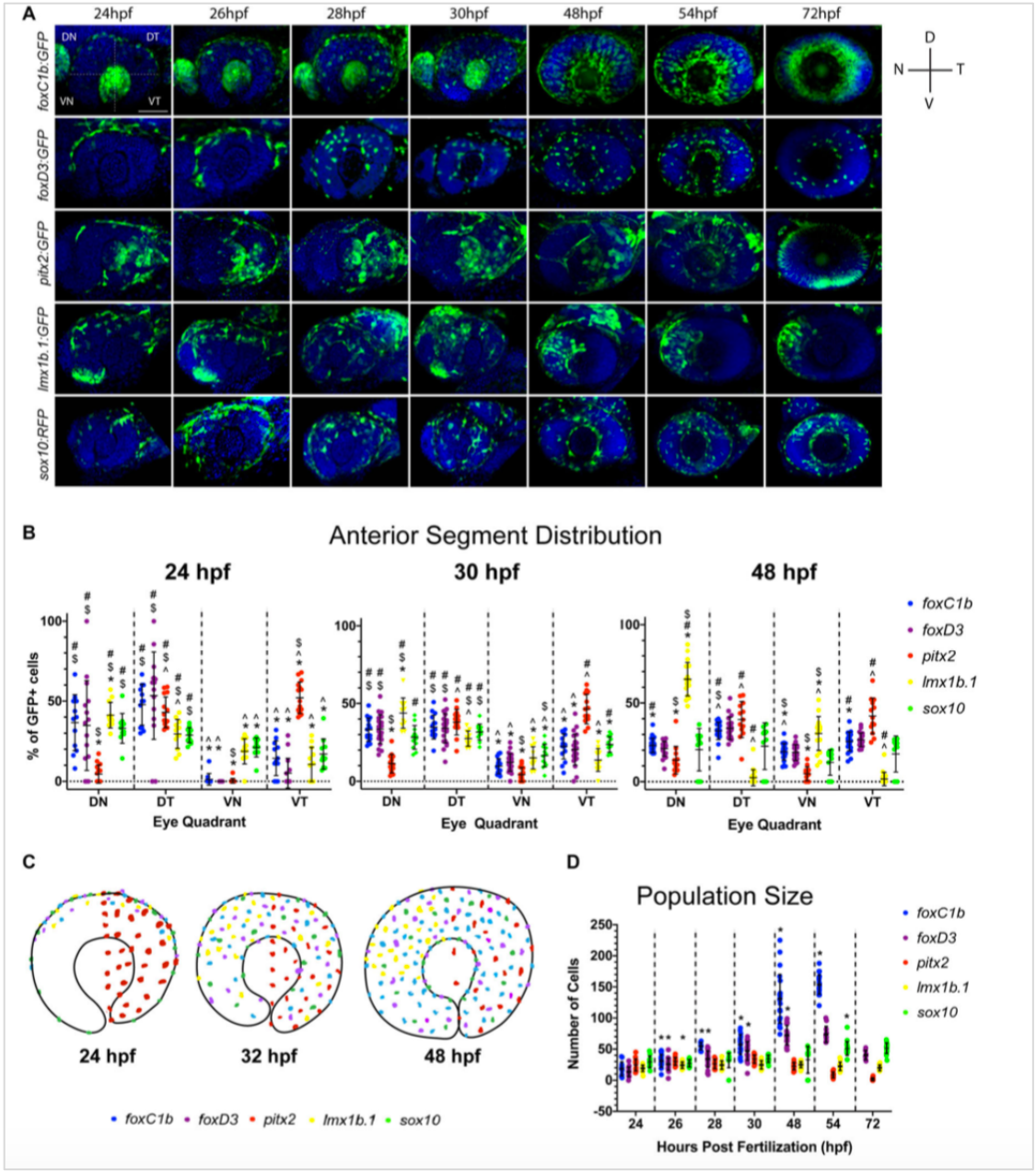

Figure 3.3: Periocular mesenchyme subpopulation distribution analysis. (A) 3D rendering of confocal stacks encompassing the AS in POM transgenic lines between 24 and 72hpf. GFP+ cells are green, DNA was stained with DAPI (blue). DN, dorsal-nasal; DT, dorsal-temporal; VN, ventral-nasal; VT, ventral-temporal. Scale bar = 50µm. **(B)** Distribution of quantified GFP+ cells within each AS quadrant (DN, DT, VN, and VT) at

24, 30, and 48hpf. Distribution is represented as an average percentage of the total number of GFP+ in each quadrant of the AS for each transgenic line. Statistically significant difference ($p < 0.05$): * vs. DT, # vs. VN, $ vs. VT and ˆ vs. DN. **(C)** Model of POM colonization at 24, 30, and 48hpf. **(D)** Average AS cell population size for each transgenic line at 24–72hpf. * indicates statistically significant ($p < 0.05$) change from previous time point.

3.3.4 Cell Proliferation Does Not Drive ASM Population Growth During AS Colonization

A distinct fluctuation in the total number of GFP+ cells within each transgenic line examined throughout the time course was also noted. While *lmx1b.1*, *pitx2*, and *sox10*-derived populations maintained a relatively consistent total number of cells, f*oxc1b* and *foxd3*-derived populations increased in size over time (**Figure 3.3 D**). This is particularly evident in the *foxc1b*-population which increased size so significantly by 72hpf that it was no longer quantifiable by our assay. Having documented the increase in population size of some ASM subpopulations, we next sought to understand the mechanisms responsible for this change. Specifically, we wanted to investigate whether the increase in population size of the *foxc1b:GFP* and *foxd3:GFP* subpopulations was the result of a continued influx of migratory cells into the AS or proliferation of cells already in the AS. Transgenic embryos were fixed at 32 and 48hpf as this window in development sees the largest increase in population size. Proliferating cells were identified using pH3 antibody staining. 3D images of the AS were collected using a confocal microscope. Cells positive for both the GFP and the pH3 signal were quantified (**Supplementary Figure S3.3**). Little to no pH3 signal at either 32 or 48hpf in *foxd3*:GFP or *foxc1b*:GFP embryos, or any of our transgenic lines, indicates that ASM cells are not actively dividing while migrating within the AS. Based on these data, we suggest that the increase in *foxc1b*:GFP and *foxd3*:GFP cell populations is the sole result of rapid and continuous migration of cells to the AS between 32 and 48hpf.

3.3.5 ASM Subpopulations Exhibit Unique Migratory Behavior

In addition to cellular distribution over time, we also sought to catalog the migratory behavior of ASM cells. Specifically, we aimed to determine if they behaved in a similar fashion to cranial NCCs. Hence, we tracked their migration within the AS using *in vivo* 4D imaging. Using this approach we documented migration of *foxc1b:*GFP, *foxd3:*GFP, *pitx2:*GFP, *lmx1b.1:*GFP, and *sox10:*GFP-derived cells (**Figure 3.4 A**). Qualitative examination of our data indicated that in all the transgenic lines, ASM cells migrated in a stochastic manner. This suggests that similar to cranial NCCs, ASM cells lack leader/follower cell identities or chain migration behavior (**Figure 3.4 A** and **Additional Files M3.1**–**M3.5**). The 4D data sets mirrored the cellular distribution trends we quantified in our previous time course assay (**Figure 3.3**). As expected based on our distribution studies, both *pitx2* and *lmx1b.1*:GFP cells displayed very specific distributions within the AS (**Figure 3.4 B**), while *foxc1b*, *foxd3*, and *sox10:*GFP had more homogenous distribution patterns.

To analyze individual migratory behavior, we performed individual cell tracking. As expected, *foxc1b:*GFP, *foxd3:*GFP, *lmx1b.1:*GFP and *sox10*:GFP-derived cells migrated in a general dorsal to ventral pattern (**Figure 3.4 B** and **Additional Files M3.6–M3.10**). *Pitx2:*GFP cells migrated in a generally temporal to nasal direction (**Figure 3.4 B**). Tracked cells were analyzed for their total distance traveled, directed migration, and velocity. *Foxc1b*-derived ASM had the highest velocities (0.115 ± 0.048μm/min) while the cells of the *pitx2*-derived subpopulation were the slowest (0.049 ± 0.023μm/min) (**Figure 3. 4 C**). *Foxd3*, *lmx1b.1*, and *sox10*-derived ASM cells had similar velocities (0.095 ± 0.042; 0.091 ± 0.050; and 0.079 ± 0.033μm/min). When examining total

distance traveled, *foxc1b*-derived cells displayed the farthest distances overall (44.667 ± 18.531μm), while *pitx2*-derived cells exhibited the shortest (20.719 ± 9.936μm) (**Figure 3.4 D**). *Foxd3*, *lmx1b.1*, and *sox10*-derived ASM all exhibited similar overall distances traveled (37.339 ± 16.769; 33.267 ± 15.869; and 31.688 ± 13.289μm). Differences in total migratory distance and velocity based on the AS quadrant of entry were also compared. Only *foxc1b*- derived cells originating in the dorsal temporal quadrant showed differences in migration displaying shorter total distance traveled and slower velocity (data not shown). Based on analysis of migration velocity and distance traveled we conclude that ASM exhibit of a mixture of migration patterns and behaviors. This further supports our hypothesis that during colonization of the AS, the ASM are a heterogenous population.

Lastly, we measured the degree of directed migration by examining individual cell displacement within the AS (**Figure 3.4 E**). Displacement was used as a measure of purposeful, or targeted, migration. We saw that cells within the *sox10* subpopulation showed the highest overall displacement (136.885 ± 63.327 pixels), followed by cells in the *foxd3* subpopulation (109.70 ± 75.434 pixels). Displacement of *foxc1b* and *lmx1b.1* was found to be 84.632 ± 49.223 and 95.559 ± 61.285 pixels, respectively. Similar to our previous observations for velocity and distance, the *pitx2* subpopulation exhibited the least amount of displacement (44.698 ± 33.008 pixels). Our data indicate that all ASM cells are highly migratory, but that as observed for POM marker gene expression, there is heterogeneity when comparing the various reporter lines.

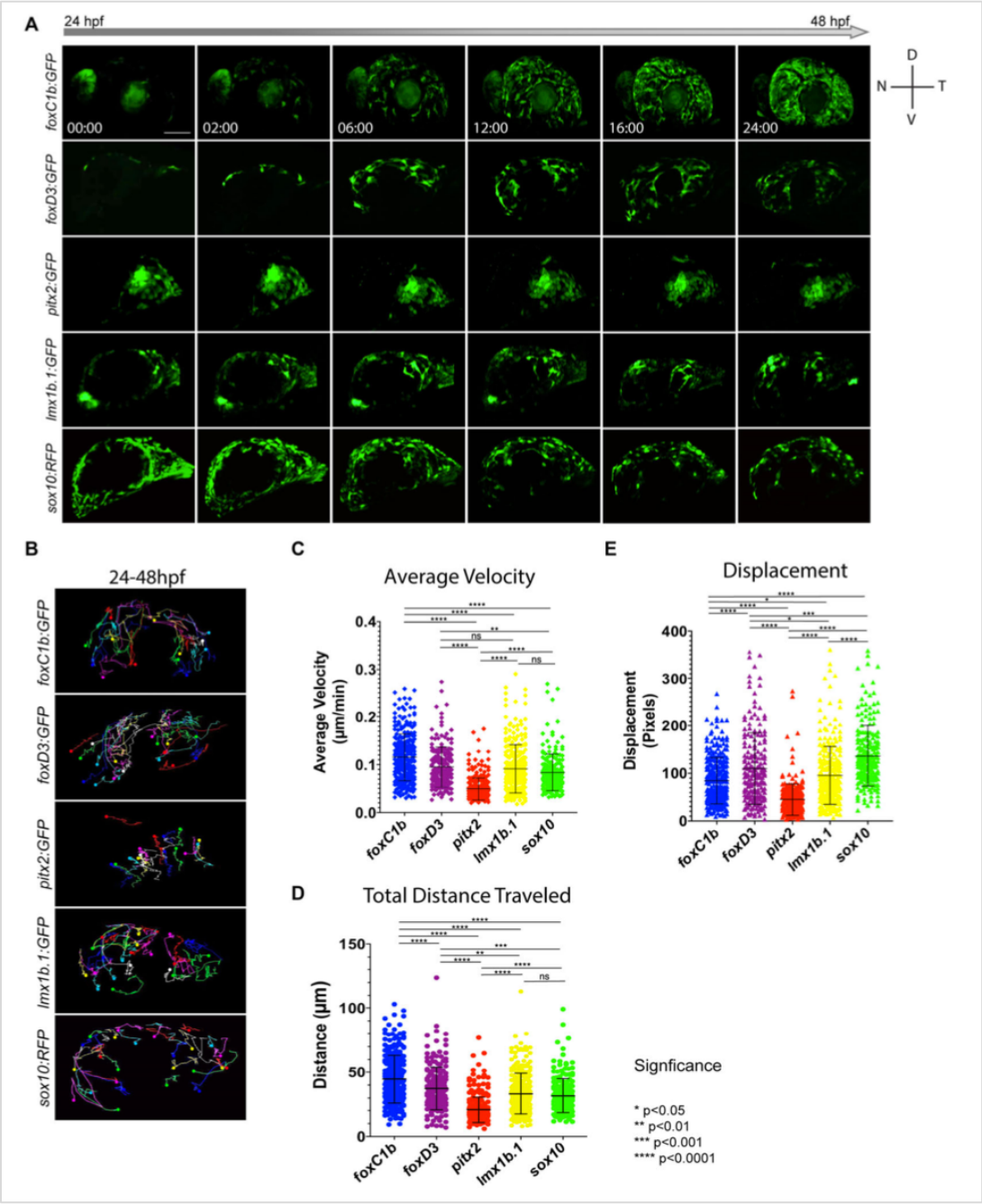

Figure 3.4: *In vivo* 4D imaging of POM anterior segment colonization. (A) 4D *in vivo* imaging of the AS conducted between 24–48hpf using POM transgenic lines. Time stamp hours:minutes. Scale bar = 50µm. Representative movie files for each line can be found under Additional Files. **(B)** Individual cell tracking for each POM transgenic line reveals migratory patterns during early AS colonization. Solid spheres indicate terminal end of

track. Representative racking movies for each line can be found under Additional Files. **(C–E)** Cell tracking measurements of average migratory velocity (ANOVA $p < 0.0001$), total migration distance (ANOVA $p < 0.0001$), and migratory displacement within the AS (ANOVA $p < 0.0001$).

3.3.6 ASM Subpopulations Cluster According to Developmental Transcriptomic Profiles

Having observed the AS-associated POM subdivide into several ASM subpopulations, based on distribution and migratory behavior, our final goal was to analyze single cell transcriptomic profiles of ASM cells during AS colonization. To do so, we dissected the eyes off of our transgenic embryos at 48hpf, isolated GFP+ cells via FACS, and subsequently employed the Chromium 10X genomics platform to generate single cell transcriptomes (scRNA). Resulting transcriptomes were sequenced using Illumina technology and analyzed using Cell Ranger3.1 and Loupe software. In total we sequenced 2,460 individual cells with per cell reads of greater than 100,000.

K-means clustering (t-SNE) of all five data sets resulted in four distinct clusters (**Figure 3.5 A** and **Supplementary Figure S3.4**). We identified one predominantly NCC-like cluster (Cluster 1) with cells largely originating from the *foxd3* and *sox10* transgenic lines (**Figure 3.5 B**). 85.6% of *sox10*:GFP and 84.3% of *foxd3*:GFP cells were found in cluster 1. *Sox10*:GFP and *foxd3*:GFP cells were also found in cluster 3 with 11.5 and 15% of their total distribution, respectively. A majority of cells isolated from the *foxc1b:*GFP line were found in Cluster 2, 70.1%, with a small proportion also present in cluster 3, 10.2%, and cluster 4, 15.8% (**Figure 3.5 B**). *Pitx2:GFP* isolated cells were predominantly found in cluster 3, 83.9%, and cluster 2, 7.1%, with a low proportion found in clusters 1 and 4, 5.3% and 3.6% distribution, respectively. *Lmx1b*:GFP derived cells have the unique classification of being almost equally represented throughout all 4 clusters, 24.3% in cluster 1, 15.7% in cluster 2, 29% in cluster 3 and 31% in cluster 4 (**Figure 3.5 B**). When comparing spatially, UMAP-based plotting of the clusters

indicated a continuous or connected expression profile suggestive of interaction or progression between the clusters (**Figure 3.5 A** and **Supplementary Figure S3.4**). The placement of the clusters within the UMAP graph predicts interaction between *sox10/foxd3* with *pitx2*, *pitx2* and *lmx1b/foxc1b* and finally *lmx1b/foxc1b* with *foxc1b*-derived cells (**Figure 3.5 C**). Interestingly, cluster 4 appears to represent a transition stage where multiple AS cell fates are possible. Taken together, we observed that none of the clusters are made up solely of cells originating from one individual transgenic line. This observation is supported by our two-color fluorescent *in situ* expression analysis (**Figure 3.2**) and is particularly relevant in terms of the relationships amongst POM associated genes, particularly *pitx2* and *foxc1* whose products are actually known to physically interact (Matt et al., 2005; Chawla et al., 2018). Finding four distinct subpopulations of ASM cells further supports our previous findings that suggest ASM are a developmentally heterogenous population during colonization of the AS.

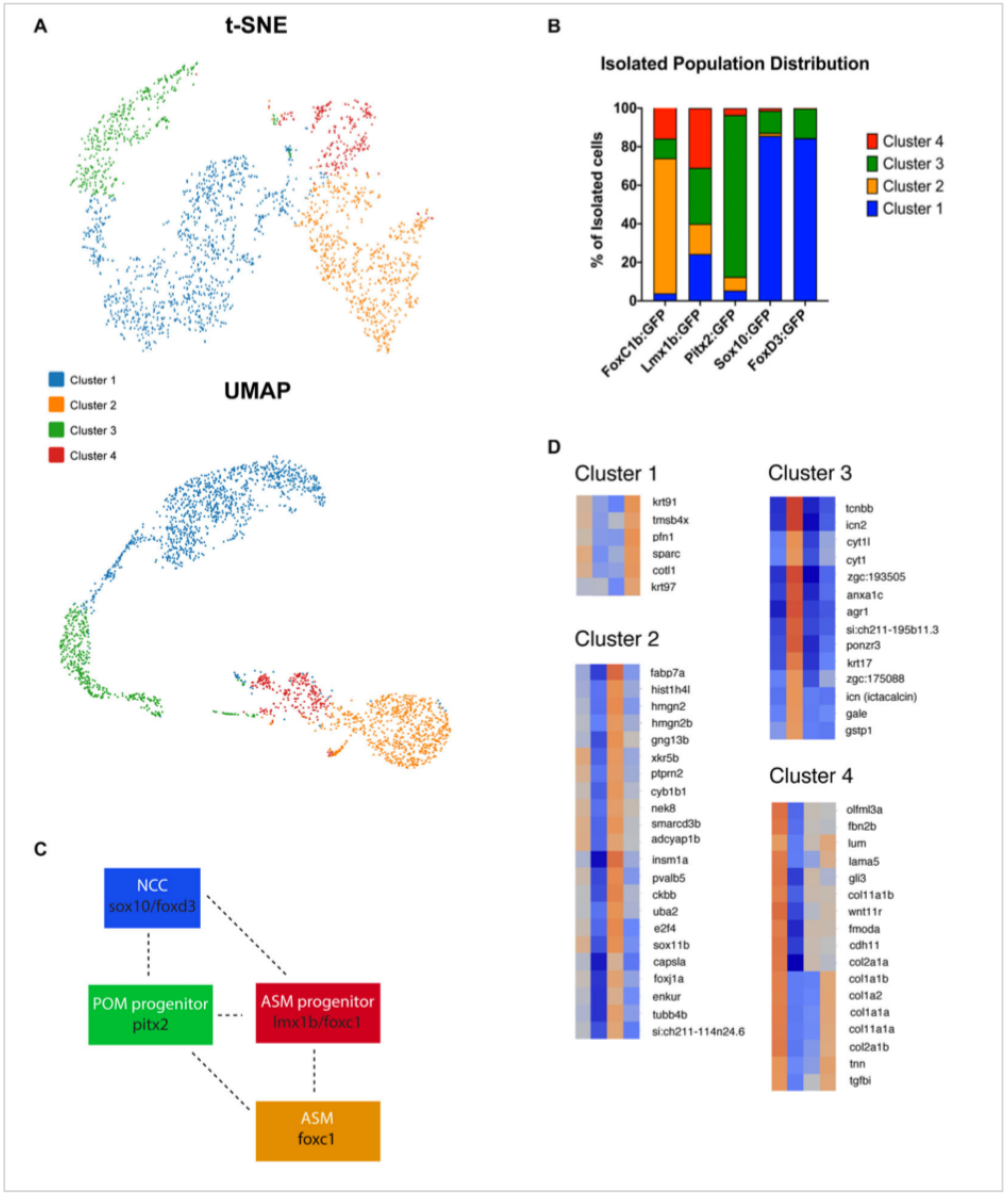

Figure 3.5: Anterior segment mesenchyme single cell clustering analysis at 48hpf. **(A)** K-means clustering of scRNA sequencing of isolated 48hpf *foxc1b:GFP, lmx1b:GFP, sox10:GFP, foxd3:GFP*, and *pitx2:GFP* ASM cells in both tSNE and UMAP readouts. Both plots identified four general clusters. **(B)** Distribution of isolated ASM cells within each of the clusters generated by the Cell Ranger3.1 software. **(C)** Model of identified cluster interactions. Interaction and overlap are indicated by dashed lines. **(D)** Heat maps of cluster specific gene expression patterns.

3.3.7 scRNA Analysis of ASM Uncovers Novel AS Markers

Based on the clustering analysis we generated heatmaps and gene ontology analysis of the most representative expression patterns for each cluster (**Figure 3.5 D** and **Supplementary Figure S3.5**). Within some of the clusters, genes with possible links to one or more AS structures were identified based on association with ASD-related disorders or potential similarities to POM/NCC- like expression patterns. For example, *cyp1b1*, known to be associated with glaucoma predisposition (Zhao et al., 2015), was identified in cluster 2, while *tgfbi*, isolated in cluster 4, is associated with corneal dystrophy (Poulaki and Colby, 2008). We also noted expression of several collagen (*col2a1a*, *1a1b*, *1a2*, *1a1a*, *2a1b*, *11a1a*, and *11a1b*) and laminin (*lama5*) genes, known to be associated with extracellular matrix properties of AS trabecular meshwork cells (Abu-Hassan et al., 2014), in cluster 4 (**Figure 3.5 D**). Importantly, our analysis also identified novel candidate genes potentially associated with AS specification and development. We therefore analyzed expression of several potential novel target genes to assess their contribution to AS development at 48 and 72hpf. Our expression analysis included *sparc* (cluster 1); *gng13b*, *hmgn2* and *adcyap1b* (cluster 2); *cyt1*, *arg1*, *ponzr3*, and *si:ch211-195b11.3* (cluster 3); and *lum*, *fmoda*, *tgfbi*, and *col2a1a* (cluster 4) (**Figure 3.6**). Examining expression of cluster 1 associated gene *sparc* revealed that at 48 and 72hpf *sparc* mRNA was associated with the developing AS, in particular the periphery of the lens and iris regions (**Figure 3.6 A**). From cluster 2, we examined expression of *hmgn2*, *gng13b*, and *adcyap1b*. We observed strong expression of *hmgn2* throughout the AS by 72hpf, and strong expression of *adcyap1b* in the lens periphery and future iris region (**Figure 3.6 B**). Cluster 3 targets included *agr1*, *cyt1*, *ponzr3*, and the currently

uncharacterized *si:ch211- 195b11.3*. Both *cyt1* and *agr1* appear to label dermal cells in the periocular and AS regions (**Figure 3.6 C**). *Ponzr3* did not display AS associated expression patterns (**Figure 3.6 C**), while *si:ch211- 195b11.3* does not appear to be related to the AS development (data not shown). Lastly, from cluster 4 we examined *col2a1a*, *fmoda*, *lum,* and *tgfbi* expression. By 72hpf, we observed strong expression of *fmoda* in the AS as well as some overlapping expression of *tgfbi* and *col2a1a* (**Figure 3.6 D**). Several genes in our list including *sparc*, *col2a1a*, *lum*, and *tgfbi* also demonstrated periocular expression patterns similar to other known ASM genes at 48hpf. In particular, *sparc* expression was reminiscent of *sox10*, *lum* expression was reminiscent of *foxc1a* while *tgfbi*, *col2a1a,* and *fmoda* expression were reminiscent of *foxc1b* and *eya2* (**Figures 3.1, 3.6**). In summary, our single cell transcriptomic analysis of ASM cells identified several novel markers associated with early AS formation which may represent uncharacterized regulators of AS development and/or function.

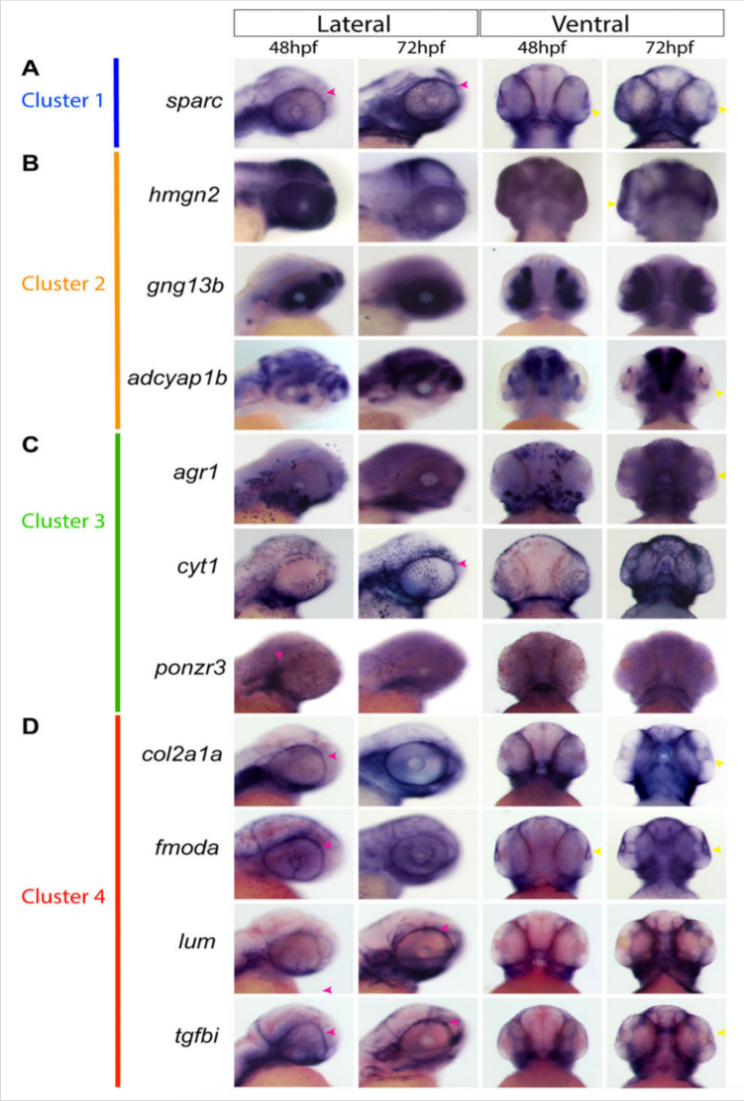

Figure 3.6: Gene expression of sequencing-derived genes. Whole mount *in situ* hybridization for novel ASM marker gene mRNA expression patterns was performed during early (48hpf) and intermediate stages (72hpf) of AS development and observed in lateral and ventral views. **(A)**, Sparc expression representing cluster 1. **(B)** *gng13b, hmgn2*, and *adcyap1b* expression representing cluster 2. **(C)** *cyt1, agr1,* and *ponzr3* expression representing cluster 3. **(D)** *lum, fmoda, col2a1a,* and *tgfbi* expression representing cluster 4. Yellow arrowheads indicate AS expression, magenta arrowheads indicate periocular expression.

3.4 CONCLUSION

In the literature, POM has become an umbrella term associated with a host of developmental events including cranial-facial, vascular, retinal as well as anterior segment development. In order to provide some much-needed clarity, our study aimed to characterize specifically the AS associated subset of POM cells, which we term the ASM. As such, our focus was strictly on POM cells that have entered the AS and ultimately contributed to its formation. We used a combination of *in situ* hybridization, real-time imaging of transgenic reporter lines and single cell transcriptomic analysis. Based on our results of ASM distribution, migration dynamics and lastly single cell transcriptional profiles, we conclude that AS colonization employs several distinct, yet developmentally connected, subpopulations of ASM. Overall, our work is the first comprehensive examination of ASM during AS development in zebrafish which we believe will serve as a starting point for future studies of novel regulators of this critical developmental event.

Observing a lack of total co-expression for POM marker genes in ASM cells suggested to us a lack of uniformity within the population. Furthermore, when co-expression of POM markers occurred, the degree and localization within the AS varied between genes examined (**Figures 3.1**, **3.2**). *Sox10* and *foxd3*, both NCC markers, appear to be co-expressed in ASM cells distributed over the entire AS at 32hpf (**Figures 3.2 A–C,E,F**). Co-expression of *pitx2* and *foxc1* was limited to the periphery of the AS while co-expression of *pitx2* and *eya2* was detected throughout the AS (**Figure 3.2 D** and **Supplementary Figure S3.2**). *Pitx2* displayed a high degree of co-expression with all other POM and NCC markers which likely coincides with its predicted wide-reaching role during AS development. Although we do see some degree of co-localization

amongst all POM marker genes, the distinction between each gene's expression pattern remains evident. Individual ASM cells therefore exhibit a range of POM marker expression patterns which supports our hypothesis that the ASM is heterogenous during AS development. Our findings also speak for the fact that when deciding on a marker for analysis of ASM, not all of the classical POM marker genes may be representative of the entire population and this should be taken into consideration during experimental design.

Utilizing transgenic lines: *foxc1b:*GFP, *foxd3:*GFP, *pitx2:*GFP, *lmx1b.1:*GFP, and *sox10:*GFP we examined the dispersal and distribution of ASM cells during the critical window of POM AS colonization (24–72hpf). Our detailed imaging studies indicated that the first POM cells arrive on the AS between 22–24hpf (**Figure 3.3 A**). GFP+ cells of the *pitx2* subpopulation appear to arrive the earliest of all observed ASM populations, entering the AS as early as 22hpf, and specifically from the temporal quadrant. When examined as a whole, ASM colonization is, however, primarily dorsal in origin and ASM cells proceed to spread throughout the AS as development proceeds. This pattern was observed for *foxc1b*:GFP, *foxd3*:GFP, *sox10*:GFP, and *lmx1b*:GFP ASM cells. In addition to several differing entry points, we also observed varying targeting behavior of ASM cells. By 48hpf homogenous AS distribution was observed for *foxc1b*:GFP, *foxd3*:GFP, and *sox10*:GFP cells. Conversely, *lmx1b.1*:GFP and *pitx2*:GFP cells remained strictly restricted to the nasal and temporal quadrants of the AS, respectively. This is a clear indication that heterogeneity during AS colonization is also a potential mechanism for specific targeting within the AS. Lastly, we observed that migratory ASM are not actively undergoing cellular division. The rapid increase in ASM cell number between 24–48hpf within some subpopulations, in particular *foxc1b:*GFP and *foxd3:*GFP, may

therefore be primarily attributed to the continual arrival of migratory cells to the AS. This notion is supported by the fact that cranial NCCs, the main source of POM/ASM, originate dorsal to the AS and that we observe *foxd3*:GFP and *foxc1b*:GFP cells entering the AS predominantly within the dorsal quadrant. Alternatively, it remains possible that GFP+ cells represent a non-proliferative pool of ASM. Analyzing co-expression of ASM markers and cell cycle transcripts will be necessary to test this alternative. When combining all of our ASM distribution data, we propose a progressive colonization model outlined in **Figure 3.3 C**.

The ability to migrate long distances and respond to specific cues is a crucial and well documented behavior of NCCs. Cranial NCCs migrate without designated leader or follower identities, instead maintaining a large homogenous population wherein each member exhibits the same migratory capabilities as its neighbors (Clay and Halloran, 2010; Kulesa et al., 2010; Richardson et al., 2016). 4D live imaging of *foxc1b*:GFP, *foxd3*:GFP*, sox10*:GFP, *pitx2*:GFP, and *lmx1b.1*:GFP transgenic embryos aged 24–48hpf showed a uniform migration behavior pattern in ASM subpopulations indicative of cranial neural crest-like migration (**Additional Files M3.1– M3.5**). Tracking analyses indicated cells had stochastic and independent migratory capabilities, frequently pausing during migration, altering directionality, and extending filipodia to communicate with one another (**Additional Files M3.6–M3.10**). Quantification of total distance and average velocity indicated that *foxc1b:*GFP ASM cells traveled the farthest distance and with the highest velocity (**Figures 3.4 C,D**). Conversely, *pitx2:*GFP ASM cells traveled the shortest distances and with the slowest velocities, but also with the least amount of stochastic movement (**Figures 3.4 B–D**). Interestingly, since *pitx2*:GFP+ cells are the

first POM cells to colonize the AS, we hypothesize that they may serve as sentinels to mark the AS for later arriving POM. Their need for timely arrival at the AS may explain their unique, highly targeted, migratory behavior. Displacement, also referred to as directed migration, was measured as a way to characterize the purposeful migration of ASM cells. We wanted to quantify whether certain ASM cells migrated with more directionality than their counterparts. Interestingly, our data indicates that cells in the *sox10*:GFP and *foxd3*:GFP subpopulation, associated with NCC identity (Stewart et al., 2006; Drerup et al., 2009; Wang et al., 2011), engage the most in directed migration (**Figure 3.4 E**). These likely pluripotent, NCC-like cells may be directly targeting to specific regions of the AS in order to ensure equal distribution. Cells likely associated with a more traditional POM identity, *foxc1b*:GFP and *pitx2*:GFP (Liu and Semina, 2012; Reis et al., 2012), appear to have more stochastic migration paths (**Figure 3.4 E**). A more stochastic migration pattern may be indicative of ASM cells further along the differentiation spectrum and no longer needing to target to specific AS regions. Similar to our observations of ASM expression patterns and distribution (**Figures 3.1–3.3**), migratory behavior is also clearly variable amongst ASM cells which further supports the notion of a heterogenous population.

Lastly, we investigated the transcriptomic differences amongst the ASM. Utilizing the 10× Genomics process of scRNA sequencing, we isolated 48hpf eyes from transgenic embryos (*foxc1b*:GFP, *foxd3*:GFP, *lmx1b*:GFP, *sox10*:GFP, and *pitx2*:GFP) and used FACS to isolate our GFP+ ASM cells. This approach aimed to ensure only AS associated cells were included in our analysis. ASM specific single cell cDNA libraries were generated, sequenced, and based on transcriptomic profiles, grouped into four

distinct clusters (**Figures 3.5 A,B**). We classified these clusters into a NCC-like cluster (*sox10/foxd3*), POM progenitor cluster (*pitx2*), a ASM progenitor cluster (*lmx1b/foxc1b*) and finally a specified ASM cluster (*foxc1b*) (**Figures 3.5 B,C**). UMAP analysis of the data indicates a connection between clusters suggesting that ASM cells may be found along a heterogenous, but connected, spectrum during AS colonization. This connection is also apparent when examining the cluster associated percentage distribution of our isolated cells. The four clusters all appear to be connected along a plausible trajectory of AS development starting with the NCC-like cluster (cluster 1), then the POM progenitor cluster (cluster 3) followed by the ASM progenitor cluster (cluster 4) and finally an ASM-like cluster (cluster 2). We predict that early AS is therefore likely colonized by a heterogenous population of ASM that may represent different stages of differentiation along the path to an AS cell fate. This combination could ensure that while some ASM enter already poised to begin differentiation and assembly of functional AS structures, such as the *pitx2*, *foxc1b*, or *lmx1b* driven subpopulations, others that are likely more pluripotent, *foxd3/sox10* driven, serve to ensure that proper numbers of ASM arrive at all points along the AS and then further differentiate in response to local signaling cues. It is therefore not surprising that distributions, migratory patterns and transcriptomic profiles of *sox10:*GFP and *foxd3:*GFP cells are highly similar when compared to *foxc1b:*GFP, *lmx1b.1:*GFP, or *pitx2:*GFP. Finally, while transcriptomic differences observed in our data support the notion of a heterogenous ASM population, they do not infer lineage marking. Future fate mapping experiments will need to be performed to determine whether specific transcriptomic differences directly determine cell fate or simply represent transitional states along the ASM differentiation pathway.

Expression analysis of cluster specific targets identified by our scRNA assay revealed a number of genes of particular interest including *sparc*, *hmgn2*, *adcyap1b*, *agr1*, *col2a1a tgfbi*, and *fmoda* (**Figure 3.6**). Several of these genes are associated with regulation and function of the extracellular matrix including *sparc*, *col2a1a*, and *fmoda*, indicating a possible relationship with the drainage systems of the iridocorneal angle (Abu-Hassan et al., 2014). While the drainage networks are the last to fully differentiate in the AS, their importance to the function of the eye cannot be understated. *Tgfbi* is associated with head mesenchyme and neural crest and is also predicted to be localized to the extracellular matrix (Chakravarthi et al., 2005; Kannabiran and Klintworth, 2006). Interestingly, the t*gfbi* gene is associated with a subset of familial corneal dystrophies (Nielsen et al., 2020). *Hmgn2* is a non-histone component of nucleosomal DNA and is associated with transcriptionally active chromatin, especially in cells that remain undifferentiated, and is involved in DNA replication, transcription, and repair (Lucey et al., 2008; Furusawa and Cherukuri, 2010). Although not yet associated with AS development or ASD pathology, *hmgn2* is abundantly expressed throughout the ocular structures of the AS and retina in mice, especially in the lens fibers and epithelium layer of the cornea (Lucey et al., 2008). *Adcyap1b* is a neuropeptide also known as PACAP associated with brain and camera-type eye development, meaning that it plays a role in the development of the lens and retina of the eye (Wu et al., 2006; Denes et al., 2019). PACAP also appears to have retinoprotective attributes (Shioda et al., 2016). The mechanisms of *adcyap1b* function during AS development is unclear at this time. Finally, *agr1* is associated with the negative regulation of cell death, regenerative abilities of fish and frogs and is strongly associated with liver function (Ivanova et al., 2015, 2018).

While it's function within the eye remains unclear at this time, *agr1* does show expression in the corneal region (**Figure 3.6**) (Ivanova et al., 2015). Future studies will focus on examining the functional roles of the aforementioned AS associated target genes as well as others from our transcriptomic screen (**Figure 3.5 D**). We will also seek to determine whether the identified clusters also represent lineages of specific AS structures, such as the cornea, iridocorneal angle (annular element in zebrafish) or iris.

Heterogeneity within the early colonizing POM and subsequent ASM poses an important question: what is the functional interplay between such subpopulations? Previous studies of AS development in several models suggest that there are in fact "master regulators" of this process, in particular *foxc1* and *pitx2*. Loss of function of either has significant consequences on AS formation and function. However, the status of other POM/ASM markers, or subpopulations, in these circumstances has not been thoroughly examined. It therefore remains unknown whether all ASM subpopulations are affected and to what degree. We know even less about the consequences of other POM/ASM regulators, such as *eya2*, *foxd3*, or *lmx1b*, in this context. Future work will need to concentrate on carefully teasing out how individual regulators of POM influence the entire process of AS colonization, rather than simply observing for physiological consequences in juvenile or adult AS tissues.

In conclusion, our findings, based on distribution, migration and transcriptomic profiles, indicate that POM cells targeted to the anterior segment, which we have termed the Anterior Segment Mesenchyme (ASM), are not homogenous. Rather, the ASM simultaneously comprises of several subpopulations likely divided along the ASM differentiation pathway. Our findings open a wide range of possible new investigative

paths in the area of AS development and ASD disorders. Future examination of the interplay between these subpopulations will be prudent to further our understanding of eye development and ultimately predisposition to ASD associated blinding disorders.

3.5 MATERIALS AND METHODS

3.5.1 Zebrafish Maintenance

Zebrafish lines were bred and maintained in accordance with IACUC regulations (IACUC protocol 2015-1380) at the University of Kentucky. AB strain was used as wildtype. Transgenic lines used were: Tg[*foxc1b:GFP]* (Dr. Bryan Link), Tg[*foxd3:GFP]* (Dr. Lister), Tg[*pitx2C4:GFP]* (Dr. Elena Semina), and Tg[*lmx1b.1:GFP]* (Dr. Brian Link), Tg[*sox10:RFP]* (Dr. Lister). All embryos were raised for the first 24 hours post fertilization in embryo media (E3) at 28°C. After 24 hours, E3 media was replaced with embryo media containing 1-phenyl 2-thiourea (PTU) every 24 h to maintain embryo transparency.

3.5.2 Whole-Mount *in situ* Hybridization (WISH)

Whole-mount *in situ* hybridizations were performed using a minimum of 20–25 embryos for each time point (12, 18, 24, 32, 48, and 72hpf). DIG and FITC labeled RNA probes were created using PCR incorporating T7 promoters in the primers and transcribed with T7 polymerase (Roche). Forward and Reverse primer sequences are listed in **Supplementary Table S3.1**. WISH protocol was performed as previously described (Holly et al., 2014). Dorsal, lateral, and ventral images of embryos were captured using a Nikon Digital Sight DS-U3 camera and Elements software. Images were

adjusted for brightness using Adobe Photoshop and assembled into figures using Adobe Illustrator.

3.5.3 Immunohistochemistry (IHC) for Distribution and Proliferation Analysis

Approximately 30 embryos were imaged for each transgenic line at each of the given time points (24, 26, 28, 30, 48, 54, and 72hpf). Embryos were fixed overnight at 4°C using 4% PFA. PFA was washed out with PBST 4 times for 5 min each. Embryos were permeabilized with Proteinase K (10 μg/ml) at the following times (24hpf = 5 min; 26hpf = 6 min; 28hpf = 7 min; 30hpf = 9 min; 48hpf = 20 min; 54hpf = 25 min; 72hpf = 40 min), washed with PBST and then blocked with 5% goat serum (1 g/100 ml), 1% BSA in a solution of 1x PBST for at least 2 h at room temperature. Primary antibody (Rockland rabbit anti-GFP) was diluted at 1/200 in blocking buffer and incubated overnight at 4°C on rotation. The following day, the primary antibody solution was washed out with PBST 5 times for 15 min each. Secondary antibody (Alexa Fluor 488 anti rabbit, 1/1000) and DAPI (1/2500) were diluted in blocking buffer and incubated for 1 h on rotation in the dark at room temperature. Embryos were washed 2× for 15 min with PBST in the dark.

After staining, embryos were embedded in a 1.2% Low- gelling agarose in a 1-inch glass bottom cell culture dish (Fluorodish, World Precision Instruments) and visualized using a Nikon C2+ confocal microscope with a 20× (0.95 NA) oil immersion objective. The anterior segment of the eye was imaged in 3D in the lateral position as a 100 μm z-stack using 3.50 μm steps. All images were captured using Nikon Elements software, adjusted for contrast and brightness using Adobe Photoshop and assembled into

figures using Adobe Illustrator. Images generated from IHC analysis were rendered in 3D using Nikon Elements Viewer software. Eyes were divided into 4 quadrants: dorsal nasal, dorsal temporal, ventral nasal, and ventral temporal. Nasal and temporal regions were divided by a vertical straight line through the center of the lens, while dorsal and ventral were divided by a horizontal straight line through the center of the lens. For distribution analysis, GFP+ cells were manually counted based on their position within one of the four quadrants of a 3D constructed anterior segment. For each timepoint 25+ embryos from three independent trials were imaged for quantification.

3.5.4 Two-Color Fluorescent WISH

RNA probes were generated using the MEGAscript T7 transcription Kit (Ambion) in combination with RNA labeling mixes for both DIG and FITC (Roche). Double *in situ* hybridization was performed according to the protocol by Lauter et al. (2011). This included exposing embryos to acidified methanol and adding Dextran Sulfate into the hybridization reaction. Staining was done by combining Fast Blue and Fast Red dyes (Sigma) (50 μg/ml). After successful *in situ* double staining, embryos were additionally stained using DAPI and imaged using a NIKON C2+ confocal microscope. Images were adjusted for brightness and contrast using Adobe Photoshop and assembled into figures using Adobe Illustrator. 15–20 embryos were analyzed for each probe combination.

3.5.5 Time-Lapse Confocal *in vivo* Imaging

Embryos from each of the previously mentioned transgenic lines were collected and raised in E3 media at 28°C. Fluorescent embryos were placed in E3 PTU media including 3-amino benzoic acid ethyl ester (Tricaine) to prevent pigmentation and to anesthetize them, respectively. They were then dechorionated and embedded laterally in 1% low-gelling agarose in a 35 mm glass bottom cell culture dish (Fluorodish, World Precision instruments). Real-time imaging was conducted at 28°C using a Nikon C2+ confocal microscope and a 20× (0.95 NA) oil immersion objective. 3D *z*-stacks over a 75µm thickness with a slice size of 3.5µm were collected to encompass the entire developing anterior segment. *Z*-stack images were taken at 10 min intervals over a 24 h period (embryos imaged: $n = 12$ *foxc1b:GFP*, $n = 9$ *foxd3:GFP*, $n = 13$ *pitx2:GFP*, $n = 10$ *lmx1b.1:GFP*, $n = 7$ *sox10:RFP*). Data were collected and rendered using Nikon Elements software. Images were adjusted for brightness using Adobe Photoshop and assembled into figures using Adobe Illustrator.

3.5.6 Cell Migration Tracking and Displacement Analysis

Completed 4D live imaging files were uploaded into FIJI software for analysis. Approximately 25 cells were manually tracked per video file using manual tracking tools. Tracked cells were measured for total distance traveled (µm), average velocity (µm/min), and total displacement (pixels). Tracked cells were randomly selected from all four eye quadrants to ensure all eye regions were represented, as well as all time frames. After tracking, data were exported to Microsoft Excel for statistical analysis. Displacement was measured using the line measurement tool in FIJI software. Previously tracked lines were

identified as “completed” tracks in one of two ways: (1) at the end of the migration video or (2) the track was seen in the last frames of video before the specific track disappeared. Once the completed track was identified, the line measurement tool was used to measure the straight-line distance (in pixels) from the first point of the track to the last point of the track. Statistics were analyzed in Microsoft Excel and Graphpad Prism8.

3.5.7 Single Cell Transcriptomic Analysis

Embryos from each of the POM subpopulation transgenic lines were dechorionated and incubated in E3 media at 28°C until 48hpf. At this time, embryos were anesthetized using 3-amino benzoic acid ethyl ester (Tricaine) and their eyes dissected and collected on ice. Eyes were incubated for 2 min in 0.25% Trypsin + EDTA at 37°C. After incubation, a 20G needle and syringe were used to dissociate the tissue before the tube was placed back at 37°C for 2 min. This process was repeated four times. After incubation, the dissociated cells were strained using a 40 μm filter (VWR) and spun down for 10 min at 3,500 rpm at 4°C. The supernatant was removed and the pellet resuspended in 1x PBS + 2 mM EDTA and goat serum. Cells were sorted for GFP+ identity at the University of Kentucky Flow Cytometry and Immune Monitoring Core at the Markey Cancer Center. After sorting, cells were spun down and resuspended using PBS and goat serum. Approximately 1,000 cells from each transgenic line were then loaded onto the Chromium 10× V3 chip (10× genomics) and processed in the University of Kentucky Department of Biology Imaging Core to generate single cell barcoded cDNA. Sequencing was performed using NovaSeq SP, 2 × 150 bp paired ends to achieve 100,000 reads per cell at University of Illinois at Urbana-Champaign Roy J. Carver Biotechnology Center.

Sequencing results were processed and subsequently aggregated (incorporating mapped normalization), using the Cell Ranger3.1 pipeline and results analyzed using Loupe Cell Browser 3.1.1 software (10× genomics).

3.5.8 Statistics

One-way ANOVA analysis (multiple point analysis) and unpaired *t*-tests (individual comparison analysis) were performed using Microsoft Excel and GraphPad Prism8 software. All graphs are shown with their respective means and standard deviations. Values were considered significant by the conventional standard: *P*-value of 0.05 or less.

3.5.9 DATA AVAILABILITY STATEMENT

The raw data supporting the conclusions of this article will be made available by the authors, without undue reservation, to any qualified researcher.

3.5.10 ETHICS STATEMENT

The use of zebrafish in this study was approved by the University of Kentucky IACUC committee, Institutional PHS Assurance #D16-00217 (A3336-01) with a protocol number: 2015-1370. All experimental protocols were approved by the University of Kentucky Institutional Biosafety Committee, registration number B18-3186-M.

3.5.11 AUTHOR CONTRIBUTIONS

JF and KV wrote the manuscript. KV, OV, MW, and NM performed the experiments and analysis. JF oversaw the project secured funding. JF and KV contributed to conception and design of the study. All authors contributed to manuscript revision, read and approved the submitted version.

3.5.12 FUNDING

This work was supported by the NIH-NEI grant EY027805-01. MW was supported by the Lyman T. Johnson Scholarship from the University of Kentucky. OV was supported by the Knights Templar Eye Foundation Career Starter Grant.

3.5.13 ACKNOWLEDGMENTS

We thank Dr. Link, Dr. Semina, and Dr. Lister for providing transgenic zebrafish lines. We thank members of the Famulski lab for helpful discussions. We also thank Dr. Jeramiah Smith for assistance with single cell sequencing analysis. This manuscript has been released as a pre-print at Biorxiv (Van Der Meulen et al., 2019).

CHAPTER 4: LOSS OF NEURAL CREST REGULATORY GENES NEGATIVELY IMPACTS PERIOCULAR MESENCHYME GENE EXPRESSION AND ANTERIOR SEGMENT DEVELOPMENT

Kristyn L. Van Der Meulen, Oliver Vöcking, and Jakub K. Famulski

4.1 ABSTRACT

Development of the ocular anterior segment (AS) is a crucial component in the assembly of the visual system in vertebrates. Composed of the cornea, iris, ciliary body, and iridocorneal angle, the AS is a critical network of structures for visual acuity and eye homeostasis. Failures in the process of AS assembly lead to Anterior Segment Dysgenesis (ASD), a spectrum of conditions characterized by congenital blindness and/or defects and a predisposition to glaucoma. AS development is largely regulated via a neural crest-derived population of cells called the Periocular Mesenchyme (POM). The neural crest (NC) is a vertebrate specific, transient, and highly migratory population of cells that contribute to many different systems around the developing embryo including pigmentation, the nervous system, cardiac tracts, cartilage, inner ear bones, teeth, and the AS. Much of the research focus has been directed at POM specification later in eye development and how it relates to certain ASD conditions, but little attention has been given to the origins of the POM within the NC and how it relates to POM health and AS formation. In this study, we aimed to determine the relationship between the POM and NC in the zebrafish embryo using various NC knock outs. While the loss of *Sox10* gene expression appears to show no negative effects on the expression of POM genes at 24 or 48hpf, a more complete knock out of the NC using *Tfap2a* or *Foxd3* shows a complete loss of POM gene expression within the AS at 32hpf. This near total loss of POM gene

expression is likely, we believe, to severely impact the migration and specification of POM cells and, therefore, negatively effects the overall development of the AS. Our evidence thus far indicates that proper NCC gene function is required for POM-associated genes to be activated in AS-associated POM cells and that, when these genes are missing or mutated, AS development cannot proceed.

4.2 INTRODUCTION

The ocular Anterior Segment (AS) in vertebrates is a crucial collection of structures tasked with focusing and manipulating light onto the retina and for maintaining eye homeostasis via regulation of intraocular pressure. The AS is comprised of structures including the cornea, lens, iris, anterior chamber, ciliary body, and iridocorneal angle. Without the proper formation of these structures vision and overall eye health may be compromised, resulting in disorders broadly termed as Anterior Segment Dysgenesis (ASD). These malformations may affect one or more AS structures and can lead to minor or significant visual impairment. Mis-steps during the formation of the AS can lead to congenital ASDs which may include corneal opacity, iris hypoplasia, polycoria, corectopia, posterior embryotoxon, juvenile glaucoma, and disorders including Peter's Anomaly (PA) and Axenfeld-Rieger Syndrome (ARS) (Gould et al., 2004; Volkmann et al., 2011; Akula et al., 2018). In addition to their AS-associated phenotypes, these rare autosomal dominant disorders also often exhibit systemic phenotypes that may include dental malformations, hearing loss, and craniofacial defects (Volkmann et al., 2011; Bohnsack et al., 2012; Ji et al., 2016).

Development of the AS arises from several diverse embryonic cell lineages working in a complex and coordinated partnership with one another. By its completion, the AS will include tissues coming from the surface ectoderm, head mesoderm, and neural crest (Trainor and Tam, 1995; Langenberg et al., 2008; Williams and Bohnsack, 2015). Vertebrate AS development starts once the neuroectoderm derived bi-layered optic cup has been established. During this time, the surface ectoderm invaginates at the anterior of the optic cup to form the lens placode and the surface ectoderm comes back together to form the outer most layer of the cornea, the corneal epithelium (Fuhrmann, 2012, Lang, 2004, Soules and Link, 2005; Cavodeassi, 2018). A highly migratory and specified population of cells called the Periocular Mesenchyme (POM), derived from the Cranial Neural Crest (cNC) and the head mesoderm, will then migrate into the space between the corneal epithelium and the anterior neural retina and lens (Creuzet et al., 2005; Cavodeassi, 2018; Fuhrmann et al., 2000). These POM cells, upon completion of their migration, will differentiate into the various structures of the AS. Little is presently understood about how POM cells develop, the mechanism(s) needed to arrive at the AS, and how they are able to form the various structures of the mature AS. Our previous work showed that the POM is a collection of subpopulations which are differentiated by their unique distributions around the AS, migratory behaviors, and transcriptional profiles (Van Der Meulen et al., 2020). Several genes associated with these POM subpopulations, and also therefore heavily implicated in several ASD disorders, include the transcription factors *Foxc1, Pitx2, Foxd3, Lmx1b*, and *Eya2*. *Foxc1* and *Pitx2*, for example, are considered regulators of AS development and have been implicated in human cases of ARS and ASD (Berry et al., 2006; Liu and Semina, 2012, Chen and Gage, 2016, Seo et

al., 2017; Hendee et al., 2018; Volkmann Kloss et al., 2012). As previously mentioned, ARS is a systemic disorder affecting other NC-derived tissues throughout the organisms, suggesting that these developmental defects share a common origin point within the NC and that multiple NC-derivatives are affected. The roles of *Foxd3, Lmx1b*, and *Eya2* are less defined during AS development, but have also been implicated in human conditions (Volkmann Kloss et al, 2012; McMahon et al., 2009; Liu and Johnson, 2010; Matt et al., 2008; Lupo et al., 2011). However, missing from our work was an in-depth analysis of where, when, and how the various POM subpopulations originate.

The neural crest is a transient and highly migratory embryonic cell population unique to vertebrates. These specialized cells migrate throughout the developing embryo to contribute to a wide range of tissues and subtypes including but not limited to myofibroblasts, cartilage, bone, smooth muscle, teeth, components of the ear, eye, and heart, pigment cells, neurons, and glial cells (Williams and Bohnsack, 2015; Trainor and Tam, 1995; Mayor and Theveneau, 2013; Langenberg et al., 2008). No other cell population exhibits as much diversification in derivatives as the neural crest. While the later cell specification possibilities for a NCC are varied, the beginning stages are uniform. Presumptive NCCs are induced on the borders of the neural plate by intermediate levels of BMP and high levels of Wnt, RA, and FGF (Bronner and LeDouarin, 2012; Simões-Costa and Bronner, 2015; Mayor and Theveneau, 2013; Hoffman et al., 2007). As the plate folds itself into the neural tube, these border region cells come together at the anterior of the tube below the surface ectoderm (Bronner and LeDouarin, 2012; Simões-Costa and Bronner, 2015; Mayor and Theveneau, 2013; Noisa and Raivio, 2014; Zhang et al., 2014). Cells in this region then lose their strong epithelial

connections to one another through the Epithelial-to-Mesenchymal Transition (EMT) and migrate away from the neural tube region throughout the embryo to their various targets. While not currently well understood, a collection of positive and negative signaling cues help to guide NCCs to their appropriate targets and away from inhospitable locations. The specification of these cells into more distinctive cell types, their migration behaviors, and other population specifics are dependent on where the cells originate and what environmental cues they're exposed to along the way (Clay and Halloran, 2010; Theveneau and Mayor, 2012; Kulesa et al., 2010; Richardson et al., 2018; Mayor and Etienne-Manneville, 2016).

The number of genes needed for the proper induction, proliferation, migration, survival, and specification of NCCs is an extremely vast and complex web of gene interactions known as the Neural Crest Gene Regulatory Network (GRN). While still being studied to this day, the GRN consists of many different stages of the NCCs, with genes turning on and off rapidly, with some genes creating feedback loops and/or being of benefit in multiple stages. While morphogenic genes such as Wnts, FGFs, and BMPs are vital in establishing the fate of the neural plate border cells, it is the activation of transcription factors like *Tfap2, Snail1/2, Foxd3, AP2α,* and *Sox8/9/10* that actually specify the NC (Bronner and LeDouarin, 2012; Simões-Costa and Bronner, 2015; Mayor and Theveneau, 2013; Zhang et al., 2014). These genes work to maintain the NC multipotent state, control cell proliferation, migration, and survival through cell adhesion and motility, and mediate the EMT (Bronner and LeDouarin, 2012; Simões-Costa and Bronner, 2015; Mayor and Theveneau, 2013; Noisa and Raivio, 2014; Clay and Halloran, 2010; Zhang et al., 2014). Because of the complex web of interactions within the NC-

GRN, it becomes quite difficult to focus on only one gene at a time and maintain the expectation of altering the entire NC network of genes and cells. This is especially true when trying to target a specific subgroup of NCCs, such as those that specifically target the eye. However, previous work has shown that several genes knocked out in conjunctions with one another, such as a *Tfap2a/Foxd3* double mutant, can significantly reduce the NCC population or eliminate it entirely.

Two genes have been shown in previous studies to be both NCC-specifier genes as well as POM-specific markers with documented, standalone effects on AS development: *Foxd3* and *Sox10*. Forkhead box D3 (*Foxd3*) is a transcription factor vitally important to the NC-GRN expressed during induction of NCCs, EMT, and as pre-migratory and migratory NCCs (Lister et al., 2006; Volkmann Kloss et al., 2012; Wang et al., 2011; Stewart et al., 2006; Simões-Costa and Bronner, 2015; Mayor and Theveneau, 2013; Noisa and Raivio, 2014; Hanna et al., 2002). *Foxd3* expression begins to decrease as differentiation begins, remaining active in a small subset of cells (Volkmann Kloss et al., 2012). Derivatives of cells that express/expressed *Foxd3* and migrate successfully to the AS have been documented and defects in *Foxd3* have been associated with ASD phenotypes in humans (Van Der Meulen et al., 2020; Volkmann Kloss et al, 2012). In zebrafish lacking *Foxd3*, phenotypes like craniofacial defects, cardiac abnormalities, and increased embryonic lethality have been observed (Volkmann et al., 2012; Lister et al., 2006; Wang et al., 2011; Stewart et al., 2006).

The second NC and POM related gene is SRY-box 10, or *Sox10.* Another important transcription factor, *Sox10* is critical in the specification of NC identity and migration (Dutton et al., 2001; Kulesa et al., 2003; Bronner and LeDouarin, 2012;

Simões-Costa and Bronner, 2015; Mayor and Theveneau, 2013; Noisa and Raivio, 2014). Unlike *Foxd3* which is needed as a NCC induction and pre-migratory gene used during EMT, it is currently believed that *Sox10* expression commences after NCC induction and is required for the initiation and continuation of migration (Simões-Costa and Bronner, 2015; Mayor and Theveneau, 2013; Noisa and Raivio, 2014). *Sox10* is expressed in other migratory cells not related to POM cells or the development of the AS, such as endothelial cells. These *Sox10*-expressing endothelial cells enter into the developing eye via the ventrally located optic fissure and establish the transient hyaloid vasculature (Williams and Bohnsack, 2015; Weaver et al., 2020). While located in the anterior portions of the eye, the hyaloid vasculature in humans is an embryonic structure only and therefore not considered to be part of the AS or a POM cell-derived structure (Creuzet et al., 2005; Williams and Bohnsack, 2015).

Several genes within the NC-GRN can be used either independently or in conjunction with one another to diminish or inhibit the NCs ability to function, migrate, or specify. Early neural plate border induction genes like *Tfap2a* have been used together with pre-migratory genes like *Foxd3* to effectively knock out cNCCs (Bryan et al., 2020; Arduini et al., 2009; Wang et al., 2011). Transcription factor AP-2 alpha (*Tfap2a*) is a gene vital in early neural crest development and is often associated with *Foxd3* as both are expressed in the early NC-GRN in distinct, but complementary, domains (Wang et al., 2011). Evidence suggests that *Tfap2a* is upstream of *Foxd3* and that they work together to maintain the balance of BMP and Wnt during NCC induction at the neural plate borders (Wang et al., 2011; Powell et al., 2013). *Tfap2a* has also been shown to directly activate another well-known NCC transcription factor, *Sox10* (Van Otterloo et

al., 2012). In zebrafish, a loss of *Tfap2a* has resulted in apoptosis of NC progenitors and NC-derived tissues, while a loss of *Foxd3* in zebrafish has also led to a loss of NCC derivatives (Wang et al., 2011). Given that defects seen in *Tfap2a* mutants and *Foxd3* mutants are so similar, it has been suggested that both genes work within the same developmental pathway needed for the induction and maintenance of early NCCs (Wang et al., 2011). In fact, *Prdm1a* has been shown to directly bind to the enhancer regions of both *Tfap2a* and *Foxd3* (Powell et al., 2013). Current research is unclear on how individual knock outs of either *Tfap2a* or *Foxd3* effect the development of the AS, much less the POM. But when creating double mutant embryos with both *Tfap2a* and *Foxd3*, a thorough and near complete loss of all NCCs can be achieved where individual gene mutations failed, including in regards to eye development (Bryan et al., 2020; Arduini et al., 2009; Wang et al., 2011).

Critical to our understanding of POM biology is determining when and how these cells originate within the organism. Currently, little is defined about where POM cells come from and how they ultimately achieve their POM identity. It is widely understood that POM cells derive largely from the transient neural crest cell population, with a small contribution from the mesoderm, however the exact details of this process have not been documented. In this study utilizing zebrafish, we aim to determine when and where the transition from neural crest to POM occurs, characterize the effects of NC gene knock outs on POM subpopulations and their interactions with one another, and how the loss of NCCs impacts of the development of the anterior segment.

4.3 RESULTS

4.3.1 *Sox10* partial or complete KO does not affect the expression patterns of POM genes

With a large number of genes being implicated in the NC-gene regulatory network, we first chose to look at the effects on POM subpopulations and AS development under the loss of function of just one gene: *Sox10*. As a key transcription factor involved in the migration and viability of NCCs, we believed that *sox10* loss of function would prevent POM colonization of the AS and therefore, development of some, if not all, AS structures. We obtained the *Sox10* Colorless t3 (*Sox10-CLS)* mutant fish line (Dutton et al., 2001; Kelsh and Elsen, 2000), which contains a 1.4kb transposon insertion in the *Sox10* coding sequence upstream of the HMG domain, resulting in 8 amino acids being added to the C-terminal domain before a premature termination (Dutton et al., 2001). The CLS mutation causes NCCs to fail to migrate appropriately (Dutton et al., 2001; Kelsh and Elsen, 2000). To determine the effect of this loss-of-function on POM subpopulations, we performed Whole Mount *in situ* Hybridization (WISH) on wildtype, *Sox10-CLS* heterozygous and *CLS* homozygous embryos at 24 and 48hpf using RNA probes for POM-related genes *Foxc1a, Foxc1b, Foxd3, Pitx2*, and *Eya2* (**Supplemental Table S3.1**). Imaging of both heterozygous and homozygous *Sox10-CLS* embryos indicated no change in expression patterns of any POM-related genes (**Figure 4.1**). All genes tested displayed the same patterns of expression seen in wildtype embryos. Briefly, at 24hpf POM probes showed various degrees of expression surrounding the periocular space and displaying close contact with the optic cup, similar to what was observed in time matched wildtype counterparts. *Sox10* expressing cells

were also detected in close contact with the eye, as well as throughout the craniofacial space. At 48hpf, expression patterns of *foxc1, foxc1b*, and *eya2* are more easily observed on the border of the eye, as well as its surface, while expression patterns of *foxd3* and *pitx2* are more segregated on the surface of the eyes and within the cranial space. *Sox10* expression in *Sox10-CLS* heterozygous embryos showed similar expression patterns to wildtype embryos at 24 and 48hpf, but a reduced expression in *Sox10-CLS* mutants (**Figure 4.1**).

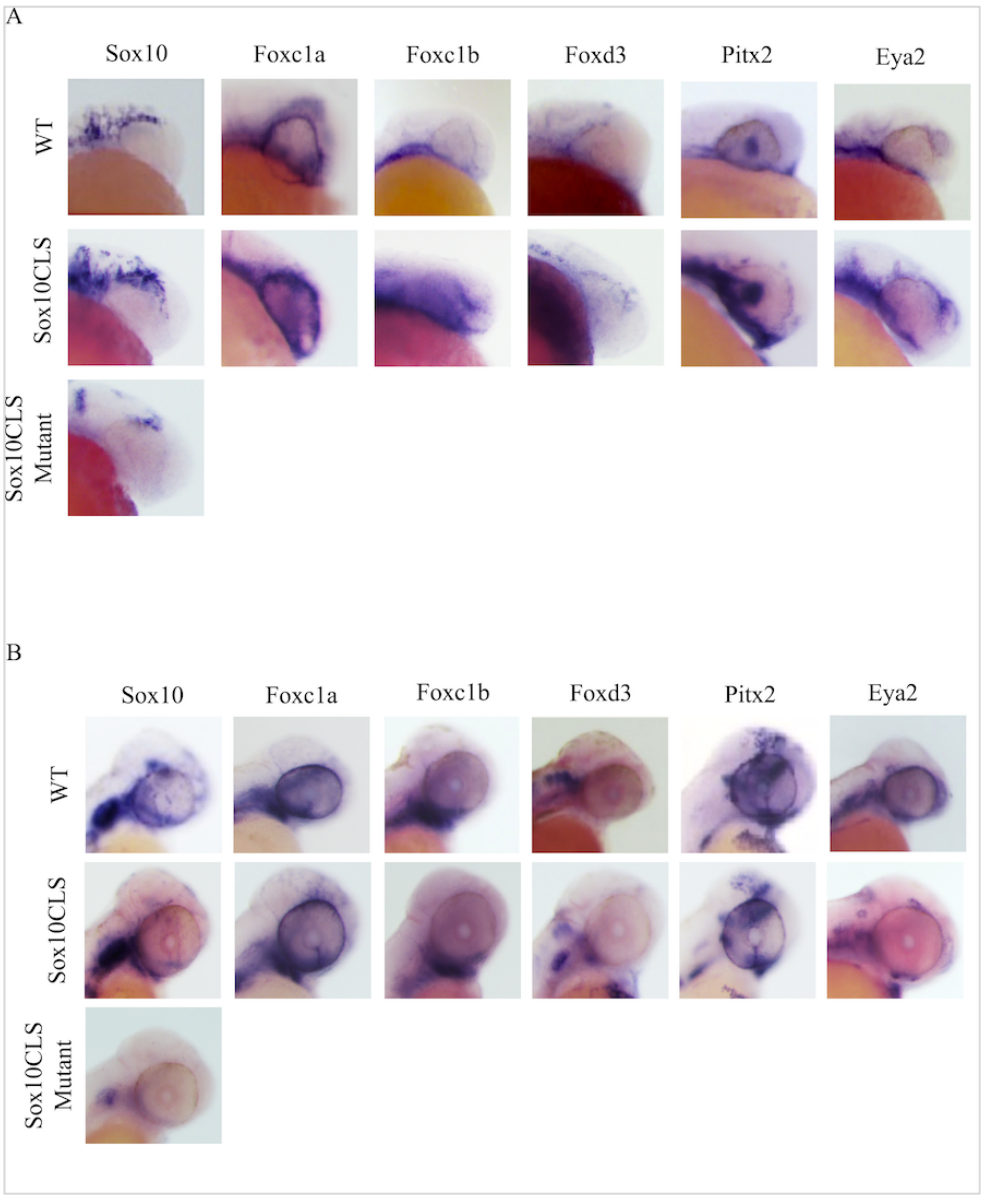

Figure 4.1: POM gene expression patterns in *Sox10-CLS* embryos. Lateral images seen at 24 **(A)** and 48hpf **(B).** No changes in expression patterns between wildtype, heterozygous, and mutant embryos were observed at either time point, despite the loss of *Sox10*.

Real-Time Quantitative PCR (qPCR) was performed using wildtype and *Sox10-CLS* homozygous embryos at 36hpf to confirm the lack of disruption in POM-related gene expression (**Figure 4.2**). ΔΔCt calculations showed mutant samples within the margin of error for all genes tested. With these results, we suspected that the loss of *Sox10* was not a robust enough knockout of the NC to disrupt the formation of the POM populations. *Sox10* is thought to be primarily responsible for the migratory capabilities of NCCs and while *Sox10-CLS* appears to be enough to alter the migration of NCCs throughout the body, in particular pigment cells, it does not show an effect on the NC-derived POM or the development of the AS (Dutton et al., 2001). With this in mind, we sought to knock out other NC genes that appear earlier in the NC-GRN, both individually and in conjunction, to find a more robust knock out model.

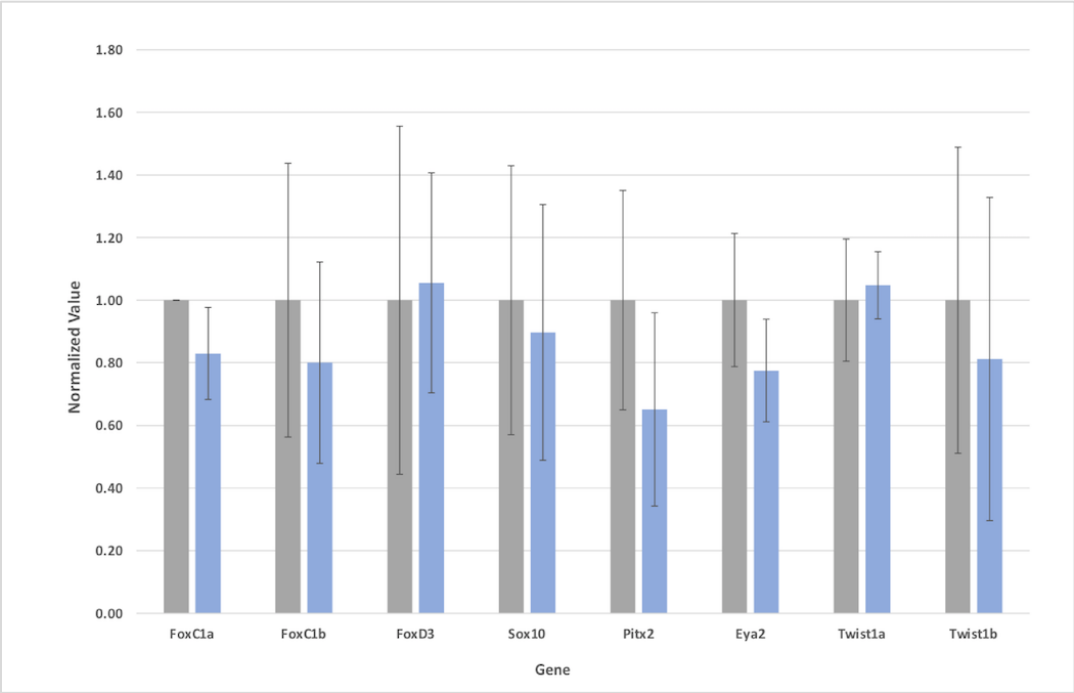

Figure 4.2: qPCR of *Sox10-CLS* at 36hpf. Wildtype is denoted by a gray bar and *Sox10-CLS* mutant is denoted by a blue bar. None of the differences in expression values seen between wildtype and *Sox10-CLS* mutant embryos were statistically significant.

4.3.2 *Tfap2* and *Foxd3* mutants independently knock out POM subpopulations on the anterior segment

Prior to the activation of migratory genes like *Sox10*, NCCs must first be induced at the neural plate border and undergo an EMT in order to become individual, migratory cells. Within the NC-GRN we can identify genes important in these early processes such as *Tfap2a* and *Foxd3*, respectively. Previous work on NC KO lines has shown that *Tfap2a*/*Foxd3* double mutants display an almost complete loss of NCCs, as well as gross morphological defects in eye development (Bryan et al., 2020; Arduini et al., 2009; Wang et al., 2011). To study the effect of these genes on the POM subpopulations, we performed WISH using Fast Blue coloration and 3D confocal imaging to assess POM colonization in both *Tfap2a* and *Foxd3* knockouts. *Tfap2a*^{sa24445} contains a single point mutation resulting in truncation, while a frameshift point deletion in the DNA binding domain creates a premature truncation in the *Foxd3*$^{\Delta 537}$ mutant line. Probes for *Foxc1a, Foxd3, Pitx2, Lmx1b.1,* and *Eya2* were used to detect possible defects in POM specification or migration. At 32hpf, we saw a dramatic reduction or total loss in expression of POM genes on the AS of all probes tested (**Figure 4.3**).

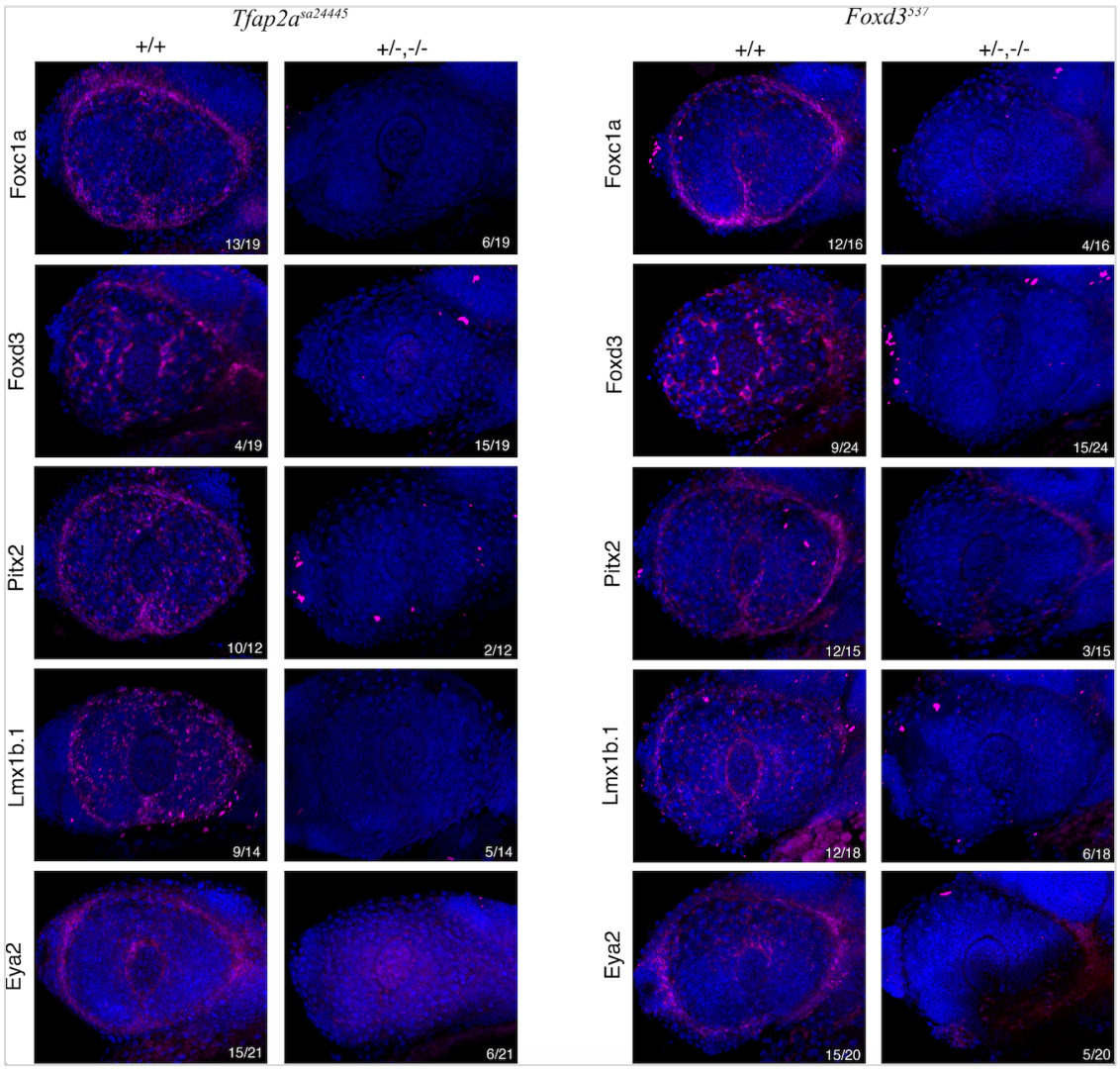

Figure 4.3: POM gene expression patterns in *Tfap2a*^{sa2445} and *Foxd3*$^{\Delta 537}$ embryos at 32hpf. (A) *Tfap2a*^{sa24445} embryos all showed a reduction or complete loss of POM gene expression on the surface of the AS. **(B)** *Foxd3*$^{\Delta 537}$ embryos showed the same reduction or loss of POM gene expression. Numbers in lower right of image indicate the total number of embryos that displayed that expression type for each gene.

Quantification of these results indicated the following the percentage of embryos containing the defect for each mutant line. For *Tfap2a*^{sa24445} embryos: *Foxc1a* (31%), *Foxd3* (78%), *Pitx2* (16%), *Lmx1b.1* (35%), and *Eya2* (28%). For *Foxd3*$^{\Delta 537}$ embryos: *Foxc1a* (25%), *Foxd3* (62%), *Pitx2* (20%), *Lmx1b.1* (33%), and *Eya2* (25%). These numbers indicate that certain POM-related genes are more affected than others by a partial or complete loss of either *Tfap2a* or *Foxd3*. For example, in both mutants, loss of *Pitx2* gene expression is seen in only about 20% of embryos tested, indicating that heterozygous embryos in both lines may retain the wildtype expression pattern. However, loss of *Foxd3* probe expression is seen in much higher overall numbers, indicating that even a partial loss of either NC marker has a profound impact on the *Foxd3* POM subpopulation. With these mutant lines, we can see that loss of *Tfap2a* or *Foxd3* individually can reduce or eliminate the expression of POM-related genes within the AS.

4.4 DISCUSSION

The influence of the NC on the development of the vertebrates cannot be understated, with involvement in skin pigmentation to ganglia development. While further research is needed to understand the role of NCCs in many aspects of vertebrate development, it is perhaps most needed in relation to the development of the ocular AS and the resulting congenital defects associated with failures in NC-derived POM subpopulations and AS tissue development. In order to provide some of this much sought-after clarity, our study here aimed to characterize the negative effects associated with a loss in NCCs on the development of the AS, as well as the individual POM subpopulations. We used a combination of mutant lines, CRISPR injections, and *in situ*

hybridization to analyze these effects. Based on our findings, we conclude that the POM subpopulations are NC-derived and that a loss of NCCs severely diminishes, or completely eliminates, all POM subpopulation colonization and development of the AS. While previous work in the community has shown some ties between the NC and AS development, our work here is the first to show the effects of the NCC loss on each of the POM subpopulations in zebrafish, which we believe will serve as the basis for future work concerning the relationship between NC population health and ASD phenotypes and disorders.

Our previous work on POM cells showed a lack of uniformity within the population observed through a lack of co-expression, differing migratory patterns, and distinct genetic profiles (Van Der Meulen et al., 2020). However, the work lacked evidence supporting the origins of these distinct collections of cells. Believing POM subpopulations originate within the cranial NC, we first sought to eliminate the NC using a mutant line for the NC gene *Sox10*. Surprisingly, loss-of-function mutants for *Sox10* did not show any negative effects in the expression patterns of POM-related transcription factors *Foxc1a, Foxc1b, Foxd3, Pitx2*, and *Eya2* at 24 or 48hpf (**Figure 4.1**). qPCR using 36hpf *Sox10-CLS* mutant embryos compared to wildtype counterparts confirmed these finding (**Figure 4.2**). *Sox10*, often considered a hallmark gene of the NC, isn't activated within the NC until the later stages of the NC-GRN, during the pre-migratory stage and continuing throughout the migration process, promoting not only migration, but also cell survival and pluripotency (Dutton et al., 2001; Kulesa et al., 2003; Bronner and LeDouarin, 2012; Simões-Costa and Bronner, 2015; Mayor and Theveneau, 2013; Noisa and Raivio, 2014). It is our belief that loss of *Sox10* function is not robust enough to

reduce or eliminate the POM subpopulations as they may become specified out from the NC at an early stage or other POM or NC genes may be able to compensate for the loss of *Sox10* within the relatively small POM subpopulation. Further research is required to determine if the loss of *Sox10* has any more subtle negative effects on the development of POM or the AS. Additionally it would be prudent to determine with more clarity when the specification from NC to POM cell occurs and the molecular mechanisms of that transition.

To generate a more effective knock out of the NC, we obtained the *Tfap2a*^{sa24445} and *Foxd3*$^{\Delta 537}$ mutant lines. Previous work has shown that a *Tfap2a*/*Foxd3* double mutant results in a near complete elimination of all NCCs, as well as ocular defects (Bryan et al., 2020; Arduini et al., 2009; Wang et al., 2011). This data suggests that mutations in *Tfap2a* and *Foxd3*, both activated early within the GRN during NC induction and specification stages, can work together to knock out the NC early and effectively enough to also impact the POM. Before creating the double mutant lines, we sought to test whether either the loss of *Tfap2a*^{sa24445} or *Foxd3*$^{\Delta 537}$ independently impacts the POM subpopulations. Our 3D *in situ* work supports this as we saw a severe reduction or complete loss of POM marked by *Foxc1a, Foxd3, Pitx2, Lmx1b.1*, and *Eya2* in 32hpf embryos in both *Tfap2a*^{sa24445} and *Foxd3*$^{\Delta 537}$ lines (**Figure 4.3**). We are confident that we now have a working model to study the effects of NCC loss on POM subpopulations and AS development. Now that the effects of individual losses of either *Tfap2a* or *Foxd3* in the neural crest has been established, we are interested in diving deeper into the relationship dynamics of the POM in these situations. We have shown that POM cells are not arriving to the AS in these mutants at 32hpf, however, more time points should be

assessed to determine if a delay in migration is occurring. Additionally, with the loss of not one, but multiple POM subpopulations, the morphology of the AS and visual capabilities in juvenile and adult fish should be analyzed.

In conclusion, our findings, based on *in situ* hybridizations backed up by qPCR, show that a delicate relationship exists between the NC and the POM. This relationship is critical for the formation of the various POM subpopulations and the development of AS structures. Without a healthy cranial NC population expressing genes such as *Tfap2a* and *Foxd3*, POM subpopulation genes fail to activate and further the migration and specification of POM cells. Our findings further solidify the need for continued investigation into the cranial NC and POM populations, with particular focus on the exact timing and location of cells during the specification from NCC to POM cell, as well as a characterization of the AS defects seen with the loss of each POM gene. These future works will be prudent to our understanding of ASD phenotypes and overall eye development.

4.5 MATERIALS AND METHODS

4.5.1 Zebrafish Maintenance

Zebrafish lines were maintained according to IACUC rules and regulations (IACUC protocol 2015-1380) in a designated facility at the University of Kentucky. AB and ABix lines were used as wildtypes. Transgenic fish lines used included Tg[*sox10:GFP*] (Dr. James Lister) and Tg[*Sox10:RFP*] (Dr. James Lister). Mutant fish lines included the following: *Sox10CLS* (Dr. James Lister), $Tfap2a^{sa24445}$ (Dr. Robert Cornell), and $Foxd3^{\Delta 537}$ (Dr. Robert Cornell). All embryos were raised in incubators at

28˚C in embryo media (E3) during their first 24 hours post fertilization. After the first 24 hours, E3 media was replaced with E3 media containing 1-phenyl 2-thiourea (PTU) to maintain embryos transparency which was replenished every 24 hours.

4.5.2 Whole-Mount *in situ* Hybridization (WISH)

Whole-mount *in situ* hybridization (WISH) was performed on both WT and mutant embryos using approximately 10-18 embryos per time point. Time points used included 24, 32, 36, and 48hpf. DIG and FITC labeled RNA probes were generated using PCR incorporating T7 promoters within the primers and was transcribed with T7 polymerase (Roche). Forward and reverse primer sequences are listed in **Supplemental Table S3.1**. WISH protocol was performed as previously described in Thisse and Thisse (2008). Coloration using NBT/BCIP was used at a concentration of 45µL/10mL and 35µL/10mL, respectively. Coloration using the Fast Blue method (Sigma) were used at a concentration of 10µL/1mL for both NAMP and Fast Blue. Embryos colored with Fast Blue were also counterstained with DAPI (3µL/1mL). Dorsal, lateral, and ventral images of whole embryos colored with NBT/BCIP were captured using a Nikon Digital Sight DS-U3 camera and Nikon Elements software. Lateral 3D images of Fast Blue stained embryos were captured using a Nikon C2+ confocal microscope and utilizing a 20x (0.95 NA) oil immersion objective. All images were adjusted for brightness using Adobe Photoshop and assembled for presentation in Adobe Illustrator.

4.5.3 Real-time Quantitative PCR (qPCR)

Primers for POM and NC genes (*Foxc1a, Foxc1b, Foxd3, Pitx2, Lmx1b.1, Eya2*, and *Sox10*) as well as the endogenous control gene (GAPDH) were generated and validated **(Supplemental Table S4.1).** Total RNA was isolated from either AB control embryos or *Sox10CLS* mutant embryos at 36hpf using Trizol (Invitrogen). A total of 3 biological replicates were used for each treatment. cDNA was synthesized from the total RNA (1mg) using SuperScript reverse transcriptase (Invitrogen) and its concentration was quantified by Epoch Microplate Spectrophotometer (BioTek). cDNA was diluted to 100ng/mL. qPCR was performed in sets of three using 5µL of iTaq Universal SYBR Green Supermix (BioRad), 1µL total of Forward and Reverse Primers **(Supplemental Table S4.1),** 1µL of cDNA from either the control or *Sox10*CLS samples, and 3µL of ddH2O for a total sample volume of 10µL using the CFX Connect Real Time System (BioRad). Results were analyzed via the ΔΔCt standard method.

4.5.4 Alt-R CRISPR Injections

All gRNA, solutions, and protocols for ALT-R CRISPR experiments were obtained from Integrated DNA Technologies (IDT). Mutated sequences of *Sox10*, *Tfap2a*, and *Foxd3* crRNA:tracrRNA were predesigned by IDT to be nonfunctional knockouts for the zebrafish genome. The crRNA:tracrRNA work together to form a functional duplex wherein the crRNA contains the gene specific sequence and the tracr:RNA hybridizes to the crRNA to form a gRNA duplex that activates the Cas9. crRNA (100µm) was resuspended in 20µL of IDT Duplex Buffer (IDT) and incubated at 65°C for 10 mins. tracrRNA (100µm) was resuspended with 200µL of IDT Duplex

Buffer (IDT) and incubated at 65°C for 10 mins. To form the duplex, 5µL of crRNA (50µM) was combined with 5µL of tracrRNA (50µM) in a PCR tube. The mixture was incubated at 95°C for 5 mins before being rapidly cooled to 25°C at a rate of 0.1°C/sec. Once 25°C had been reached, the solution was incubated for 5 mins.

The desired fish (WTs, *Sox10CLS*, *Tfap2a*^{sa24445}, *Foxd3*$^{\Delta 537}$) were released to breed and embryos were collected after 30 mins. Golden was used as an injection control. The final injection mix was as follows 1.5µL of the Duplex mix (5µL of Duplex diluted in 5µL of IDT Duplex Buffer for a final concentration of 25µM), 1.5µL 25µM Cas9 protein, and 0.1µL dex red. 1-2nL of this mixture was injected into the cell of each embryo. After injection, embryos were stored at 28°C in fresh E3 media. PTU media was not supplemented on these embryos to more easily identified mutants, which do not naturally pigment. Golden injected embryos were de-pigmented using 30% hydrogen peroxide until de-pigmentation had occurred.

4.5.5 Statistics

One-way ANOVA and unpaired *t*-tests were performed using Microsoft Excel and GraphPad Prism8 software. All graphs and data points are shown as means ± standard deviation. Significant values were assessed using the conventional standard: P-value < 0.05.

CHAPTER 5: DISCUSSION

Development of the vertebrate eye is as complex as the sense of vision itself, involving precise coordination of numerous cell types undergoing rapid genetic flux, morphological movements, cell migration, and terminal specification. Vision is arguably considered the most important sense, allowing us to interact with the 3D space around us in a way not possible by our other senses. While extremely complex in nature and with key components still not well understood today, eye development has just two main steps: morphogenesis of the eye and retinal development. In general, eye field specification induces future eye cells within the front regions of the forebrain, allowing this neuroepithelial region to evaginate towards the surface ectoderm. Invagination then creates the lens and bi-layered optic cup, allowing for the differentiation and maturation of retinal cells within the cup and the retinal pigmented epithelium on the outer cup. These critical steps are controlled by several morphogenetic factors like Wnt, BMP, RA, and FGF which each control the activation of multiple transcription factors that regulate downstream targets. However, beginning during the latter stages of eye morphogenesis and continuing through retinal development is another crucial but often overlooked aspect of eye development: Periocular Mesenchyme (POM) colonization and development of the Anterior Segment (AS) region.

During formation of the optic cup, POM cells will migrate around the presumptive optic stalk and optic cup to populate into the negative space left between the anterior most portions of the cup and the surface ectoderm, also known as the corneal epithelium at later stages. These specialized migratory cells will invade this region and soon differentiate into various different structures of the AS including the inner two

layers of the cornea, the drainage networks of the iridocorneal angle, ocular muscles, and key inner components of the iris and ciliary bodies. Failures in the migration or specification of the POM can lead to a spectrum of disorders and defects termed Anterior Segment Dysgenesis (ASD).

ASDs can affect one or more structures of the AS and can present solely within the AS or as features within a broader systemic issue. These disorders may cause impaired vision or even congenital blindness. While a small number of cases of systemic disorders like Axenfeld-Rieger Syndrome (ARS) have genetic mutations implicated in their cases, the vast majority of ARS and ASD instances have not been linked to any specific known cause (Reis and Semina, 2011; Sowden, 2007; Williams, 1993; Ma, 2020). Therefore, identifying the molecular mechanics and cellular source of AS development may provide clinicians the information needed to develop new therapies and pharmaceutical interventions to identify potential cases of ASD through genetic screens and improve quality of life for patients already diagnosed.

In the literature, POM cells are broadly defined. Oftentimes, each article will define the POM in a slightly altered way, sometimes using the term to refer to all mesenchyme within the head and other times suggesting POM only refers to cells from a certain region or that target to a specific tissue type. Using the same term to refer to a number of different cell types is confusing the field and adding more chaos to an already misunderstood concept. While many articles have focused their explanations and efforts on piecing together what specific genes are related to what ASD disorders, little has been done to understand the transient POM population itself. With this in mind, our original interest was focused not on the AS specification of cells expressing certain POM genes

but rather, on the POM themselves on a population level. In other words, rather than focus on the individual components of the AS and their development, we wanted to characterize the pool of cells that are responsible for those different components and to understand, at a molecular level, how this one population of cells was capable of forming all these different, specialized structures within the AS. We wanted to finally be able to give some clarity to the field of eye development and allow researchers to have a concrete answer to the question: what is the POM?

With very limited information on POM identity, I originally first sought to define the timeline of POM arrival to the AS by performing a series of whole mount *in situs* on a list of genes known to be involved in AS development or that had previously been implicated in ASD phenotypes. I expected that the bulk of expression patterns would be observed between 24-72hpf and that all expression patterns would be uniform in appearance, marking all POM cells targeting the eye. However, I observed differences between the POM markers in both expression pattern and timing, indicating differences within the POM (**Figure 3.1**). With this information, **I hypothesized that the POM targeting the AS is heterogeneous in nature, comprised of a number of unique subpopulations.** This hypothesis was explored in detail in Chapter 3.

In chapter 3, I sought to investigate and confirmed the existence of POM subpopulations utilizing transgenic reporter lines for several known POM and NC-related transcription factors: *foxc1b, foxd3, pitx2, lmx1b.1,* and *sox10*. I used transgenic lines expressing GFP or RFP under each genes' promoters to track the arrival and dispersal of POM on the AS from 22-72hpf (**Figure 3.3**). By counting the cells in each of the 4 eye quadrants I was able to quantify the significant differences in dispersal and population

size across the subpopulations and create a model of POM subpopulation colonization (**Figure 3.3**). Using Ph3+ staining at 32hpf and 48hpf I was able to show that the changes in subpopulation size was not the result of cell proliferation, but rather the continued influx of cells migrating onto the AS surface (**Figure S3.3**). Utilizing two-color fluorescent *in situ* technology, we showed that while some overlap in expression does exist between the subpopulations, they remain largely exclusive from one another (**Figure 3.2**). To determine if these subpopulations behaved in a similar manner, I used real-time live imaging on a confocal microscope to visualize early POM colonization and manual cell tracking to determine that the cells of each subpopulation migrate on the AS in a stochastic and independent manner, with each subpopulation having different total distances traveled, average velocities, and cellular displacements (**Figure 3.4, Additional Files M3.1-M3.10**). Finally, I used FACs sorting and 10x genomics single cell sequencing technology to create genetic profiles for each of the POM subpopulations at 48hpf wherein k-means clustering identified 4 unique clusters: a neural crest cluster and 3 POM clusters (**Figure 3.5**). Heat maps and *in situs* of the highest upregulated genes in each cluster identified numerous new genes of interest, some related to general POM expression and others related to specific AS structures (**Figures 3.5-3.6**). Several genes identified may mark key AS structures as they have specific expression in key areas of the eye such as *fmoda* on the surface of the AS (cornea) or a*dcyap1b* with expression around the back of the lens (ciliary body) (**Figure 3.6).** By conducting functional analyses on these newly unearthed genes, we may be able to better link developmental genes to POM subpopulations and their final positions within AS structures. Tracking of AS structure cells from their births within the NC to their terminal endpoints would allow

us to fully understand the complexities of AS development, but with the hindsight of POM subpopulation dynamics.

Despite the pivotal work done to support the idea of POM subpopulations outlined in Chapter 3, there were still several limitations to this study. The transgenic lines used to mark the POM subpopulations used in several different experiments were not representative lines used to indicate the real time expression of these POM markers. The proteins to mark cells expressing these genes are quite stable (GFP and RFP), meaning that the protein remains present and active within the cells for a considerable time after the transcription of that gene is no longer ongoing. This means that the distributions mapped in our colonization maps and real-time live imaging may not have been of cells actively expressing the POM gene of interest, but rather cells that were or had previously been expressing that gene in the recent past. This information is still extremely valuable as it shows the unique patterns, heterogeneous nature, and lineage of POM cells within the AS during key time points, but we cannot say that the cells captured at those time points are actively expressing the gene they represent at that time. Future work with POM subpopulation mapping will need to chronicle not only the full lineage of these subpopulations from induction out of the neural crest to fully matured eye, but also more accurately characterize the timeline of POM gene expression. This would allow researchers to better understand how quickly differentiation occurs from POM cell to specified cell type and whether it differs between subpopulations. This research may indicate that some AS structures must be established before others can begin to develop, suggesting that some POM subpopulations may differentiate faster than others. Additionally, scRNA sequencing data was limited to just one specific time point,

48hpf. To capture the entire progression of all POM subpopulations, additional time points earlier and later in development need to be generated.

With fundamental characteristics of the POM and its unique subpopulations established, future work will need to focus on two distinct areas: further characterizing of POM identities and understanding the influence of the POM on one another. In regard to POM subpopulation identity, my work has only begun to scratch the surface of what these cells are and what they can do. Obtaining the full transcriptomic makeup of these cells is only just the beginning, with more work needed to focus on the scRNA sequencing data already generated, as well as creating new transcriptomic profiles at other key developmental stages. This will allow researchers to understand how these subpopulations and the clustering data change throughout development and how they may interact with one another through time. Finding markers of specific AS structures or functions will be key, as well as unearthing new POM genes that may or may not indicate new or overlapping subpopulation markers. Additionally, sequencing data at later stages will yield evidence as to which structures each of the subpopulations contribute to. Long term lineage tracing experiments would also help to show researchers the contributions of these cells to specific structures or regions.

I would also like to see work looking into the interactions of POM with one another and the collaborations amongst themselves to develop the AS. Right now, we know that POM cells are heterogeneous, with different dispersal patterns and genetic profiles, but we are very limited in understanding how these different populations work with each other and influence one another. Do these cells remain independent from each other, each working on their own to form specific tissues or structures or is it a

collaborative effort from multiple groups? In the event of failure of one subpopulation to migrate or function, are the others able to compensate for this loss? When one subpopulation fails, do the others fail as well due to lost signaling or physical interaction, thus creating a snowball effect of developmental failures leading to the multiple structural defects seen in some instances of ASD? I propose a continuation of my POM dispersal and migratory analyses using embryos generated with either a heterozygous or homozygous loss of function mutation for each of the POM genes used thus far, thereby allowing us to characterize the behaviors of the other subpopulations in the absence of one other POM gene from one other group. By generating loss-of-function zebrafish lines for each of the POM-related genes, we will be able to document the gross morphological defects of the AS seen in the absence of just one POM gene through imaging and cryosectioning. Furthermore, by crossing these mutant lines we will also be able to characterize the effect losing one POM gene has on the distribution, arrival time, population size, and migratory behaviors on the other subpopulations, including any compensation or rescuing done by the other subpopulations. Finally, I believe it would also be prudent to research the influence the POM has on the development of other ocular structures. Previous research has shown that the presence of migratory POM cells and their signal is critical for the development of the RPE, overall eye shape, and the fusion of the optic fissure (Strauss, 2005; Fuhrmann et al., 2014; Weaver et al., 2020; Bryan et al., 2020). For example, it is known that migrating endothelial cells enter into the eye via the optic fissure and form the hyaloid vasculature (Weaver et al., 2020; James et al., 2016). Some researchers call these endothelial cells POM cells, but are they truly POM or simply mislabeled in the literature? What signals or physical attributes do these migratory

cells give that induces changes in the epithelial sheets of the fissure and extracellular matrix or the development and shape of the RPE? Additionally, how do signals from the POM influence RA signaling? By further investigating the role POM cells not only play in AS development but also other aspects of eye morphogenesis, we can more clearly understand the vital influence of these cells.

Having now documented the characteristics of POM during their colonization of the AS, prior to their specification into AS tissue types, I next wanted to step farther back in the life of a POM cell. During the course of my work, it became apparent that many systemic ASD conditions, like Axenfeld-Rieger Syndrome, have defects in a wide array of tissues throughout the body that share a neural crest origin during development, including components of the AS. Neural crest cells are a vertebrate specific, highly migratory embryonic cell population with vital contributions to tissues and structures throughout the organism. Some of these contributions include cartilage, bone, myofibroblasts, smooth muscles, glial cells, teeth, and components of the heart, inner ear, and eye. Induced at the borders of the neural plate, NCCs undergo an EMT upon closure of the neural tube and proceed to migrate throughout the body, following various environmental cues. Within the literature, it is well understood that the POM are a derivative of the cranial neural crest (cNC), with small contributions from the mesoderm as well. However, our understanding of the mechanisms of the transition between cNC and POM is very limited. In order to better understand where POM come from and the direct effects of the cNC on POM and the AS, **I hypothesized that proper cNC formation and migration is required for proper development of the POM subpopulations and ocular anterior segment.**

My goals throughout Chapter 4 were to understand the relationship between the cNCCs and the POM subpopulations, as well as AS development. To investigate this relationship, I started by conducting a serious of whole mount *in situs* at 32 and 48hpf using Sox10CLS mutant embryos and probes for various POM markers of interest: *Foxc1a, Foxc1b, Foxd3, Pitx2*, and *Eya2* (**Figure 4.1**). With Sox10 being a key gene for NCCs in the Gene Regulatory Network, it was my belief that knocking it out would result in the loss of POM cell colonization of the AS and therefore AS development. However, the data showed no effect in the expression patterns of any of the POM markers in either heterozygous or homozygous mutants, suggesting that loss of Sox10 function was not enough to eliminate the POM. This was confirmed through qPCR analysis (**Figure 4.2**). I believed *Sox10CLS* to not be a mutation robust enough to eliminate the NC contributing to the POM as it may not be completely penetrant or result in a complete null. While the *Sox10CLS* mutation is able to effectively knock out NC-derived pigmentation cells, it is possible that other genes are compensating for the loss of Sox10 in the head region, particularly other SoxE family members like Sox9. With this in mind I instead chose two other NC-related genes to work with instead, ones that have previously shown a promising near complete loss of NC cells when knocked out (Bryan et al., 2020; Wang et al., 2011; Arduini et al., 2009). *Tfap2a* and *Foxd3* are activated earlier in the NCC process than *Sox10*, at the induction of NCCs on the neural plate border and through the assumption of their migratory capabilities. Conducting fluorescent *in situs* using *Tfap2a*^{sa24445} and *Foxd3*$^{\Delta 537}$ mutant embryos individually at 32hpf, I saw a complete absence of POM gene expression on the surface of the AS (**Figure 4.3**). The loss of expression of several different POM-related genes suggests a very strong relationship

between the health of the NC and the establishment of POM gene expression. While we do no not currently know if the loss of these POM genes also indicates the loss of POM cells themselves, we believe that POM cells lacking these genes may fail to migrate or distribute around the AS properly and would fail to activate the downstream targets necessary for specification into AS structures.

Having investigated the role of POM subpopulation dynamics during AS colonization, the beginning stages of AS specification, and the relationship between NC and POM, a model of POM cell birth to plausible specification in the AS was generated (**Figure 5.1**). This model outlines the possible location of POM specification from NCCs, the initial colonization and distribution of POM cell subpopulations around the AS in relation to one another, and finally speculates about possible AS structures that each of the POM scRNA clusters may contribute to.

The current work outlined here is only the foundation for the work needed to be done on the relationship between the NC and the POM. Extensive work needs to continue to elucidate the details of NC to POM specification and the impacts of NC loss-of-function on POM subpopulation dynamics. Future work will need to focus in more detail on the characteristics of AS morphology in NC knock out lines, particularly *Tfap2a*^{sa24445} and *Foxd3*$^{\Delta 537}$, both individually and in conjunction. Does the loss of NC genes, and therefore migratory NC, halt the development of the AS entirely? Do some POM cells still manage to migrate to the AS, such as

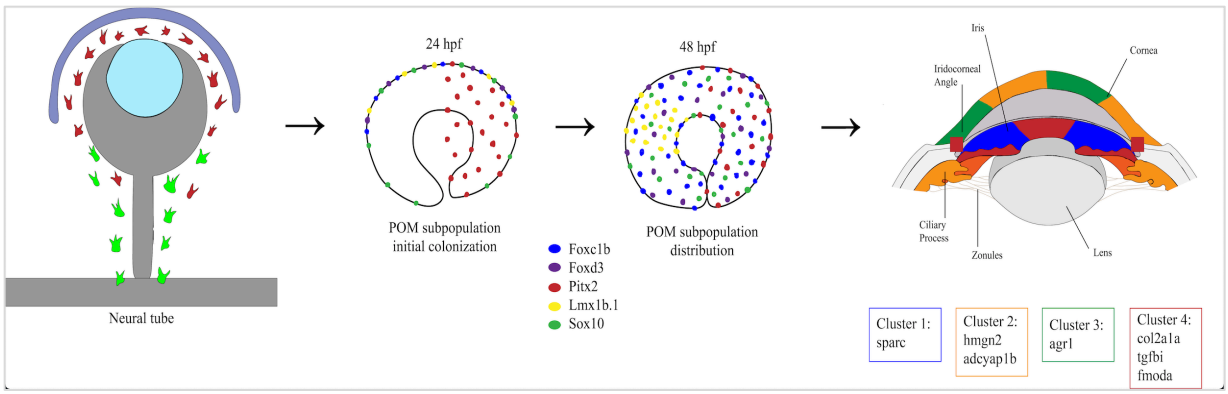

Figure 5.1: Model of POM cell development in zebrafish. A POM cell can first be identified within the neural crest stream targeting to the developing eye. Though currently not well understood, at some point between the initiation of NC migration and the arrival of these cells at the eye, NCCs (green) will specify into POM cells (red). The exact timing, location, and mechanism of this differentiation is unclear. The vast majority of these POM cells will begin to arrive at the surface of the AS between 23-24hpf, with the vast majority of cells entering via the dorsal half of the eye. As eye development continues, the POM subpopulations will begin to distribute around the AS, with some subpopulations inhabiting the entire AS surface and others isolating to specific regions. Finally, as distribution is commencing, POM cells will begin specifying further, expressing genes involved in the development and function of their terminal AS structure endpoints. While further research needs to be done to fully understand this differentiation, the expression patterns of some genes of interest within the scRNA sequencing data allows us to speculate which subpopulations, or clusters, are targeting to which structures.

the small portion derived from the mesoderm, but fail to specify or undergo apoptosis? If some POM cells do manage to arrive to the AS, can they still form partial AS structures or do they lack proper signaling from other POM cells? In addition to the work in the NC mutant lines, more research is also needed to characterize the NC and POM relationship in wildtype development specifically, when, where, and how does the specification from NCC to POM occur? By using two-color *in situ* hybridization, we can look at key time points to find cells co-expressing key NC genes like *Tfap2a* or *Sox10* and POM genes like *Foxc1* and *Pitx2*. Focus should be given to determining when this transition occurs. For instance, do POM cells specify out of the NC soon after the EMT as cells are beginning their migratory tracks indicating an early specification? Or do the POM not obtain their identities until they come into closer proximity to the eye? By ascertaining when this specification occurs, when can more accurately determine the changing dynamics of POM cells and possibly identify problems earlier on in their development.

In conclusion, the research outlined in this dissertation provides a detailed and critical analysis of the molecular make-up and developmental origins of the Periocular Mesenchyme heterogeneous population in vertebrate eye development. It examines in detail the colonization of POM during key time points of eye development, as well as an extensive list of genetic differences seen between subpopulations at the crucial moment of highest POM expression. Real-time 4D imaging showed the exact migratory behaviors of POM within the AS space, while two-color *in situs* showed the extent of heterogeneity between the subpopulations. Additionally, this dissertation provides evidence for the fundamental role of cranial neural crest cells in the development of POM and POM-derived structures. My work shows the profound impact that the NC has on the

expression of POM-related genes and on the development of the POM subpopulations. The work here demonstrates that the POM is not homogeneous and cannot be treated as such in clinical settings. By demonstrating the heterogeneity of the POM, I hope that researchers can investigate the POM through new lenses by more precisely targeting each of the subpopulations in turn, rather than blindly targeting one thinking they are reaching all POM cells. While the role POM may play in ASD disorders later in life is currently unclear, the potential to create more robust and effective therapeutic interventions for developmental disorders through specific subpopulation targeting is reasonable and promising. Future studies on POM subpopulations will need to define POM subpopulation targeting within the AS and specific differentiation mechanisms, as well as their implications in ASDs.

APPENDIX

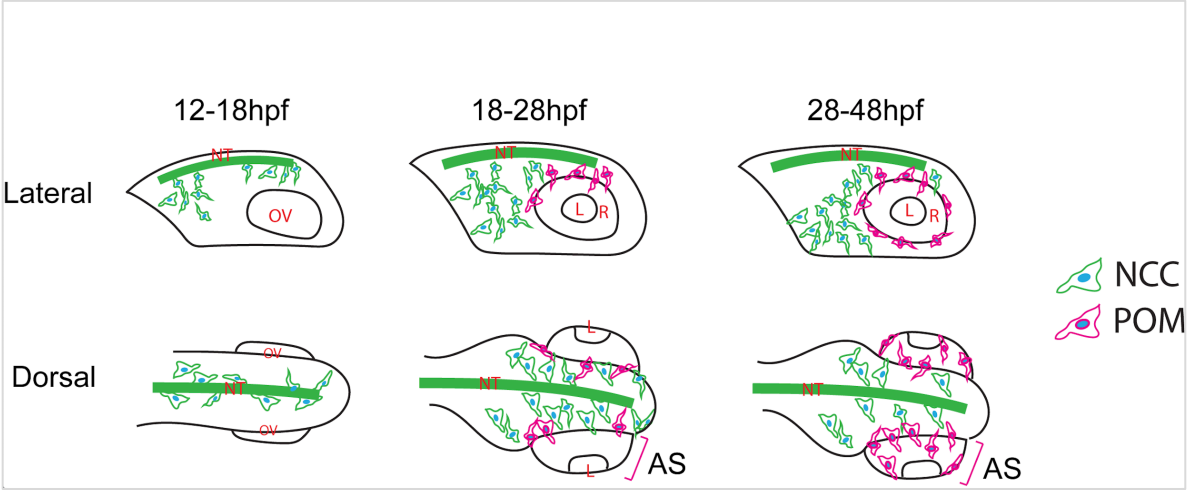

Figure S3.1: Schematic representation of AS colonization in a zebrafish embryo. Upon closure of the neural tube (NT) neural crest cells (NCC) delaminate and begin to migrate throughout the embryo (12–18hpf), including the cranial NCC within the developing head (pictured as black outline; OV, optic vesicle). Upon retinal morphogenesis and lens (L) induction (18–28hpf), NCC begin to surround the retina (R) in anticipation of AS colonization and become periocular mesenchyme (POM). POM targeted to the AS subsequently migrate onto the surface of the retina and occupy the future AS (28–48hpf).

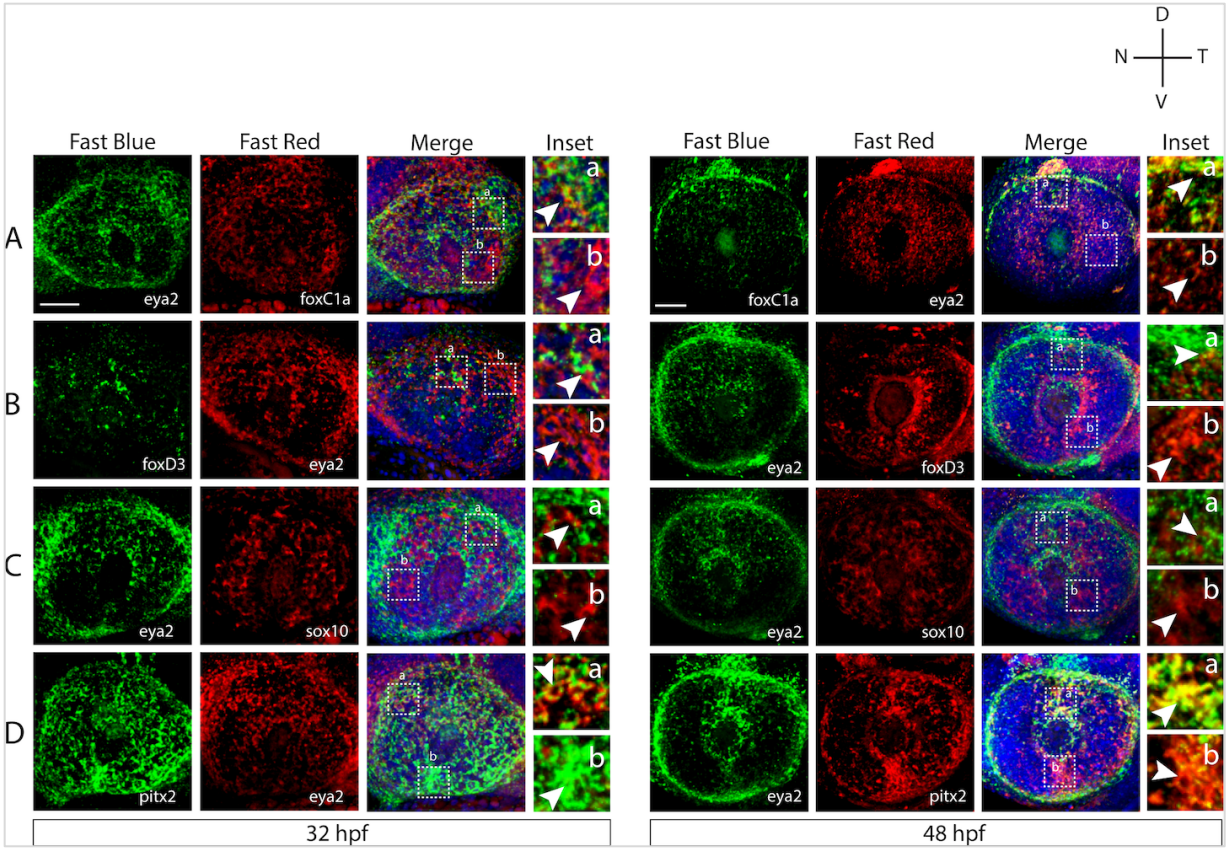

Figure S3.2: Anterior segment ASM heterogeneity for *eya2* expression. (A–D) Two-color fluorescent WISH (FWISH) performed for all possible combinations of *eya2* vs. *foxc1a, foxd3, pitx2,* and s*ox10* at 32 and 48hpf. DAPI is in blue. White arrows within inset panels (dashed squares) display instances of individual **(b)** and co-expression **(a)**. Scale bar = 50µm.

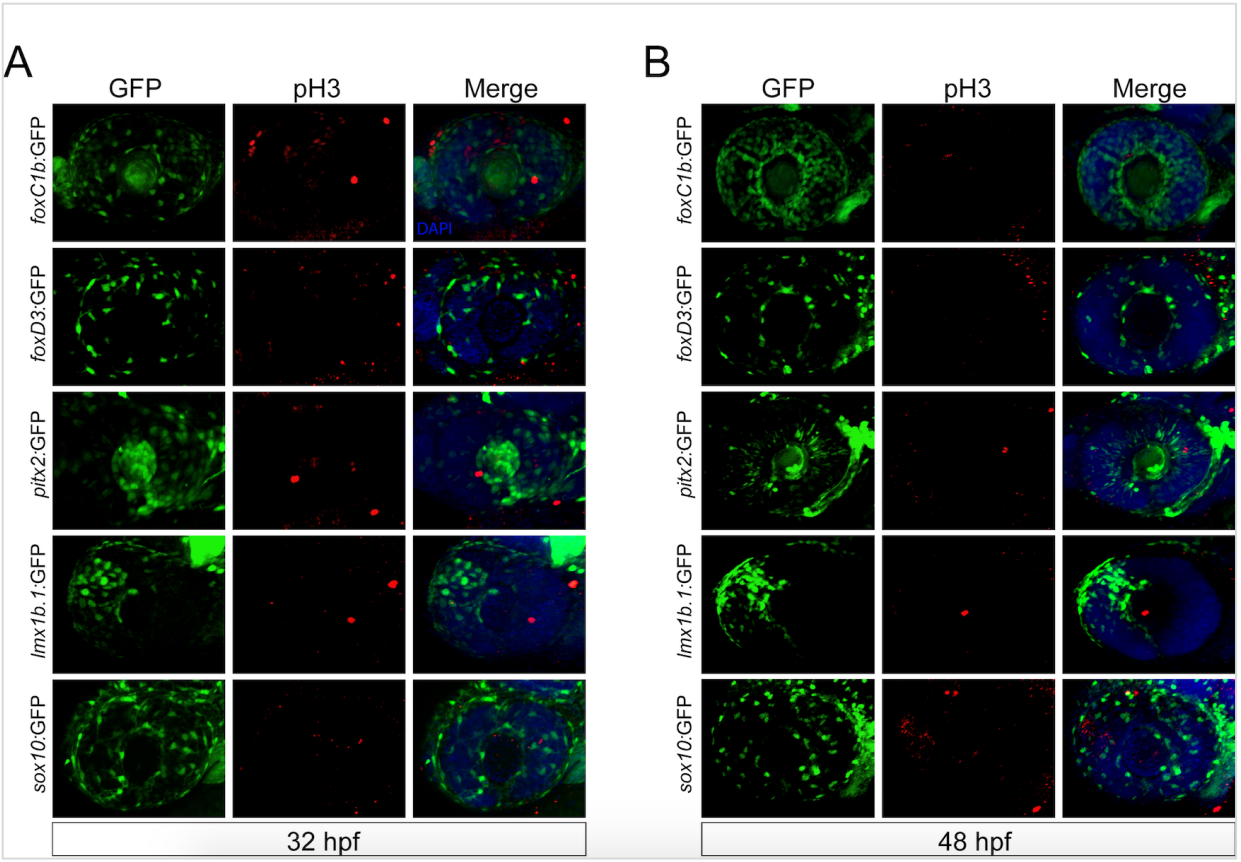

Figure S3.3: PH3 proliferation staining assay. 3D rendering of confocal stacks of the AS at 32 and 48hpf. GFP+ cells (green) are the result of transgenic lines, pH3+ cells (red) indicate active cell division, and DAPI (blue) stains the nucleus. **(A)** Few pH3+ cells can be seen on the surface of the AS at 32hpf, indicating little to no cell division is taking place. No co-expression was seen between the GFP+ cells and pH3+ cells in any of the POM subpopulations. **(B)** Similarly, the AS at 48hpf also lacked pH3+ cells and had little to no co-expression with the various POM subpopulations.

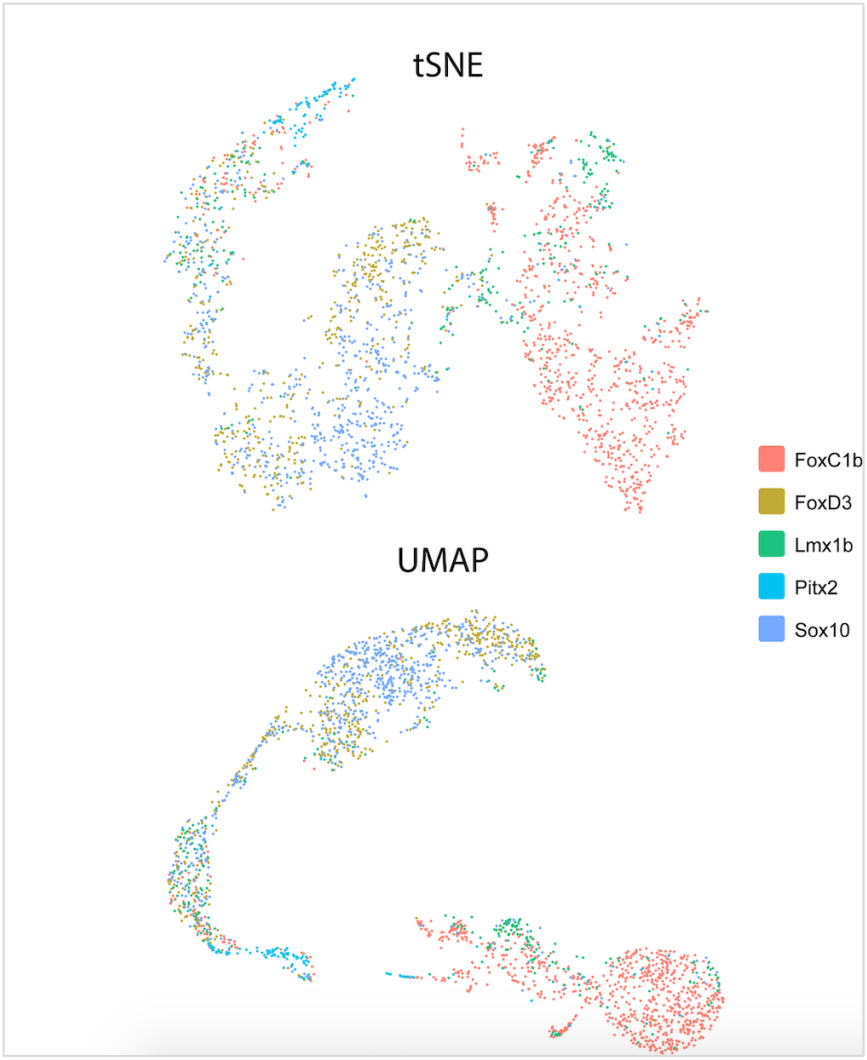

Figure S3.4: cDNA library-based t-SNE and UMAP clusters. K-means clustering of scRNA sequencing of isolated 48hpf *foxc1b:GFP* (pink), *lmx1b.1:GFP* (green), *sox10:GFP* (blue), *foxd3:GFP* (mustard) and *pitx2:GFP* (teal) ASM cells in both tSNE and UMAP readouts.

Figure S3.5: PANTHER Gene Ontology for 48hpf ASM clusters. Protein function Gene Ontology was applied to gene lists from clusters 1–4. Pie graphs display the distribution of each GO term applied.

Table S3.1: WISH Primer Sequence. mRNA forward and reverse primer sequences for all POM and NCC-related genes.

Gene	Primer Sequence
Foxc1a	Forward: ATGCAGGCGCGCTATTCCGTCTCCAGT
	Reverse: TAATACGACTCACTATAGGGCGAGATAGAGTTCTGGCTGCAGGGCGA
Foxc1b	Forward: ATGCAGGCGCGCTACCCCGTG
	Reverse: TAATACGACTCACTATAGGGGTATTCCGGTAAAGTGTCGTC
Foxd3	Forward: ATGACCCTGTCTGGAGGCAC
	Reverse: TAATACGACTCACTATAGGGTCATTGAGAAGGCCATTTCG
Eya2	Forward: ATGGCAGCTTACGGACAGACGCAGTAC
	Reverse: TAATACGACTCACTATAGGGGTTCTTGTATGTGTTGTAGATCTCTTTA
Pitx2	Forward: ATGACCTCTATGAAGGATCCGTTG
	Reverse: TAATACGACTCACTATAGGGTTACACCGGTCTATCCACTGCGTA
Lmx1b.1	Forward: ATGTTGGACGGTATAAAAATC
	Reverse: TAATACGACTCACTATAGGGTCATGAGGCGAAATAGGAGCTCTGCAT
Lmx1b.2	Forward: TGCTGGACGGAATCAAAATTG
	Reverse: TAATACGACTCACTATAGGGTCAGGAGGTGAAGTAGGAGCTCTG
Sox10	Forward: ATGTCGGCGGAGGAGCACAG
	Reverse: TAATACGACTCACTATAGGGTCACGGTCGAGACAGTGTGGTG
Sparc	Forward: AGAAAGTTTCACCAGCTGACTTC
	Reverse: TAATACGACTCACTATAGCCTCCCCCCAATAATAACTAGG
Hmgn2	Forward: CTGCAGCCAAGATGCCCAAAA
	Reverse: TAATACGACTCACTATAGGGTTTTATTCAAAACCATTTAAA
Gng13b	Forward: AACTTCTATAGCATCGTTTCAG
	Reverse: TAATACGACTCACTATAGGTTAATAAATTAAAACGAACTG
Adycap1b	Forward: ATAAAATCCGTGGTAATCGGAG
	Reverse: TAATACGACTCACTATAGCTTTTGTACAAAAAGAAAAACAATG
Agr1	Forward: GATTCGATATCGCGGCCGCGG
	Reverse: TAATACGACTCACTATAGTAATGATTCCTAATATGAAATTC
Cyt1	Forward: CTTCTTCTCCAGGCAGAGCAGG
	Reverse: TAATACGACTCACTATAGCTTTCATGCTGAGTCGGGACTG
Ponzr3	Forward: AAAAGCGCTCAGTCTCGTCTTC
	Reverse: TAATACGACTCACTATAGGGCACAGTTTATCACAATTCTT
Col2a1a	Forward: CGGCGACTTTCACCCCTTAGGAC
	Reverse: TAATACGACTCACTATAGGGCACCTGCAGCACCAGCCTCTC
Fmoda	Forward: AAAGCCACTCCATATGCTACAGG
	Reverse: TAATACGACTCACTATAGCACACTGCAGAAACTGCCCAGC
Lum	Forward: GCAACATAATATGTAACAATGTTTTC
	Reverse: TAATACGACTCACTATAGTAGTTGAGCTCATGTCTCGGTAC
Tgfbi	Forward: GACCATCAACGGCAAAGCTGTC
	Reverse: TAATACGACTCACTATAGGGCTGGACACGAGACAATGTTCTG
Si:ch211-195b11.3	Forward: GACTACAAACATATTTAACACC
	Reverse: TAATACGACTCACTATAGGGGGAACAAAGTGATATTTATTGGC

Table S4.1: qPCR Primer Sequences. Forward and reverse primer sequences for all POM and NCC-related genes.

Gene	Primer Sequence
GapDH	Forward: TCCGTCTTGAGAAACCTGCC
	Reverse: CAACCTGGTGCTCCGTGTAT
Foxc1a	Forward: ACAGAGACAACAAGCAGG
	Reverse: CGGGTTTCTTATCATCGC
Foxc1b	Forward: TGGCAGAACAGCATAAGG
	Reverse: CGGGTCTAAAGTCCAGTAG
Foxd3	Forward: AGGAGGAGAAAACGCTTC
	Reverse: TATGGATTCCCAATGCCG
Sox10	Forward: GTCGGAGGTGGAAATGAG
	Reverse: GGACATCTGAGACTGCTG
Pitx2	Forward: CTCCAGTATGGTTCCGTC
	Reverse: TAGAGAGGGGTTGCTGAG
Eya2	Forward: GACCTGGAGGAATGTGAC
	Reverse: CTGGAAACCATCTGTGCC
Twist1a	Forward: ATCATCCCCACCTTACCC
	Reverse: GCTGGACATCTTGGAGTC
Twist1b	Forward: CGGCTTTACGCAAAATCATC
	Reverse: GCTCTGTCACTCTGTAGAAC

REFERENCES

Abu-Hassan, D., Acott, T., Kelley, M., 2014. The trabecular meshwork: a basic review of form and function, Journal of Ocular Biology.

Abzhanov, A., Tzahor, E., Lassar, A., and Tabin, C., 2003. Dissimilar regulation of cell differentiation in mesencephalic (cranial) and sacral (trunk) neural crest cells in vitro. Development 130, 4567-4579.

Achary, M.S., Reddy, A.B.M., Chakrabarti, S., Panicker, S.G., Mandal, A.K., Ahmed, N., Balasubramanian, D., Hasnain, S.E., Nagarajaram, H.A., 2006. Disease-causing mutations in proteins: Structural analysis of the CYP1b1 mutations causing primary congenital glaucoma in humans. Biophysical Journal 91, 4329-4339.

Akula, M., Taiyab, A., Deschamps, P., Yee, S., Ball, A.K., Williams, T., West-Mays, J.A., 2020. AP-2 beta is required for formation of the murine trabecular meshwork and Schlemm's canal. Experimental Eye Research 195, 8.

Akula, M., Won Park, J., and West-Mays, J., 2018. Relationship between neural crest cell specification and rare ocular diseases. Journal of Neuroscience Research 97, 7-15.

Aldinger, K.A., Lehmann, O.J., Hudgins, L., Chizhikov, V.V., Bassuk, A.G., Ades, L.C., Krantz, I.D., Dobyns, W.B., Millen, K.J., 2009. FOXC1 is required for normal cerebellar development and is a major contributor to chromosome 6p25.3 Dandy-Walker malformation. Nature Genetics 41, 1037-U1116.

Alsomiry, A.S., Gregory-Evans, C.Y., Gregory-Evans, K., 2019. An update on the genetics of ocular coloboma. Human Genetics 138, 865-880.

Alward, W.L.M., 2000. Axenfeld-Rieger syndrome in the age of molecular genetics. American Journal of Ophthalmology 130, 107-115.

Arduini, B.L., Bosse, K.M., Henion, P.D., 2009. Genetic ablation of neural crest cell diversification. Development 136, 1987-1994.

Baker, C.V.H., Bronner Fraser, M., LeDouarin, N.M., Teillet, M.A., 1997. Early-and late-migrating cranial neural crest cell populations have equivalent developmental potential in vivo. Development 124, 3077-3087.

Bejjani, B.A., Xu, L., Armstrong, D., Lupski, J.R., Reneker, L.W., 2002. Expression patterns of cytochrome P4501B1 (Cyp1b1) in FVB/N mouse eyes. Experimental Eye Research 75, 249-257.

Bernardos, R.L., Barthel, L.K., Meyers, J.R., Raymond, P.A., 2007. Late-stage neuronal progenitors in the retina are radial Muller glia that function as retinal stem cells. Journal of Neuroscience 27, 7028-7040.

Bernstein, C.S., Anderson, M.T., Gohel, C., Slater, K., Gross, J.M., Agarwala, S., 2018. The cellular bases of choroid fissure formation and closure. Developmental Biology 440, 137-151.

Berry, F., Lines, M., Oas, J., Footz, T., Underhill, D., Gage, P., and Walter, M., 2006. Functional interactions between foxc1 and pitx2 underlie the sensitivity to foxc1 gene dose in axenfeld-rieger syndrome and anterior segment dysgenesis. Human Molecular Genetics 15, 905-919.

Bhandari, R., Ferri, S., Whittaker, B., Liu, M., Lazzaro, D.R., 2011. Peters Anomaly: Review of the Literature. Cornea 30, 939-944.

Bohnsack, B., Kasprick, D., Kish, P., Goldman, D., and Kahana, A., 2012. A zebrafish model of axenfeld-rieger syndrome reveals that pitx2 regulation by retinoic acid is essential for ocular and craniofacial development. Investigative Ophthalmology & Visual Science 53, 7-22.
Bohnsack, B. and Kahana, A. 2013. Thyroid hormone and retinoic acid interact to regulate zebrafish craniofacial neural crest development. Developmental Biology 373, 300-309.
Borges-Giampani, A. and Giampani Jr., J. 2013. Anatomy of the ciliary body, ciliary processes, and anterior chamber angle, and collector vessels. IntechOpen.
Brickman, J.M., Clements, M., Tyrell, R., McNay, D., Woods, K., Warner, J., Stewart, A., Beddington, R.S.P., Dattani, M., 2001. Molecular effects of novel mutations in Hesx1/HESX1 associated with human pituitary disorders. Development 128, 5189-5199.
Bronner, M.E. and LeDouarin, N.M., 2012. Development and evolution of the neural crest: An overview. Developmental Biology 366, 2-9.
Bryan, C.D., Casey, M.A., Pfeiffer, R.L., Jones, B.W., Kwan, K.M., 2020. Optic cup morphogenesis requires neural crest-mediated basement membrane assembly. Development 147, 17.
Buckley, C., Carvalho, M., Young, L., Rider, S., McFadden, C., Berlage, C., Verdon, R., Taylor, J., Girkin, J., and Mullins, J., 2017. Precise spatio-temporal control of rapid optogenetic cell ablation with mem-KillerRed in zebrafish. Scientific Reports 7.
Carmona-Fontaine, C., Matthews, H., Kuriyama, S., Moreno, M., Dunn, G., Parsons, M., Stern, C., and Mayor, R., 2008. Contact inhibition of locomotion in vivo controls neural crest directional migration. Nature Letters 456, 957-961.
Carrara, N., Weaver, M., Pereira Piedade, W., Vöcking, O., and Famulski, J., 2019. Temporal characterization of optic fissure basement membrane composition suggests nidogen may be an initial target of remodeling. Developmental Biology 452(1): 43-54.
Casazza, A., Fazzari, P., and Tamagnone, L., 2007. Semaphorin signals in cell adhesion and cell migration: Functional role and molecular mechanisms, in: Pasterkamp, R.J. (Ed.), Semaphorins: receptor and Intracellular Signaling Mechanisms. Landes Bioscience and Springer Science and Business Media, pp. 90-108.
Cavodeassi, F., 2018. Dynamic tissue rearrangements during vertebrate eye morphogenesis: insights from fish models. Journal of Developmental Biology 6.
Chak, G., Mosaed, S., and Minckler, D., 2014. Diagnosing and managing juvenile open-angle glaucoma. American Academy of Ophthalmology.
Chakravarthi, S., Kannabiran, C., Sridhar, M.S., Vemuganti, G.K., 2005. TGFBI gene mutations causing lattice and granular corneal dystrophies in Indian patients. Investigative Ophthalmology & Visual Science 46, 121-125.
Chawla, B., Schley, E., Williams, A., and Bohnsack, B., 2016. Retinoic acid and pitx2 regulate early neural crest survival and migration in craniofacial and ocular development. Birth Defects Research (Part B) 107, 126-135.
Chawla, B., Swain, W., Williams, A., and Bohnsack, B., 2018. Retinoic acid maintains function of neural crest-derived ocular and craniofacial structures in adult zebrafish. Investigative Ophthalmology & Visual Science 59, 1924-1935.
Chen, L., Martino, V., Dombkowski, A., Williams, T., West-Mays, J., and Gage, P., 2016a. AP-2B is a downstream effector of pitx2 required to specify endothelium and

establish angiogenic privilege during corneal development. Investigative Ophthalmology & Visual Science 57, 1072-1081.
Chen, L. and Gage, P., 2016b. Heterozygous Pitx2 null mice accurately recapitulate the ocular features of axenfeld-rieger syndrome and congenital glaucoma. Investigative Ophthalmology & Visual Science 57, 5023-5030.
Chhetri, J., Jacobson, G., Gueven, N., 2014. Zebrafish-on the move towards ophthalmological research. Eye 28, 367-380.
Chuang, J.C., Raymond, P.A., 2002. Embryonic origin of the eyes in teleost fish. Bioessays 24, 519-529.
Clark, S.W., Fee, B.E., Cleveland, J.L., 2002. Misexpression of the eyes absent family triggers the apoptotic program. Journal of Biological Chemistry 277, 3560-3567.
Clay, M. and Halloran, M., 2010. Control of neural crest cell behavior and migration. Cell Adhesion & Migration 4, 586-594.
Copp, A.J., Greene, N.D.E., Murdoch, J.N., 2003. The genetic basis of mammalian neurulation. Nature Reviews Genetics 4, 784-793.
Cordero, D.R., Brugmann, S., Chu, Y.N., Bajpai, R., Jame, M., Helms, J.A., 2011. Cranial Neural Crest Cells on the Move: Their Roles in Craniofacial Development. American Journal of Medical Genetics Part A 155A, 270-279.
Cox, T.C., 2004. Taking it to the max: The genetic and developmental mechanisms coordinating midfacial morphogenesis and dysmorphology. Clinical Genetics 65, 163-176.
Creuzet, S., Vincent, C., and Couly, G., 2005. Neural crest derivatives in ocular and periocular structures. International Journal of Developmental Biology 49, 161-171.
Cummings, K.J., Gray, S.L., Simmons, C.J.T., Kozak, C.A., Sherwood, N.M., 2002. Mouse pituitary adenylate cyclase-activating polypeptide (PACAP): gene, expression and novel splicing. Molecular and Cellular Endocrinology 192, 133-145.
Curado, S., Stainier, D., and Anderson, R., 2008. Nitroreductase-mediated cell/tissue ablation in the zebrafish: a spatially and temporally controlled ablation method with application in developmental and regneration studies. nature Protocols 3, 948-954.
Cvekl, A. and Tamm, E.R., 2004. Anterior eye development and ocular mesenchyme: new insights from mouse models and human diseases. Bioessays 26, 374-386.
Cvekl, A. and Wang, W.L., 2009. Retinoic acid signaling in mammalian eye development. Experimental Eye Research 89, 280-291.
Davis-Silberman, N. and Ashery-Padan, R., 2008. Iris development in vertebrates; genetic and molecular considerations. Brain Research 1192, 17-28.
de Vos, I., Stegmann, A., Webers, C., and Stumpel, C., 2017. The 6p25 deletion syndrome: an update on a rare neurocristopathy. Ophthalmic Genetics 38, 101-107.
Devotta, A., Hong, C.S., Saint-Jeannet, J.P., 2018. Dkk2 promotes neural crest specification by activating Wnt/beta-catenin signaling in a GSK3 beta independent manner. Elife 7, 17.
Distel, M., Wullimann, M., and Koster, R., 2009. Optimized Gal4 genetics for permanent gene expression mapping in zebrafish. PNAS 106, 133365-133370.
Drerup, C., Wiora, H., Topczewski, J., and Morris, J., 2009. Disc1 regulates foxd3 and sox10 expression, affecting neural crest migration and differentiation. Development 136, 2623-2632.

Dunston, J.A., Reimschisel, T., Ding, Y.Q., Sweeney, E., Johnson, R.L., Chen, Z.F., McIntosh, I., 2005. A neurological phenotype in nail patella syndrome (NPS) patients illuminated by studies of murine Lmx1b expression. European Journal of Human Genetics 13, 330-335.
Dutton, K., Pauliny, A., Lopes, S., Elworthy, S., Carney, T., Rauch, J., Geisler, R., Haffter, P., and Kelsh, R., 2001. Zebrafish colourless encodes sox10 and specifies non-ectomesenchymal neural crest fates. Development 128, 4113-4125.
Emison, E.S., Garcia-Barcelo, M., Grice, E.A., Lantieri, F., Amiel, J., Burzynski, G., Fernandez, R.M., Hao, L., Kashuk, C., West, K., Miao, X.P., Tam, P.K.H., Griseri, P., Ceccherini, I., Pelet, A., Jannot, A.S., de Pontual, L., Henrion-Caude, A., Lyonnet, S., Verheij, J., Hofstra, R.M.W., Antinolo, G., Borrego, S., McCallion, A.S., Chakravarti, A., 2010. Differential Contributions of Rare and Common, Coding and Noncoding Ret Mutations to Multifactorial Hirschsprung Disease Liability. American Journal of Human Genetics 87, 60-74.
Espinoza, H.M., Cox, C.J., Semina, E.V., Amendt, B.A., 2002. A molecular basis for differential developmental anomalies in Axenfeld-Rieger syndrome. Human Molecular Genetics 11, 743-753.
Evans, A. and Gage, P., 2005. Expression of the homeobox gene Pitx2 in neural crest is required for optic stalk and ocular anterior segment development. Human Molecular Genetics 14, 3347-3359.
Fadool, J. and Dowling, J., 2008. Zebrafish: a model system for the study of eye genetics. Progress in Retinal and Eye Research 27, 89-110.
Fadool, J.M., Dowling, J.E., 2008. Zebrafish: A model system for the study of eye genetics. Progress in Retinal and Eye Research 27, 89-110.
Ferre-Fernandez, J.J., Sorokina, E.A., Thompson, S., Collery, R.F., Nordquist, E., Lincoln, J., Semina, E.V., 2020. Disruption of foxc1 genes in zebrafish results in dosage-dependent phenotypes overlapping Axenfeld-Rieger syndrome. Human Molecular Genetics 29, 2723-2735.
Friedl, P. and Wolf, K., 2010. Plasticity of cell migration: a multiscale tuning model. Journal of Cell Biology 188, 11-19.
Fu, Y., 2010. Phototransduction in rods and cones, in: Kolb H, F.E., Nelson R (Ed.), Webvision: The Organization of the Retina and Visual System [Internet]. University of Utah Health Sciences Center, Salt Lake City (UT).
Fuhrmann, S., 2010. EYE MORPHOGENESIS AND PATTERNING OF THE OPTIC VESICLE, in: Cagan, R.L., Reh, T.A. (Eds.), Invertebrate and Vertebrate Eye Development. Elsevier Academic Press Inc, San Diego, pp. 61-84.
Fuhrmann, S., Levine, E., and Reh, T., 2000. Extraocular mesenchyme patterns the optic vesicle during early eye development in the embryonic chick. Development 127, 4599-4609.
Fuhrmann, S., Zou, C., and Levine, E., 2014. Retinal pigment epithelium development, plasticity, and tissue homeostasis (Invited review for Experimental Eye Research). Experimental Eye Research 0, 141-150.
Furusawa, T. and Cherukuri, S., 2010. Developmental function of HMGN proteins. Biochimica Et Biophysica Acta-Gene Regulatory Mechanisms 1799, 69-73.

Gage, P., Kaung, C., and Zacharias, A., 2014. The homeodomain transcription factor pitx2 is required for specifying correct cell fates and establishing angiogenic privilege in the developing cornea. Developmental Dynamics 243, 1391-1400.
Gage, P.J., Qian, M., Wu, D.Q., Rosenberg, K.I., 2008. The canonical Wnt signaling antagonist DKK2 is an essential effector of PITX2 function during normal eye development. Developmental Biology 317, 310-324.
Germanguz, I., Lev, D., Waisman, T., Kim, C., and Gitelman, I., 2007. Four Twist genes in zebrafish, four expression patterns. Developmental Dynamics 236, 2615-2626.
Gestri, g., Bazin-Lopez, N., Scholes, C., and Wilson, S., 2018. Cell behaviors during closure of the choroid fissure in the developing eye. Frontiers in Cellular Neuroscience 12.
Goel, M., Picciani, R.G., Lee, R.K., Bhattacharya, S.K., 2010. Aqueous Humor Dynamics: A Review. Open Ophthalmology Journal 4, 52-59.
Goldman, D., 2014. Muller glial cell reprogramming and retina regeneration. Nature Reviews Neuroscience 15, 431-442.
Gould, D., Smith, R., and John, S., 2004. Anterior segment development relevant to glaucoma. International Journal of Developmental Biology 48.
Graw, J., 2010. EYE DEVELOPMENT, in: Koopman, P. (Ed.), Organogenesis in Development. Elsevier Academic Press Inc, San Diego, pp. 343-386.
Gray, M., Smith, R., Soules, K., John, S. and Link, B., 2009. The aqueous humor outflow pathway of zebrafish. Investigative Ophthalmology & Visual Science 50.
Gregory-Evans, C.Y., Williams, M.J., Halford, S., Gregory-Evans, K., 2004. Ocular coloboma: a reassessment in the age of molecular neuroscience. Journal of Medical Genetics 41, 881-891.
Gross, J.M., Perkins, B.D., Amsterdam, A., Egana, A., Darland, T., Matsui, J.I., Sciascia, S., Hopkins, N. and Dowling, J.E., 2005. Identification of zebrafish insertional mutants with defects in visual system development and function. Genetics 170, 245-261.
Gross-Thebing, T., Paksa, A., and Raz, E., 2015. Simultaneous high-resolution detection of multiple transcripts combined with localization of proteins in whole-mount embryos. BMC Biology 12.
Hall, B.K., 2000. The neural crest as a fourth germ layer and vertebrates as quadroblastic not triploblastic. Evolution & Development 2, 3-5.
Hanna, L.A., Foreman, R.K., Tarasenko, I.A., Kessler, D.S., Labosky, P.A., 2002. Requirement for Foxd3 in maintaining pluripotent cells of the early mouse embryo. Genes & Development 16, 2650-2661.
Hans, S., Kaslin, J., Freudenreich, D., and Brand, M., 2009. Temporally-controlled site-specific recombination in zebrafish. PLoS One 4.
He, D.Y., Marie, C., Zhao, C.T., Kim, B., Wang, J.C., Deng, Y.Q., Clavairoly, A., Frah, M., Wang, H.B., He, X.L., Hmidan, H., Jones, B.V., Witte, D., Zalc, B., Zhou, X., Choo, D.I., Martin, D.M., Parras, C., Lu, Q.R., 2016. Chd7 cooperates with Sox10 and regulates the onset of CNS myelination and remyelination. Nature Neuroscience 19, 678-+.
Hendee, K., Sorokina, E., Muheisen, S., Reis, L., Tyler, R., Markovic, V., Cuturilo, G., Link, B., and Semina, E., 2018. Pitx2 deficiency and associated human disease: insights from the zebrafish model. Human Molecular Genetics 27, 1675-1695.
Hirose, H., Ishii, H., Mimori, K., Tanaka, F., Takemasa, I., Mizushima, T., Ikeda, M., Yamamoto, H., Sekimoto, M., Doki, Y., Mori, M., 2011. The Significance of PITX2

Overexpression in Human Colorectal Cancer. Annals of Surgical Oncology 18, 3005-3012.
Hoffman, T., Javier, A., Campeau, S., Knight, R., and Schilling, T., 2007. Tfap2a transcription factors in zebrafish neural crest development and ectodermal evolution. Journal of Experimental Zoology (Mol Dev Evol) 308, 679-691.
Holly, V.L., WIden, S. A., Famulski, J.K., and Waskiewicz, A.J., 2014. Sfrp1a and Sfrp5 function as positive regulators of Wnt and BMP signaling during early retinal development. Developmental Biology 388, 192-204.
Hsu, Y., 2015. Theory and practice of lineage tracing. Stem Cells 33, 3197-3204.
Iqbal, Z., Cejudo-Martin, P., de Brouwer, A., van der Zwaag, B., Ruiz-Lozano, P., Scimia, M., Lindsey, J., Weinreb, R., Albrecht, B., Megarbane, A., Alanay, Y., Ben-Neriah, Z., Amenduni, M., Artuso, R., Veltman, J., van Beusekom, E., Oudakker, A., Millan, J. Hennekam, R., Hamel, B., Courtneidge, S., and van Bokhoven, H., 2010. Disrution of the podosome adapter protein TKs4 (SH3PXD2B) causes the skeletal dysplasia, eye, and cardiac abnormalities of the Frank-Ter Haar syndrome. The American Journal of Human Genetics 86, 254-261.
Ittner, L., Wurdak, H., Schwerdtfeger, K., Kunz, T., Ille, F., Leveen, P., Hjalt, T., Suter, U., Karlsson, S., Hafezi, F., Born, W., and Sommer, L., 2005. Compound developmental eye disorders following inactivation of TGFbeta signaling in neural-crest stem cells. Journal of Biology 4.
Ivanova, A.S., Korotkova, D.D., Ermakova, G.V., Martynova, N.Y., Zaraisky, A.G., Tereshina, M.B., 2018. Ras-dva small GTPases lost during evolution of amniotes regulate regeneration in anamniotes. Scientific Reports 8, 16.
Iwao, K., Inatani, M., Ogata-Iwao, M., Yamaguchi, Y., Okinami, S., and Tanihara, H., 2010. Heparan sulfate deficiency in periocular mesenchyme causes microphthalmia and ciliary body dysgenesis. Experimental Eye Research 90, 81-88.
James, A., Lee, C., Williams, A., Angileri, K., Lathrop, K., and Gross, J., 2016. The hyaloid vasculature facilitates basement membrane breakdown during choroid fissure closure in the zebrafish eye. Developmental Biology 419, 262-272.
Jesuthasan, S., 1996. Contact inhibition/collapse and pathfinding of neural crest cells in the zebrafish trunk. Development 122, 381-389.
Ji, Y., Buel, S., and Amack, J., 2016. Mutations in zebrafish pitx2 model congenital malformations in axenfeld-rieger syndrome but do not disrupt left-right placement of visceral organs. Developmental Biology 416, 69-81.
Johnson, C., Holzemer, N., and Wingert, R., 2011. Laser ablation of the zebrafish pronephros to study renal epithelial regeneration. Journal of Visualized Experiments 54.
Kannabiran, C., Klintworth, G.K., 2006. TGFBI gene mutations in corneal dystrophies. Human Mutation 27, 615-625.
Kelsh, R.N., 2006. Sorting out Sox10 functions in neural crest development. Bioessays 28, 788-798.
Kim, Y.K., Lee, H., Ismail, T., Kim, Y., Lee, H.S., 2020. Dach1 regulates neural crest migration during embryonic development. Biochemical and Biophysical Research Communications 527, 896-901.
Kimmel, C.B., Ballard, W.W., Kimmel, S.R., Ullmann, B., Schilling, T.F., 1995. STAGES OF EMBRYONIC-DEVELOPMENT OF THE ZEBRAFISH. Developmental Dynamics 203, 253-310.

Kioussi, C., Briata, P., Baek, S., Rose, D., Hamblet, N., Herman, T., Ohgi, K., Lin, C., Gleiberman, A., Wang, J., Brault, V., Ruiz-Lozano, P., Nguyen, H., Kemler, R., Blass, C., Wynshaw-Boris, A., and Rosenfeld, M., 2002. Identification of a Wnt/Dvl/B-catenin drives Pitx2 pathway mediating cell-type-specific proliferation during development. Cell 111, 673-685.
Kirby, M. and Hutson, M., 2010. Factors controlling cardiac neural crest cell migration. Cell Adhesion & Migration 4, 609-621.
Kletke, S.N., Vincent, A., Maynes, J.T., Elbaz, U., Mireskandari, K., Lam, W.C., Ali, A., 2020. A de novo mutation in PITX2 underlies a unique form of Axenfeld-Rieger syndrome with corneal neovascularization and extensive proliferative vitreoretinopathy. Ophthalmic Genetics 41, 358-362.
Klymkowsky, M.W., Rossi, C.C., Artinger, K.B., 2010. Mechanisms driving neural crest induction and migration in the zebrafish and Xenopus laevis. Cell Adhesion & Migration 4, 595-608.
Kohli, V., Rehn, K., and Sumanas, S., 2011. Single cell fate mapping in zebrafish. Journal of Visualized Experiments 56.
Kulesa, P., Bailey, C., Kasemeier-Kulesa, J., and McLennan, R., 2010. Cranial neural crest migration: new rules for an old road. Developmental Biology 344, 543-554.
Kulesa, P., Ellies, D., Tranior, P., 2003. Comparative analysis of neural crest cell death, migration, and function during vertebrate embryogenesis. Developmental Dynamics 299, 14-29.
Kwan, K.M., Otsuna, H., Kidokoro, H., Carney, K.R., Saijoh, Y., Chien, C.B., 2012. A complex choreography of cell movements shapes the vertebrate eye. Development 139, 359-372.
Lang, R.A., 2004. Pathways regulating lens induction in the mouse. International Journal of Developmental Biology 48, 783-791.
Langenberg, T., Kahana, A., Wszalek, J., and Halloran, M., 2008. The eye organizes neural crest cell migration. Developmental Dynamics 237, 1645-1652.
Lauter, G., Soll, I., Hauptmann, G., 2011. Two-color fluorescent in situ hybridization in the embryonic zebrafish brain using differential detection systems. Bmc Developmental Biology 11, 11.
Le Douarin, N and Teillet, M., 1974. Experimental analysis of the migration and differentiation of neuroblasts of the autonomic nervous system and of the neuroectodermal mesenchymal derivatives, using a biological cell marking technique. Developmental Biology 41, 162-184.
Lister, J., Cooper, C., Ngyen, K., Modrell, M., Grant, K., and Raible, D., 2006. Zebrafish foxd3 is required for development of a subset of neural crest derivatives. Developmental Biology 290, 92-104.
Liu, P. and Johnson, R., 2010. Lmx1b is required for murine trabecular meshwork formation and for the maintenance of corneal transparency. Developmental Dynamics 239, 2161-2171.
Liu, Y. and Semina, E., 2012. Pitx2 deficiency results in abnormal ocular and craniofacial development in zebrafish. PLoS One 7.
Loosli, F., Staub, W., Finger-Baier, K.C., Ober, E.A., Verkade, H., Wittbrodt, J., Baier, H., 2003. Loss of eyes in zebrafish caused by mutation of chokh/rx3. Embo Reports 4, 894-899.

Lovatt, M., Yam, G.H.F., Peh, G.S., Colman, A., Dunn, N.R., Mehta, J.S., 2018. Directed differentiation of periocular mesenchyme from human embryonic stem cells. Differentiation 99, 62-69.
Lovett, M., Yam, G., Peh, G., Colman, A., Dunn, N., and Mehta, J., 2018. Directed differentiation of periocular mesenchyme from human embryonic stem cells. Differentiation 99, 62-69.
Lu, M.F., Pressman, C., Dyer, R., Johnson, R.L., Martin, J.F., 1999. Function of Rieger syndrome gene in left-right asymmetry and craniofacial development. Nature 401, 276-278.
Lucey, M.M., Wang, Y., Bustin, M., Duncan, M.K., 2008. Differential expression of the HMGN family of chromatin proteins during ocular development. Gene Expression Patterns 8, 433-437.
Lupo, G., Gestri, G., O'Brien, M., Denton, R.M., Chandraratna, R.A.S., Ley, S.V., Harris, W.A., Wilson, S.W., 2011. Retinoic acid receptor signaling regulates choroid fissure closure through independent mechanisms in the ventral optic cup and periocular mesenchyme. Proceedings of the National Academy of Sciences of the United States of America 108, 8698-8703.
Lupo, G., Liu, Y., Qiu, R., Chandraratna, R.A.S., Barsacchi, G., He, R.Q., Harris, W.A., 2005. Dorsoventral patterning of the Xenopus eye: a collaboration of Retinoid, Hedgehog and FGF receptor signaling. Development 132, 1737-1748.
Ma, A., Yousoof, S., Grigg, J.R., Flaherty, M., Minoche, A.E., Cowley, M.J., Nash, B.M., Ho, G., Gayagay, T., Lai, T., Farnsworth, E., Hackett, E.L., Fisk, K., Wong, K., Holman, K.J., Jenkins, G., Cheng, A., Martin, F., Karaconji, T., Elder, J.E., Enriquez, A., Wilson, M., Amor, D.J., Stutterd, C.A., Kamien, B., Nelson, J., Dinger, M.E., Bennetts, B., Jamieson, R.V., 2020. Revealing hidden genetic diagnoses in the ocular anterior segment disorders. Genetics in Medicine 22, 1623-1632.
Maj, E., Kunneke, L., Loresch, E., Grund, A., Melchert, J., Pieler, T., Aspelmeier, T., Borchers, A., 2016. Controlled levels of canonical Wnt signaling are required for neural crest migration. Developmental Biology 417, 77-90.
Mannino, G., Abdolrahimzadeh, B., Calafiore, S., Anselmi, G., Mannino, C., Lambiase, A., 2016. A review of the role of ultrasound biomicroscopy in glaucoma associated with rare diseases of the anterior segment. Clinical Ophthalmology 10, 1453-1459.
Mao, M., Kiss, M., Ou, Y., and Gould, D., 2017. Genetic dissection of anterior segment dysgenesis caused by a Col4a1 mutation in mouse. Disease Models and Mechanisms 10, 475-485.
Martik, M.L., Gandhi, S., Uy, B.R., Gillis, J.A., Green, S.A., Simoes-Costa, M., Bronner, M.E., 2019. Evolution of the new head by gradual acquisition of neural crest regulatory circuits. Nature 574, 675-+.
Martino, V., Sabljic, T., Deschamps, P., Green, R., Akula, M., Peacock, E., Ball, A., Williams, T, and West-Mays, J., 2016. Conditional deletion of Ap-2B in mouse cranial neural crest results in anterior segment dysgenesis and early-onset glaucoma. Disease Models and Mechanisms 9, 849-861.
Matt, N., Dupe, V., Garnier, J., Dennefeld, C., Chambon, P., Mark, M., and Ghyselinck, N., 2005. Retinoic acid-dependent eye morphogenesis is orchestrated by neural crest cells. Development 132, 4789-4800.

Matt, N., Ghyselinck, N., Pellerin, I., and Dupe, V., 2008. Impairing retinoic acid signaling in the neural crest cells is sufficient to alter entire eye morphogenesis. Developmental Biology 320, 140-148.
Mayor, R. and Theveneau, E., 2013. The neural crest. Development 140, 2247-2251.
Mayor, R. and Etienne-Manneville, S., 2016. The front and rear of collective cell migration. Nature Reviews Molecular Cell Biology 17, 97-109.
McMahon, C., Gestri, G., Wilson, S., and Link, B., 2009. Lmx1b is essential for survival of periocular mesenchymal cells and influences fgf-mediated retinal pattering in zebrafish. Developmental Biology 332, 287-298.
McMahon, C., Semina, E., and Link, B., 2004. Using zebrafish to study the complex genetics of glaucoma. Comparative Biochemistry and Physiology, Part C 138, 343-350.
Medeiros, D.M., 2013. The evolution of the neural crest: new perspectives from lamprey and invertebrate neural crest-like cells. Wiley Interdisciplinary Reviews-Developmental Biology 2, 1-15.
Murphy, D., Diaz, B., Bromann, P., Tsai, J., Kawakami, Y., Maurer, J., Stewart, R., Izpisua-Belmonte, J., and Courtneidge, S., 2011. A src-Tks5 pathway is required for neural crest cell migration during embryonic development. PLoS One 6.
Nieminen, P., Kotilainen, J., Aalto, Y., Knuutila, S., Pirinen, S., Thesleff, I., 2003. MSX1 gene is deleted in Wolf-Hirschhorn syndrome patients with oligodontia. Journal of Dental Research 82, 1013-1017.
Noisa, P. and Raivio, T., 2014. Neural Crest Cells: From Developmental Biology to Clinical Interventions. Birth Defects Research Part C-Embryo Today-Reviews 102, 263-274.
Or, L., Barkana, Y., Hecht, I., Weiner, C., Einan-Lifshitz, A., Pras, E., 2020. FOXC1 variant in a family with anterior segment dysgenesis and normal-tension glaucoma. Experimental Eye Research 200, 6.
Parichy, D.M., Elizondo, M.R., Mills, M.G., Gordon, T.N., Engeszer, R.E., 2009. Normal Table of Postembryonic Zebrafish Development: Staging by Externally Visible Anatomy of the Living Fish. Developmental Dynamics 238, 2975-3015.
Pingault, V., Ente, D., Dastot-Le Moal, F., Goossens, M., Marlin, S., Bondurand, N., 2010. Review and Update of Mutations Causing Waardenburg Syndrome. Human Mutation 31, 391-406.
Powell, D.R., Hernandez-Lagunas, L., LaMonica, K., Artinger, K.B., 2013. Prdm1a directly activates foxd3 and tfap2a during zebrafish neural crest specification. Development 140, 3445-3455.
Pressman, C.L., Chen, H.X., Johnson, R.L., 2000. Lmx1b, a LIM homeodomain class transcription factor, is necessary for normal development of multiple tissues in the anterior segment of the murine eye. Genesis 26, 15-25.
Qin, Y.Y., Gao, P., Yu, S.S., Li, J.Z., Huang, Y.W., Jia, D.N., Tang, Z.H., Li, P.C., Liu, F., Liu, M.G., 2020. A large deletion spanning PITX2 and PANCR in a Chinese family with Axenfeld-Rieger syndrome. Molecular Vision 26, 670-678.
Quigley, H. and Broman, A., 2006. The number of people with glaucoma worldwide in 2010 and 2020. British Journal of ophthalmology 90, 262-267.
Rausch, R., Libby, R., and Kiernan, A., 2018. Trabecular meshwork morphogenesis: a comparative analysis of wildtype and anterior segment dysgenesis mouse models. Experimental Eye Research 170, 81-91.

Reade, A., Motta-Mena, L., Gardner, K., Stainier, D., Weiner, O., and Woo, S., 2017. TAEL: a zebrafish-optimized optogenetic gene expression system with fine spatial and temporal control. Development 144, 345-355.
Reis, L., Tyler, R., Volkmann Kloss, B., Schilter, K., Levin, A., Lowry, R. B., Zwinjnenburg, P., Stroh, E., Broeckel, U., Murray, J., and Semina, E., 2012. Pitx2 and Foxc1 spectrum of mutations in ocular syndromes. European Journal of Human Genetics 20, 1224-1233.
Reis, L. and Semina, E., 2011. Genetics of anterior segment dysgenesis disorders. Current Opinion in Ophthalmology 22, 314-324.
Richardson, J., Gauert, A., Montecinos, L., Fanlo, L., Alhashem, Z., Assar, R., Marti, E., Kabla, A., Hartel, S., and Linker, C., 2016. Leader cells define directionality of trunk, but not cranial, neural crest cell migration. Cell Reports 15, 2076-2088.
Richardson, R., Tracey-White, D., Webster, A., Moosajee, M., 2017. The zebrafish eye-a paradigm for investigating human ocular genetics. Eye 31, 68-86.
Saffari, A., Ziegler, A., Merkenschlager, A., Kruger, S., Kolker, S., Hoffmann, G.F., Syrbe, S., 2020. Axenfeld-Rieger Anomaly and Neuropsychiatric Problems-More than Meets the Eye. Neuropediatrics 51, 192-197.
Scarpa, E., Szabo, A., Bibonne, A., Theveneau, E., Parsons, M., and Mayor, R., 2015. Cadherin switch during EMT in neural crest cell leads to contact inhibition of locomotion via repolarization of forces. Developmental Cell 34, 421-434.
Schumacher, J., Zhao, E., Kofron, M., and Sumanas, S., 2014. Two-color fluorescent in situ hybridization using chromogenic substrates in zebrafish. BioTechniques 57, 254-256.
Scott, A.W., Bressler, N.M., Ffolkes, S., Wittenborn, J.S., Jorkasky, J., 2016. Public Attitudes About Eye and Vision Health. Jama Ophthalmology 134, 1111-1118.
Sedykh, I., Yoon, B., Roberson, L., Mskvin, O., Dewey, C., and Grinblat, Y., 2017. Zebrafish zic2 controls formation of periocular neural crest and choroid fissure morphogenesis. Developmental Biology 429, 92-104.
Seo, S., Chen, L., Liu, W., Zhao, D., Schultz, K., Sasman, A., Liu, T., Zhang, H., Gage, P., and Kume, T., 2017. FoxC1 and FoxC2 in the neural crest are required for the ocular anterior segment development. Investigative Ophthalmology & Visual Science 58, 1368-1377.
Seo, S., Singh, H., Lacal, P., Sasman, A., Fatima, A., Liu, T., Schultz, K., Losordo, D., Lehmann, O. and Kume, T., 2012. Forkhead box transcription factor FoxC1 preserves corneal transparency by regulating vascular growth. PNAS 109, 2015-2020.
Siggs, O.M., Souzeau, E., Taranath, D.A., Dubowsky, A., Chappell, A., Zhou, T., Javadiyan, S., Nicholl, J., Kearns, L.S., Staffieri, S.E., Narita, A., Smith, J.E.H., Pater, J., Hewitt, A.W., Ruddle, J.B., Elder, J.E., Mackey, D.A., Burdon, K.P., Craig, J.E., 2020. Biallelic CPAMD8 Variants Are a Frequent Cause of Childhood and Juvenile Open-Angle Glaucoma. Ophthalmology 127, 758-766.
Simo, R., Villarroel, M., Corraliza, L., Hernandez, C., Garcia-Ramirez, M., 2010. The Retinal Pigment Epithelium: Something More than a Constituent of the Blood-Retinal Barrier-Implications for the Pathogenesis of Diabetic Retinopathy. Journal of Biomedicine and Biotechnology, 15.
Simoes-Costa, M. and Bronner, M.E., 2015. Establishing neural crest identity: a gene regulatory recipe. Development 142, 242-257.

Simon, E., Theze, N., Fedou, S., Thiebaud, P., and Faucheux, C., 2017. Vesitigial-like 3 is a novel Ets1 interacting partner and regulates trigeminal nerve formation and cranial neural crest migration. Biology Open 6, 1528-1540.
Sinagoga, K.L., Larimer-Picciani, A.M., George, S.M., Spencer, S.A., Lister, J.A., Gross, J.M., 2020. Mitf-family transcription factor function is required within crania neural crest cells to promote choroid fissure closure. Development 147, 8.
Skarie, J. and Link, B., 2009. FoxC1 is essential for vascular basement membrane integrity and hyaloid vessel morphogenesis. Investigative Ophthalmology & Visual Science 50, 5026-5034.
Snider, P., Olaopa, M., Firulli, A., and Conway, S., 2007. Cardiovascular development and the colonizing cardiac neural crest lineage. The Scientific World JOURNAL 7, 1090-1113.
Solek, C., Feng, S., Perin, S., Mendes, H., and Ekker, M., 2017. Lineage tracing of dlx1a/2a and dlx5a/6a expressing cells in the developing zebrafish brain. Developmental Biology 427, 131-147.
Sommer, P., Napier, H., Hogan, B., and Kidson, S., 2006. Identification of TgfB1i4 as a downstream target of FoxC1. Developmental Growth and Differentiation 48, 297-308.
Soules, K. and Link, B., 2005. Morphogenesis of the anterior segment in the zebrafish eye. BMC Developmental Biology 5.
Sowden, J.C., 2007. Molecular and developmental mechanisms of anterior segment dysgenesis. Eye 21, 1310-1318.
Sridhar, M.S., 2018. Anatomy of cornea and ocular surface. Indian Journal of Ophthalmology 66, 190-194.
Stamer, W. and Clark, A., 2017. The many faces of the trabecular meshwork cell. Experimental Eye Research 158, 112-123.
Stewart, R., Arduini, B., Berghmans, S., George, R., Kanki, J., Henion, P., and Look, A., 2006. Zebrafish foxd3 is selectively required for neural crest specification, migration, and survival. Developmental Biology 292, 174-188.
Strauss, O., 2005. The retinal pigment epithelium in visual function. Physiological Reviews 85, 845-881.
Strungaru, M.H., Footz, T., Liu, Y., Berry, F.B., Belleau, P., Semina, E.V., Raymond, V., Walter, M.A., 2011. PITX2 Is Involved in Stress Response in Cultured Human Trabecular Meshwork Cells through Regulation of SLC13A3. Investigative Ophthalmology & Visual Science 52, 7625-7633.
Takamiya, M., Stegmaier, J., Kobitski, A.Y., Schott, B., Weger, B.D., Margariti, D., Delgado, A.R.C., Gourain, V., Scherr, T., Yang, L.X., Sorge, S., Otte, J.C., Hartmann, V., van Wezel, J., Stotzka, R., Reinhard, T., Schlunck, G., Dickmeis, T., Rastegar, S., Mikut, R., Nienhaus, G.U., Strahle, U., 2020. Pax6 organizes the anterior eye segment by guiding two distinct neural crest waves. Plos Genetics 16, 36.
Tamimi, Y., Skarie, J.M., Footz, T., Berry, F.B., Link, B.A., Walter, M.A., 2006. FGF19 is a target for FOXC1 regulation in ciliary body-derived cells. Human Molecular Genetics 15, 3229-3240.
Taneyhill, L. and Schiffmacher, A., 2013. Cadherin dynamics during neural crest cell ontogeny, Progress in molecular Biology and translational Science, Maryland, USA.
Teddy, J. and Kulesa, P., 2004. In vivo evidence for short- and long-range cell communication in cranial neural crest cells. Development 131, 6141-6151.

Teh, C., Chudakov, D., Poon, K., Mamedov, I., Sek, J., Shidlovsky, K., Lukyanov, S., and Korzh, V., 2010. Optogenetic in vivo cell manipulation in KillerRed-expressing zebrafish transgenics. BMC Developmental Biology 10.
Thanikachalam, S., Hodapp, E., Chang, T.C., Swols, D.M., Cengiz, F.B., Guo, S.R., Zafeer, M.F., Seyhan, S., Bademci, G., Scott, W.K., Grajewski, A., Tekin, M., 2020. Spectrum of Genetic Variants Associated with Anterior Segment Dysgenesis in South Florida. Genes 11, 10.
Theveneau, E. and Mayor, R., 2012. Neural crest delamination and migration: from epithelium-to-mesenchyme transition to collective migration. Developmental Biology 366, 34-54.
Thisse, C. and Thisse, B., 2008. High-resolution in situ hybridization to whole-mount zebrafish embryos. Nature Protocols 3, 59-69.
Todorova, M.G., Grieshaber, M.C., Camara, R.J.A., Miny, P., Palmowski-Wolfe, A.M., 2014. Anterior segment dysgenesis associated with Williams-Beuren syndrome: a case report and review of the literature. Bmc Ophthalmology 14, 5.
Trainor, P.A., 2010. Craniofacial Birth Defects: The Role of Neural Crest Cells in the Etiology and Pathogenesis of Treacher Collins Syndrome and the Potential for Prevention. American Journal of Medical Genetics Part A 152A, 2984-2994.
Trainor, P. and Tam, P., 1995. Cranial paraxial mesoderm and the neural crest cells of the mouse embryo: co-distribution in the craniofacial mesenchyme but distinct segregation in the branchial arches. Development 121, 2569-2582.
Tumer, Z., Bach-Holm, D., 2009. Axenfeld-Rieger syndrome and spectrum of PITX2 and FOXC1 mutations. European Journal of Human Genetics 17, 1527-1539.
Van Der Meulen, K.L., Vocking, O., Weaver, M.L., Meshram, N.N., Famulski, J.K., 2020. Spatiotemporal Characterization of Anterior Segment Mesenchyme Heterogeneity During Zebrafish Ocular Anterior Segment Development. Frontiers in Cell and Developmental Biology 8, 16.
Van Otterloo, E., Li, W., Garnett, A., Cattell, M., Medeiros, D.M., Cornell, R.A., 2012. Novel Tfap2-mediated control of soxE expression facilitated the evolutionary emergence of the neural crest. Development 139, 720-730.
Vasiliou, V., Gonzalez, F.J., 2008. Role of CYP1B1 in glaucoma, Annual Review of Pharmacology and Toxicology. Annual Reviews, Palo Alto, pp. 333-358.
Vincent, A., Billingsley, G., Priston, M., Glaser, T., Oliver, E., Walter, M., Ritch, R., Levin, A., Heon, E., 2006. Further support of the role of CYP1B1 in patients with Peters anomaly. Molecular Vision 12, 506-510.
Volkmann, B., Zinkevich, N., Mustonen, A., Schilter, K., Bosenko, D., Reis, L., Broeckel, U., Link, B., and Semina, E., 2011. Potential novel mechanism for axenfeld-rieger syndrome: deletion of a distant region containing regulatory elements of pitx2. Investigative Ophthalmology & Visual Science 52.
Volkmann Kloss, B., Reis, L., Bremond-Gignac, D., Glaser, T., and Semina, E., 2012. Analysis of FoxD3 sequence variation in human ocular disease. Molecular Vision 18, 1740-1749.
Walker, H., Akula, M., West-Mays, J.A., 2020. Corneal development: Role of the periocular mesenchyme and bi-directional signaling. Experimental Eye Research 201, 7.

Wan, Y.N., Almeida, A.D., Rulands, S., Chalour, N., Muresan, L., Wu, Y.M., Simons, B.D., He, J., Harris, W.A., 2016. The ciliary marginal zone of the zebrafish retina: clonal and time-lapse analysis of a continuously growing tissue. Development 143, 1099-1107.
Wang, W., Melville, D., Montero-Balaguer, M., Hatzopoulos, A., and Knapik, E., 2011. Tfap2a and Foxd3 regulate early steps in the development of the neural crest progenitor population. Developmental Biology 360, 173-185.
Weaver, M.L., Piedade, W.P., Meshram, N.N., Famulski, J.K., 2020. Hyaloid vasculature and mmp2 activity play a role during optic fissure fusion in zebrafish. Scientific Reports 10, 16.
Weigele, J. and Bohnsack, B.L., 2020. Genetics Underlying the Interactions between Neural Crest Cells and Eye Development. Journal of Developmental Biology 8, 24.
Williams, A. and Bohnsack, B., 2015. Neural crest derivatives in ocular development: discerning the eye of the storm. Birth Defects Research (Part C).
Williams, A.L. and Bohnsack, B.L., 2019. What's retinoic acid got to do with it? Retinoic acid regulation of the neural crest in craniofacial and ocular development. Genesis 57, 13.
Williams, A.L. and Bohnsack, B.L., 2020. The Ocular Neural Crest: Specification, Migration, and Then What? Frontiers in Cell and Developmental Biology 8, 13.
Williams, A.L., Eason, J., Chawla, B., Bohnsack, B.L., 2017. Cyp1b1 Regulates Ocular Fissure Closure Through a Retinoic Acid-Independent Pathway. Investigative Ophthalmology & Visual Science 58, 14.
Williams, D.L., 1993. A COMPARATIVE APPROACH TO ANTERIOR SEGMENT DYSGENESIS. Eye 7, 607-616.
Xia, Z., Tong, X., Liang, F., Zhang, Y., Kuok, C., Zhang, Y., Liu, X., Zhu, Z., Lin, S., and Zhang, B., 2013. Eif3ba regulates cranial neural crest development by modulating p53 in zebrafish. Developmental Biology 381, 83-96.
Xu, P.X., Woo, I., Her, H., Beier, D.R., Maas, R.L., 1997. Mouse Eya homologues of the Drosophila eyes absent gene require Pax6 for expression in lens and nasal placode. Development 124, 219-231.
Yu, H., and Moens, C., 2005. Semaphorin signaling guides cranial neural crest cell migration in zebrafish. Developmental Biology 280, 373-385.
Zentner, G.E., Layman, W.S., Martin, D.M., Scacheri, P.C., 2010. Molecular and Phenotypic Aspects of CHD7 Mutation in CHARGE Syndrome. American Journal of Medical Genetics Part A 152A, 674-686.
Zhang, B.N., Liu, Y., Yang, Q.C., Leung, P.Y., Wang, C.D., Wong, T.C.B., Tham, C.C., Chan, S.O., Pang, C.P., Chen, L.J., Dekker, J., Zhao, H., Chu, W.K., 2020. rad21 Is Involved in Corneal Stroma Development by Regulating Neural Crest Migration. International Journal of Molecular Sciences 21, 17.
Zhang, D., Ighaniyan, S., Stathopoulos, L., Rollo, B., Landman, K., Hutson, J., and Newgreen, D., 2014. The neural crest: a versatile organ system. Birth Defects Research (Part C) 102, 275-298.
Anterior Segment Dysgenesis. American Academy of Ophthalmology.
Centers for Disease Control.
National Health Institute (NIH): Genetics Home Reference.
ZFIN (Zebrafish Information Network). 1994-2021. The University of Oregon, Oregon.
World Health Organization. 2010.
American Academy of Ophthalmology (AAO). 2019.

Eye Disease Statistics: All Vision Impairment. 2019. National Eye Institute.

VITA

Author's Name: Kristyn Van Der Meulen

Education:

2015 - present Ph.D. in Biology, University of Kentucky, Lexington, KY.

2011 - 2015 Bachelor of Science with Honors, Wittenberg University, Springfield, OH.

Professional Positions:

2015 - present Research Assistant, Famulski Lab, University of Kentucky

2015 - 2018 Teaching Assistant, University of Kentucky

Scholastic Honors:

2019 2nd Place Poster Presentation, 5th Annual Meeting of the Society of Postdoctoral Scholar, Lexington, KY

2018 Outstanding Graduate Student Presenter, 34th Annual BGSFN Spring Neuroscience Day, Lexington, KY

2016 Knights Templar Eye Foundation Scholarship for Vision Research

Professional Publications:

Van Der Meulen, K.L., Vocking, O., Weaver, M.L., Meshram, N.N., Famulski, J.K., 2020. Spatiotemporal Characterization of Anterior Segment Mesenchyme Heterogeneity

During Zebrafish Ocular Anterior Segment Development. *Frontiers in Cell and Developmental Biology* 8, 16.